DRIFT SPEED DISTRIBUTION OF ICEBERGS ON THE GRAND BANKS AND INFLUENCE ON DESIGN LOADS

PAUL D. STUCKEY

Drift Speed Distribution of Icebergs on the Grand Banks and Influence on Design Loads

by

© Paul D. Stuckey, B.Eng.

A Thesis Submitted to the School of Graduate Studies
in Partial Fulfillment of the Requirements for the Degree of
Master of Engineering

Faculty of Engineering and Applied Science
Memorial University of Newfoundland

May, 2008

St. John's Newfoundland Canada

Abstract

With increasing oil and gas exploration on the Grand Banks during the 1970's and 1980's, there was a need to better understand the risk of icebergs impacting an offshore structure, and the consequences should such an event occur. As a result of industry demand, a probabilistic iceberg design load methodology was developed to estimate the risk of impacts and the resultant impact forces.

Since the original framework was developed, there have been numerous improvements and enhancements. Distributions and relationships used to define input parameters have been refined due to the availability of new data. Several models have been improved as a result of ongoing research. The author has been extensively involved in many of the updates and improvements to the methodology, including improvements in the eccentricity model, the area-penetration model, and most recently, the drift speed model.

The iceberg drift speed model, a key component, was developed by balancing the environmental forces acting on the iceberg. The model was deterministic; there was only one iceberg drift speed for a given iceberg in a specific significant wave height. The model agreed with the overall drift speed distribution based on available data. However, with the availability of new data, it was shown the model did not fully capture the randomness observed in the data.

A new probabilistic drift speed model was developed to replace the deterministic model. It is based on the statistical analysis of available drift speed data. This model addresses the randomness in the data by incorporating probability distributions. The input parameters for the distributions are defined in terms of the iceberg waterline length and the significant wave height.

Acknowledgments

First and foremost, I would like to thank my supervisor, Dr. Ian Jordaan, for all the support and guidance he has provided over the years. Dr. Jordaan first introduced me to the field of ice engineering and the relationship with mechanics, probability and statistics, and risk assessment and its application to ice. It has been constant learning process and fully enjoyable.

I extend special thanks to Dr. Chuanke Li for his insightful thoughts and comments during our time working together. His motivation during the last stages of this work was well appreciated. I would also like to thank Mr. Daryl Burry and Mr. Freeman Ralph for proofreading and providing suggestions.

Finally, the author wishes to thank the following groups or organizations for their financial support: Newfoundland Offshore Career Development Awards Committee and the Faculty of Engineering and Applied Sciences, Memorial University of Newfoundland, and C-CORE.

Contents

List of Figures

List of Tables

Nomenclature

Abbreviations and Acronyms

AES40	Atmospheric Environmental Services Wind Hindcast Database
ARIMA	Auto-regressive, Integrated Moving Average
CIOM	Community Ice Ocean Model
CMG	Course Made Good
IIP	International Ice Patrol
CDF	Cumulative Distribution Function
FPSO	Floating, Production, Storage and Offloading (vessel)
GBS	Gravity Based Structure
PDF	Probability Density Function
PERD	Program of Energy Research and Development

Symbols

When defining probabilistic variables, upper case letters generally refer to random quantities, and lower case letters generally refer to fixed quantities.

A, a	Contact area
A_1	Square matrix containing the dimensions of the repeating variables
A_2	Matrix containing the dimensions of the non-repeating variables
$\vec{a}$	Iceberg acceleration
A_A	Above water projected area of an iceberg
A_B	Below water projected area of an iceberg
A_R	Geographical area of a region
A_W	Cross sectional area of layer of iceberg keel
B	Matrix solution to ${A_1}^{-1}A_2$
C_A	Coefficient in random area-penetration relationship

C_a	Wind drag coefficient
C_D, C_{wf}	Wave drift coefficient
C_P	Coefficient in random pressure-area relationship
C_w	Water drag coefficient
D	Iceberg draft
D_A	Coefficient in random area-penetration relationship
D_E	Ekman depth
D_I	Characteristic dimension of an iceberg
D_P	Coefficient in random pressure-area relationship
d_S	Distance travelled (encounter model)
$dist$	Total distance iceberg moves between two consecutive observations
$dist_x$	Distance in x-direction between two consecutive observations
$dist_y$	Distance in y-direction between two consecutive observations
e	Normally distributed random number
F	Ice crushing force
$\mathbf{F}$	Force vector
$\vec{f}$	Coriolis parameter
$\vec{F_A}$	Wind drag force
$\vec{F_C}$	Coriolis force
$\vec{F_D}$	Wave drift force
F_{H_S}, f_{H_S}	Significant wave height CDF and PDF
$F_L(l), f_L(l)$	Waterline length CDF and PDF
F_N	Cumulative normal distribution
$\vec{F_P}$	Pressure gradient force
F_R	Cumulative Rayleigh distribution
$\vec{F_W}$	Water drag force
$F_X(x)$	Distribution of events x
$F_Z(z)$	Extreme distribution of events z
F_{max}	Maximum crushing force
F_{SR}	Special Rayleigh cumulative distribution function
G	Non-dimensional eccentricity factor
g	Gravitational acceleration
H	Regular wave height

H_S	Significant wave height
$H_S{}^*$	Critical significant wave height
$I_{max,min}$	Maximum and minimum moments of inertia
I_x	Moment of inertia in the x-direction
I_y	Moment of inertia in the y-direction
I_{xy}	Moment of inertia in the xy plane
K	Constant; number of seconds in a year
k	Constant used in non-linear spring expression
k_D	Number of π-terms required to completely describe a problem
$\widehat{k}$	Vertical unit vector
k_i	Unit normal vector
KE_0	Iceberg initial kinetic energy
L, l	Iceberg waterline length
L_W	Wave length
L, **M**, **T**	Basic dimensions of length, mass and time (dimensional analysis)
l_S	Length of ship
$l_{1,2,3}$	Principal axes of inertia
lat_1	Latitude at the starting position
lat_2	Latitude at the end position
$long_1$	Longitude at the starting position
$long_2$	Longitude at the end position
M, m	Iceberg mass
$\tilde{m}$	Iceberg mass, including added mass
m_D	Number of variables in dimensional analysis problem
N	Time conversion constant
P	Global ice crushing pressure
$P(A)$	Prior or marginal distribution of A
$P(A\|B)$	Posterior or conditional distribution of A given B
$P(B\|A)$	Posterior or conditional distribution of B given A
p_{L,H_S}	Generic joint distribution between L and H_S
p'_{L,H_S}	Updated joint distribution between L and H_S
p_{V_D}	Iceberg drift speed as a function of L and H_S
$P_{dis}{}^*$	Probability of a successful disconnect
p_E	Probability of collision
p_i	Probability of an iceberg in the region

q_i	Proportion of force acting in the ith direction
r^2	Correlation coefficient
r_{g_i}	Radius of gyration
s	Normalization constant (iceberg collision speed model)
T	Time
T_{dis}	Time required for an emergency disconnect
$time_1$	Date and time at the starting position
$time_2$	Date and time at the end position
U_A	Velocity of air relative to iceberg
U_C	Current speed
U_W	Wind speed
$\vec{u_W}$	Wind speed
u	Iceberg collision speed (Section 2.4.2)
v_D	Iceberg drift speed
V_0	Surface current speed
$\vec{V}_{mw}$	Mean current velocity
v_R	Relative speed between iceberg and ship
v_S	Ship speed
W_D	Water depth
w_i	Average width of iceberg
w_S	Structure width
x, y, z	Cartesian coordinates
x_{CM}, y_{CM}, z_{CM}	Coordinates of iceberg center of mass
x_{CP}, y_{CP}, z_{CP}	Coordinates of initial contact point between iceberg and structure
x, $\dot{x}$, and $\ddot{x}$	Displacement, velocity and acceleration in the x-direction
z	Depth from the surface
β_0	Angle between the maximum principal axis and the x-axis
γ	Constant used in non-linear spring expression
δ, $\dot{\delta}$, and $\ddot{\delta}$	Iceberg penetration displacement, velocity and acceleration
δ_{max}	Iceberg penetration resulting in maximum force
Δt	Time interval
$\epsilon_{x,y,z}$	Eccentricity distances with respect to the x,y,z coordinate system
ϵ_i	Eccentricity distances with respect to principal axes
η_E	Expected number of iceberg impacts

ρ_A	Density of air
ρ_D	Average annual areal density of icebergs
ρ_I	Density of ice
ρ_W	Density of water
θ_R	Relative angle between iceberg and vessel headings
θ, $\dot{\theta}$, and $\ddot{\theta}$	Iceberg angular rotation, velocity and acceleration
ν	Expected number of impacts per year
σ	Variance of iceberg surge velocity
ϕ	Relative direction between iceberg and ship
ϕ_{lat}	Latitude (in degrees)
ω	Coriolis constant

Chapter 1

Introduction

1.1 Overview

Icebergs pose a significant risk to oil and gas exploration, development and production facilities operating on the Grand Banks, off Canada's east coast. Without adequate resistance, an iceberg collision with a fixed gravity based structure (GBS) may cause severe structural damage, resulting in an environmentally disastrous oil spill, or even loss of life. A floating production, storage and offloading (FPSO) vessel, which can disconnect and avoid an approaching iceberg, may lose millions of dollars in revenue due to downtime associated with disconnecting, and eventually reconnecting, the turret/riser system. Icebergs also pose a threat to vessels operating in, or transiting through the Grand Banks region. The *Titanic* sank after colliding with an iceberg, resulting in the loss of over 1500 passengers and crew. In more recent years, the bow of the bulk carrier *Canadian Bulker* was damaged seriously after colliding with an iceberg; the vessel made it safely to port. These are just two examples of ship-iceberg collisions. Brian Hill has compiled a database entitled "Ship Iceberg Collision Database" (Hill 2005) which contains information on ship-ice collisions which have

occurred during the last couple centuries. The database is focused primarily on the Grand Banks and North Atlantic but also includes regions, and includes over 600 incidents.

Exploration and development on the Grand Banks will continue in an effort to keep up with the ever-increasing energy demands of the world. Discoveries of hydrocarbons on the Grand Banks indicate that the region could be one of the top oil producing regions in Canada. To address risk of icebergs to offshore structures, an iceberg design load methodology was developed. The initial framework was laid by Fuglem et al. (1996a), Fuglem et al.(1996b) and Fuglem (1997).

During the past decade, the methodology has been expanded and improved mainly due to industry demand. The author has been primarily involved in many of the improvements and additions to the methodology, including

- improvements to the iceberg drift and collision speed models;
- improvements to the iceberg eccentricity model;
- the addition of a contact height model; and
- the improvement of the area-penetration model.

The iceberg design load methodology is probabilistic, accounts for the range of iceberg shapes, sizes and strengths, and environmental conditions. The approach is applicable to both fixed gravity based structures or jackups, as well as floating structures such as a semi-submersibles or FPSOs. The methodology incorporates the effectiveness of iceberg detection, physical management, and disconnection (where applicable) to help mitigate the risk of impact with an iceberg. This is consistent with the provisions provided in the Canadian Standards Association CAN/CSA-S.471-04,

General Requirements, Design Criteria, the Environment, and Loads, part of the *Code for the Design, Construction, and Installation of Fixed Offshore Structures.*

1.2 Methodology and Scope

This thesis describes the many components, and input parameters and relationships of the iceberg design load methodology. Typical results from the application of the methodology to a generic shaped GBS and FPSO located on the Grand Banks are presented. A detailed literature review describes some of the different approaches used in the past to model iceberg drift speed.

The theory of dimensional analysis is applied to the drift speed of icebergs on the Grand Banks. Several dimensional analysis methods are introduced briefly. The matrix method is explained in detail and is applied to the drift speed problem. Results are then compared with the approach adopted in the deterministic model.

The deterministic iceberg drift speed model is reviewed in detail. Individual components of the model are discussed, and output data from the model are compared with observed data collected on the Grand Banks.

A new probabilistic iceberg drift speed model is presented. Output data from the probabilistic model are compared with observed data. A sensitivity analysis is performed using the iceberg design load methodology, and both the deterministic and probabilistic drift speed models.

The methodology and scope of this thesis can be summarized in the following steps.

1. Literature review of past and present iceberg drift speed modeling.

2. Dimensional analysis of the iceberg drift speed phenomenon.

3. Detailed review of the deterministic iceberg drift speed model currently used in the iceberg design load methodology.

4. Statistical analysis of all available iceberg drift speed data for the Grand Banks region and a comparison with output from the deterministic model.

5. Development of a new probabilistic drift speed model, and sensitivity of iceberg design loads to the different drift speed models.

1.3 Significance of Study

The research and new probabilistic iceberg drift speed model presented in this thesis have considerable value. The research helps to provide a better understanding of the iceberg drift speed phenomenon. The development of a probabilistic iceberg drift speed model improves design load estimates for offshore structures. With lower, but yet safe, iceberg design load estimates, economically marginal fields may become feasible due to more efficient designs.

Chapter 2

Review of Iceberg Design Load Methodology

2.1 Introduction

A probabilistic methodology has been developed for determining iceberg impact loads on offshore structures (Fuglem et al. 1996a, Fuglem et al. 1996b and Fuglem 1997). The overall framework of the approach is illustrated in Figure 2.1. A probabilistic algorithm is adopted which incorporates a Monte Carlo approach to simulate a distribution of global impact forces. The methodology takes into account the size of the iceberg as well as the speed at which it is moving. The sea state conditions and associated hydrodynamic effects are also included in the model. The impact force calculation is based on a kinetic energy approach in which energy is dissipated due to ice crushing and iceberg rotation caused by eccentric impacts. Pressure-area relationships are developed to determine global loads. Local pressures are calculated accounting for the size of the loaded area, the duration and frequency of the impacts. The design load methodology can be divided into four distinct modules, including:

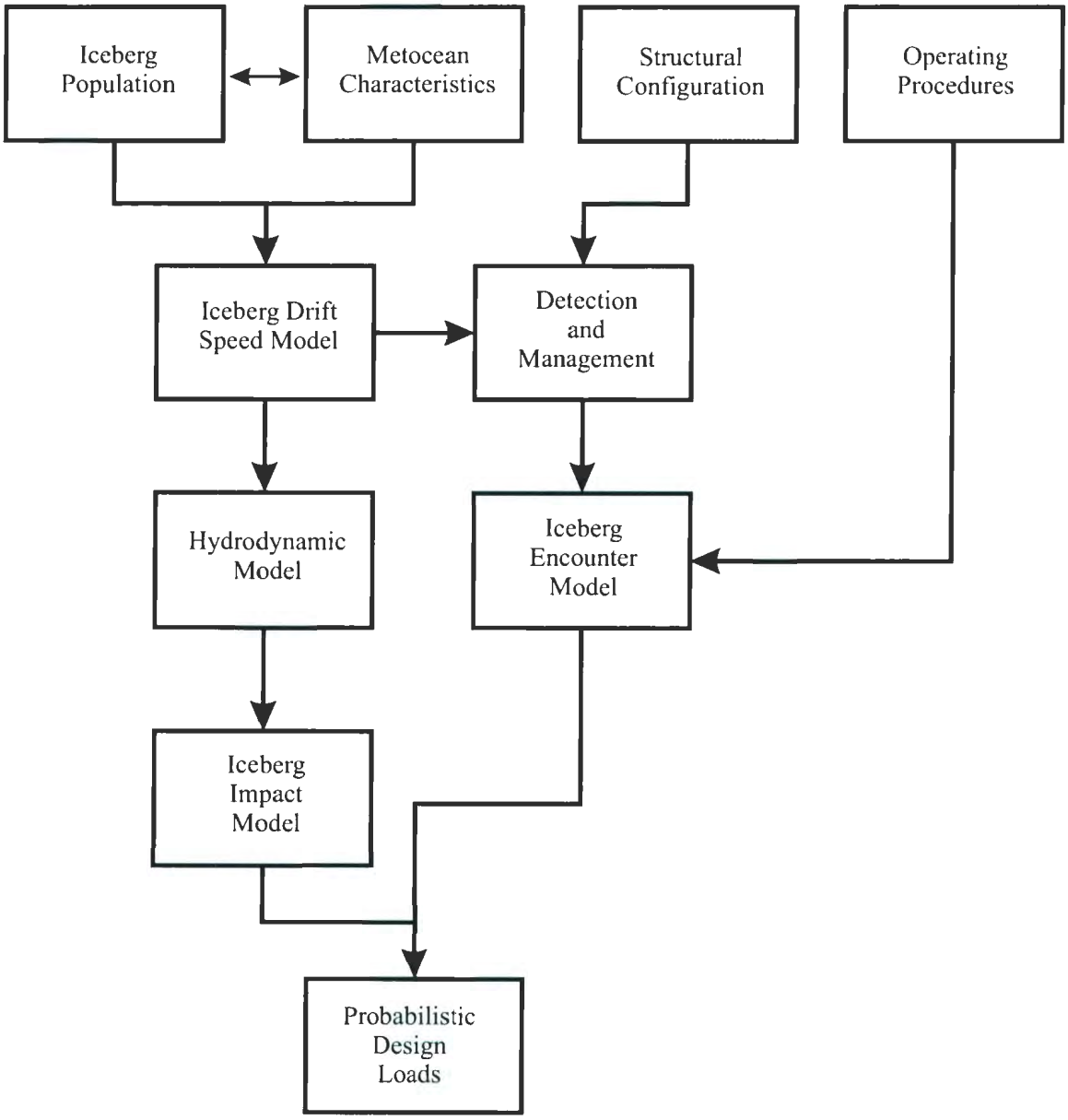

Figure 2.1: Illustration of iceberg design load methodology

- data input;
- encounter frequency;
- iceberg impact; and
- probabilistic design load calculations.

Within the data input module, the iceberg population and metocean characteristics of the region are described. The structural configuration of the GBS or FPSO is defined using a coordinate point system. Operational aspects are defined, including options such as the ability of an FPSO to disconnect and move out of the path of oncoming icebergs. The environmental inputs are then passed into the iceberg drift speed model which calculates the drift speed as a function of the iceberg size and the significant wave height. The encounter frequency module calculates the probability of an iceberg impacting the structure given the structural configuration, operating procedures and generic input distributions for iceberg length and significant wave height. If applicable, iceberg detection and management models are incorporated to help mitigate the risk of an iceberg impact. The iceberg impact module consists of the simulation of data, the calculation of the collision speed, including hydrodynamic effects, and the ice mechanics model. The ice mechanics model accounts for the decrease in both global and local ice pressures with increasing contact area, the rate of growth of contact area with penetration, and the iceberg rotational/inertial effects. The probabilistic design load module calculates the annual design loads for probabilities of exceedence of 10^{-2}, 10^{-3} and 10^{-4}.

In nature, the relationship between ice pressure and contact area is complex. During an iceberg-structure interaction event the iceberg undergoes an array of changes, including spalling of large ice pieces, microcracking, damage processes and extrusion.

The following random relationships are used to attempt to capture the complex process of global ice failure. The global pressure P is defined as a function of the nominal interaction area, and is given as,

$$P(a) = C_P a^{D_P}, \tag{2.1}$$

where C_P and D_P are coefficients determined from the analysis of full-scale ship ram data and a is the global contact area. Similarly, the impact force F can be written as

$$F(A) = C_P a^{D_P+1}. \tag{2.2}$$

A detailed description of the relationship and determination of the the coefficients C_P and D_P are given in (Carter et al. 1996).

Growth of global contact area depends on the rate of the iceberg penetration onto the structure as well and the physical shape of the iceberg. Detailed underwater profiles of icebergs are difficult and expensive to obtain. An analysis of the few existing iceberg profiles resulted in the following relationship between global contact area and penetration

$$A(\delta) = C_A \delta^{D_A}, \tag{2.3}$$

where δ is the penetration distance in meters and C_A and D_A are the coefficients resulting from the analysis (Fuglem et al. 1998). Combining equations (2.2) and (2.3) results in the following force-penetration relationship

$$F(\delta) = C_P C_A^{D_P+1} \delta^{D_A(D_P+1)}. \tag{2.4}$$

Defining

$$k = C_P C_A^{D_P+1} \text{ and } \gamma = D_A (D_P + 1), \tag{2.5}$$

one can rewrite Equation 2.4 as a nonlinear spring function

$$F(\delta) = k\delta^{\gamma}. \tag{2.6}$$

The following sections provide details on the four modules – data input, encounter frequency, iceberg impact and probabilistic design loads – and the relationship with the basic force equations defined above. Typical results for a generic GBS and FPSO operating on the Grand Banks are also summarized.

2.2 Data Input Model

In this module, the generic iceberg population and the metocean characteristics are determined for the specified location. It is important to note that distributions of iceberg size and drift speed for impacting icebergs are different than the measured distributions. For example, if a snapshot of a region is taken and the iceberg waterline length and drift speed distributions are determined, the resulting distributions would be termed **generic**. Generic distributions refer to all the icebergs in the region, including those that may or may not impact the structure. The distributions relating to icebergs that impact a structure are different from the generic ones, and are termed **updated**. The difference arises from the fact that, based on a geometric encounter model, larger and faster moving icebergs are more likely to impact, and the resulting distributions have to be calculated by modifying the generic ones. Details of this procedure, termed Bayesian updating, are given in Section 2.3.1.

2.2.1 Iceberg Population

The iceberg population on the Grand Banks is characterized using the iceberg frequency and the iceberg size distribution.

Iceberg frequency is best expressed in terms of areal density, defined as the average number of icebergs in an area (for example, a degree square) at a given instance of time. It can be likened to a series of snapshots of a specific region containing icebergs, taken throughout a period of time. The areal density would be the number of icebergs counted in the snapshots, averaged over the the year.

Iceberg size is best characterized using the waterline length, L, defined as the maximum extent of the iceberg at the water surface. This dimension is readily measured and extensive data sets have been collected. The iceberg population is divided into two separate populations, bergy bits and growlers which are less than 15 m in length, and all other icebergs having a length greater than 15 m. Icebergs with a length less than 5 m are not included in the analysis since they do not pose any significant threat to offshore structures.

The larger iceberg population is best represented using an exponential distribution with a mean of 59 m (Muggeridge et al. 1998)

$$f_L(l) = \frac{1}{59} \exp\left(-\frac{l}{59}\right), \tag{2.7}$$

where $l \geq 5$ m. Recently, new data has been included in the database, however the resultant distribution remains unchanged. This distribution is supplemented with a population of bergy bits and growlers.

Icebergs less than 15 m in size are harder to detect due to the rounded shape and smaller surface area of the ice pieces. The size distribution of these icebergs is based on data collected by Crocker (1992) and Crocker and Cammaert (1994). The data

are best represented using an exponential distribution with a mean of 2.7 m, and is expressed as

$$f_L(l) = \frac{1}{2.7} \exp\left(-\frac{l}{2.7}\right), \tag{2.8}$$

where $l < 15$ m.

The overall population is the summation of the two individual populations, weighted to achieve the correct proportion of each group. Based on the work of Fuglem et al. (1995), the proportion of icebergs less than 15 m, and the proportion greater than 15 m, has been estimated to be approximately equal to 1. The main conclusion was that for each 'parent' iceberg, there exists one 'offspring' iceberg, namely a bergy bit or growler.

The resulting overall population of icebergs is calculated by combining and renormalizing the two individual distributions, and is given as

$$f_L(l) = 0.24\left[\frac{1}{59}\exp\left(-\frac{l}{59}\right)\right] + 0.76\left[\frac{1}{2.7}\exp\left(-\frac{l}{2.7}\right)\right], \tag{2.9}$$

where 5 m $\leq l \leq$ 400 m. Figure 2.2 shows the two individual waterline length distributions, plus the combined distribution.

Using the measured iceberg size data, several other iceberg dimensions can be estimated in terms of the waterline length.

Iceberg Length-to-Draft

Water depth will influence the size of icebergs capable of entering a region. Icebergs having drafts greater than the water depth will generally scour and come to rest. While these icebergs will melt, calve, or overturn, they are unlikely to contact the structure until the draft is less than the water depth and they are free to move again. Using recorded iceberg dimensions (C-CORE 2001), a best-fit length-to-draft

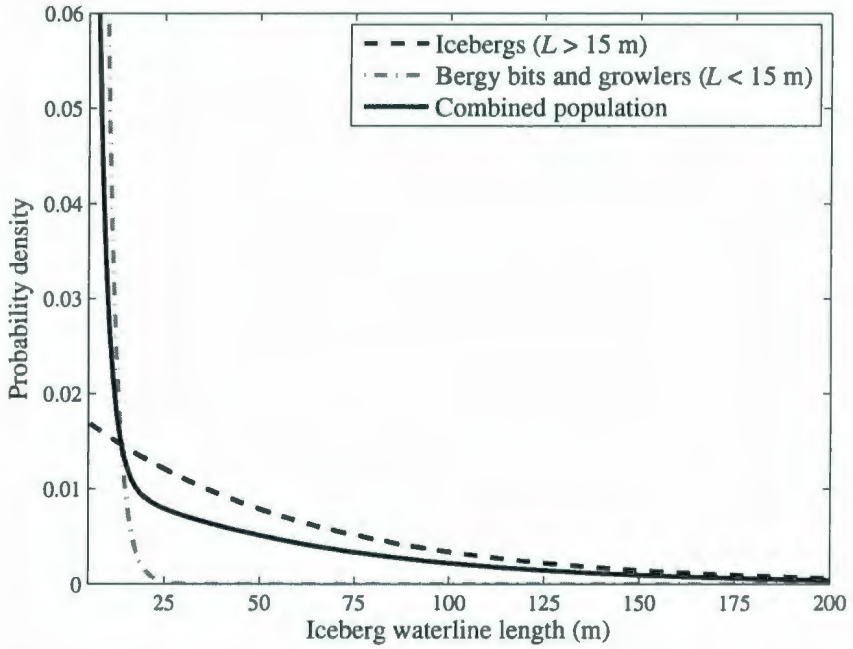

Figure 2.2: Exponential distributions representing the two individual icebergs populations and the combined iceberg waterline length distribution

relationship was determined to be

$$D = 3.14L^{0.68} \exp(e), \tag{2.10}$$

where D is the iceberg draft, L is the waterline length and e is a normally distributed random number with a mean of 0 and a standard deviation of 0.25. The data, best fit curve and the residuals are shown in Figure 2.3.

Iceberg Length-to-Mass

Iceberg mass has been estimated in various studies conducted for the Hibernia and Terra Nova developments. This effort has relied primarily on measurements of the above-water volume. Using recorded iceberg dimensions (C-CORE 2001), a best-fit

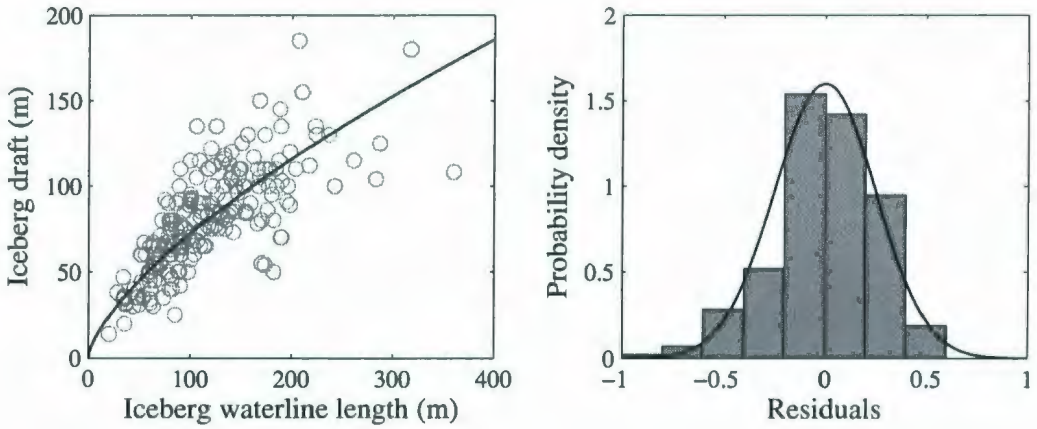

Figure 2.3: Iceberg length-to-draft relationship - data and best fit curve on left and residuals on the right

length-to-mass relationship and is given as

$$M = 1.05L^{2.68} \exp(e), \tag{2.11}$$

where M is the iceberg mass and e is a normally distributed random number with a mean of 0 and a standard deviation of 0.61. The data, best fit curve and the residuals are shown in Figure 2.3.

2.2.2 Metocean Characteristics

The metocean requirements for the iceberg design load methodology are limited to characterization of the sea state. Sea state has a direct impact on iceberg drift and collision speeds as well as the ability to detect and physically manage icebergs. The sea state is best represented using the significant wave height, H_S, defined as the mean height of the highest one third of all waves recorded during a given period.

The iceberg design load methodology uses a significant wave height distribution based on data from the AES40 Wind Hindcast database (Swail et al. 2000). The data

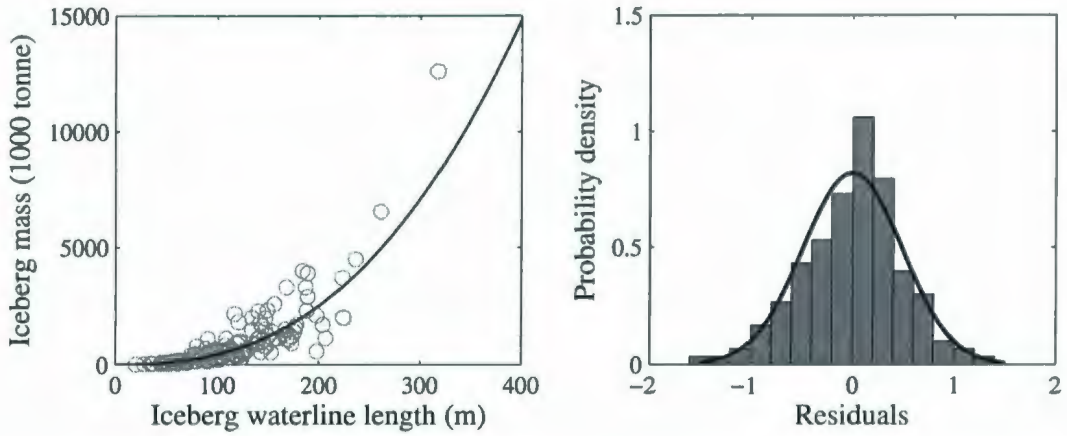

Figure 2.4: Iceberg length-to-mass relationship - data and best fit curve on left and residuals on the right

consists of 41 years of consecutive wind and wave records corresponding to specific gridpoints throughout the north Atlantic Ocean. Data from Gridpoint 5551 (46.25 N, 48.33 W) were chosen to model conditions on the Grand Banks.

Icebergs have a strong seasonal presence, with March to May being typically the months with the most icebergs present. These months also correspond to the months with lower significant wave heights, as shown in Figure 2.5. Given this variation, the significant wave height distribution is weighted according to the presence of icebergs. The annual significant wave height distribution was obtained by weighting the monthly H_S distributions by the monthly iceberg frequencies and averaging it over the entire year. The resultant annual significant wave height distribution is shown in Figure 2.6.

2.2.3 Structural Configuration and Operating Procedures

The structure configuration is defined in terms of coordinate pairs. A GBS is defined in elevation view by defining structure radii at various water depths. An FPSO is defined in plan view by defining a bow and stern outline using $x - y$ coordinates.

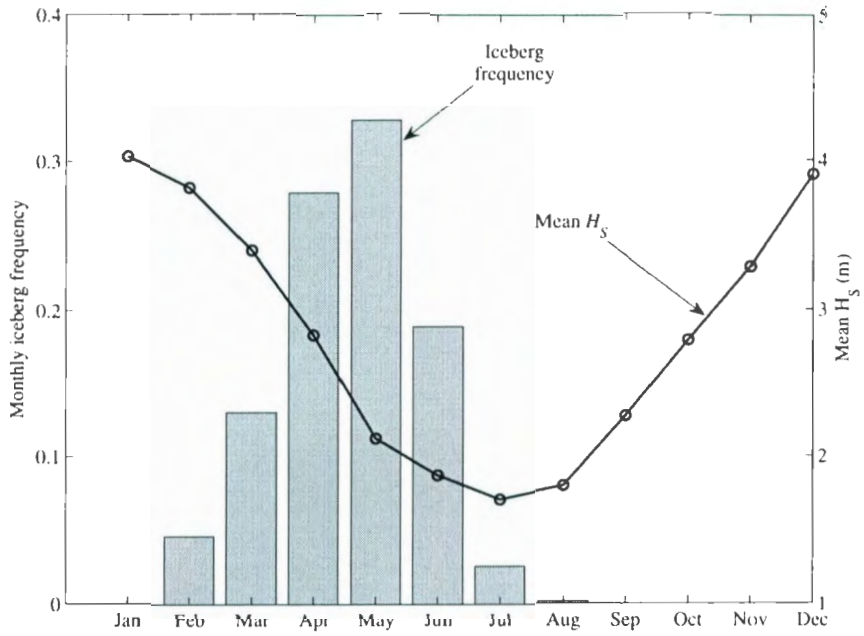

Figure 2.5: Distribution between monthly mean significant wave height and the probability of occurrence of icebergs

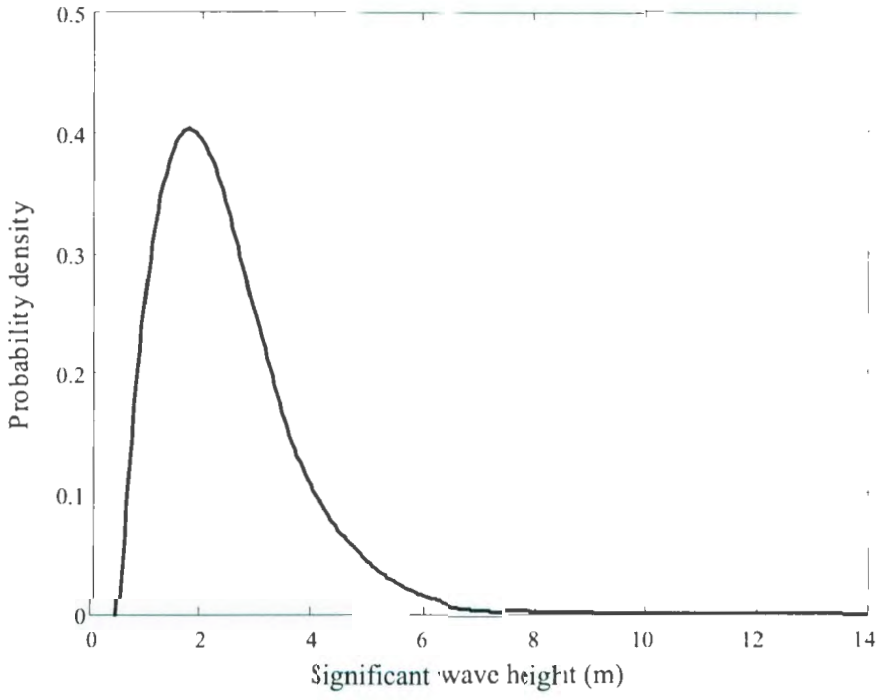

Figure 2.6: Weighted annual significant wave height distribution

Specific operating procedures, such as the time required to disconnect and move offsite are also defined. These inputs are generally reserved for FPSOs and semi-submersibles which have the ability to disconnect.

2.2.4 Iceberg Drift Speed

Modelling iceberg drift speed is a complex process. Icebergs travel in different directions with different speeds depending on the wave and current regimes, the wind speed and direction, and the iceberg shape and size. Many theories and models have been developed in an attempt to model the drift speed process. The majority capture the fundamental trends of the iceberg motions, however, none capture fully the drift speed process.

A deterministic iceberg drift speed model was developed by Fuglem (1997) to model iceberg drift speed as a function of only the iceberg waterline length and the significant wave height. The model is based on a balance of environmental forces acting on the iceberg. The resultant iceberg drift speed is the magnitude of the vector summation of all the environmental forces acting on the iceberg. The model compares well with the limited data set that was available at the time. However with a significant increase in the number of data collected in recent years, it has become apparent that the deterministic model does not capture the randomness in the data. Sensitivity analyses have shown that the iceberg drift speed is an important parameter in the design load methodology. The drift speed is used in the iceberg impact frequency calculation, the kinetic energy calculation, and is a fundamental component of the detection and management models. It is important that the process is captured as accurately as possible.

A detailed description of the deterministic model is given in Chapter 4. The results

of a statistical comparison of the model with observed data is presented in Chapter 5. A new probabilistic model based on observed data is presented in Chapter 6.

2.3 Iceberg Encounter Module

An iceberg encounter model is used to determine the expected annual number of iceberg encounter events (impact frequency) for a given structure configuration. Methods for determining the probability of impacts by ice floes on offshore structures were developed during the 1980s by Jordaan (1983), Dunwoody (1983) and Sanderson (1988).

The encounter model is based on the premise that the probability of impact of an iceberg, of size L and drift speed v_D, traveling through a region equals the ratio of the area swept out during a period of time, Δt, to the area of the entire region. This concept is expanded for GBS and FPSO configurations in the following sections.

The detection and management model uses the same combinations of L and H_S to determine which icebergs would be detected and managed and the probabilities of these events. The probabilities of non-detection and non-management can be deduced from this. Iceberg detection and management is further expanded upon in Section 2.3.3.

2.3.1 GBS Encounters

Consider a structure having a mean diameter, w_s. An approaching iceberg has an effective collision width, w_i, defined as the maximum extent of the iceberg, averaged over all orientations, projected normal to its direction of movement. A single iceberg in a region, A_R, will transit an area equaling $w_i v_D \Delta t$ in a time, Δt as illustrated in Figure 2.7. However, when determining the probability of impact, it is easier to

consider an equivalent system of an iceberg having an extended width of $w_S + w_i$ hitting a point representing the center of the structure. Given that the iceberg is randomly located with respect to the structure, the probability of collision, p_E, during time, Δt, is the probability that the center of the structure is within the new swept out area and given as

$$p_E = \frac{(w_i + w_s)\, v_D \Delta t}{A_R}. \tag{2.12}$$

The expected number of impacts, η_E, equals the probability that an iceberg in area A_R will impact in time Δt, times the sum of the number of time intervals each iceberg is in area A_R. This is given by

$$\eta_E = \frac{1}{A_R} \left[\sum_{\infty}^{i=1} i \cdot p_i \right] N \Delta t \, (w_i + w_s)\, v_D, \tag{2.13}$$

where p_i is the probability of an iceberg being in the region and N is the number of time intervals per year.

The geometric solution for the expected annual number of iceberg encounters is computed as

$$\eta_E = \rho_D \, (w_i + w_s)\, v_D K, \tag{2.14}$$

where ρ_D is the average annual areal density of icebergs and K is the number of seconds per year.

2.3.2 FPSO Encounters

A floating structure may include a ship navigating through a region or a FPSO moored at a specific location. A moored FPSO may have a weathervaning turret which allows it to assume a head-on orientation into the prevailing environmental

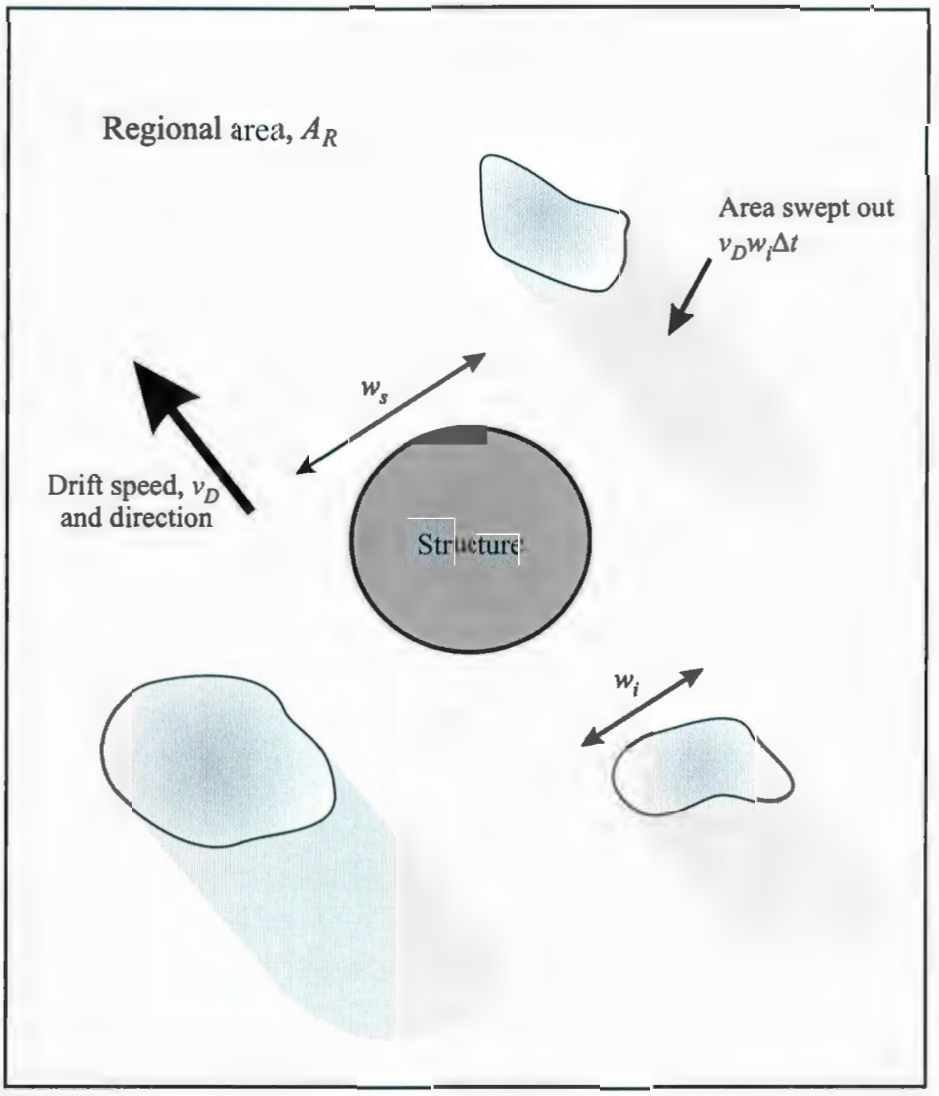

Figure 2.7: Illustration of expected number of iceberg encounters with a GBS

winds and currents which may be at some angle relative to an approaching iceberg.

Consider a vessel of width w_s and having a velocity v_s, and an iceberg with an effective collision width w_i and drift speed v_D, moving at an angle θ_R relative to the heading of the vessel (see Figure 2.8). The relative velocity and direction of the iceberg are denoted v_R and ϕ respectively. The probability that an iceberg will hit a particular section of the ship in time Δt is equal to the probability that the iceberg is within a distance $v_R \Delta t$ in front of the location.

The area from which an iceberg will collide with the side of the vessel is given by

$$A\left(v_i, \phi\right) = l_s v_R \sin\phi \Delta t = l_s v_D \sin\theta_R \Delta t, \tag{2.15}$$

where l_s is the length of the vessel. Assuming that icebergs come from all directions and that their size and velocity distributions are independent, the expected number of collisions in a time period T, is

$$\eta_E = \frac{1}{\pi} \rho_D l_s \overline{v_i} T. \tag{2.16}$$

A similar equation for bow impacts with a slowly moving vessel requires the exact bow shape. However, when the vessel is moving faster than the icebergs, ϕ approaches 180°, and the effective width of the vessel can be taken as w_s. The area from which an iceberg will collide with the bow is given by

$$A = \left(w_s + w_i\right)\left(v_s + v_D \cos\theta_R\right) \Delta t. \tag{2.17}$$

Again, since icebergs are assumed to approach from all directions, the expected

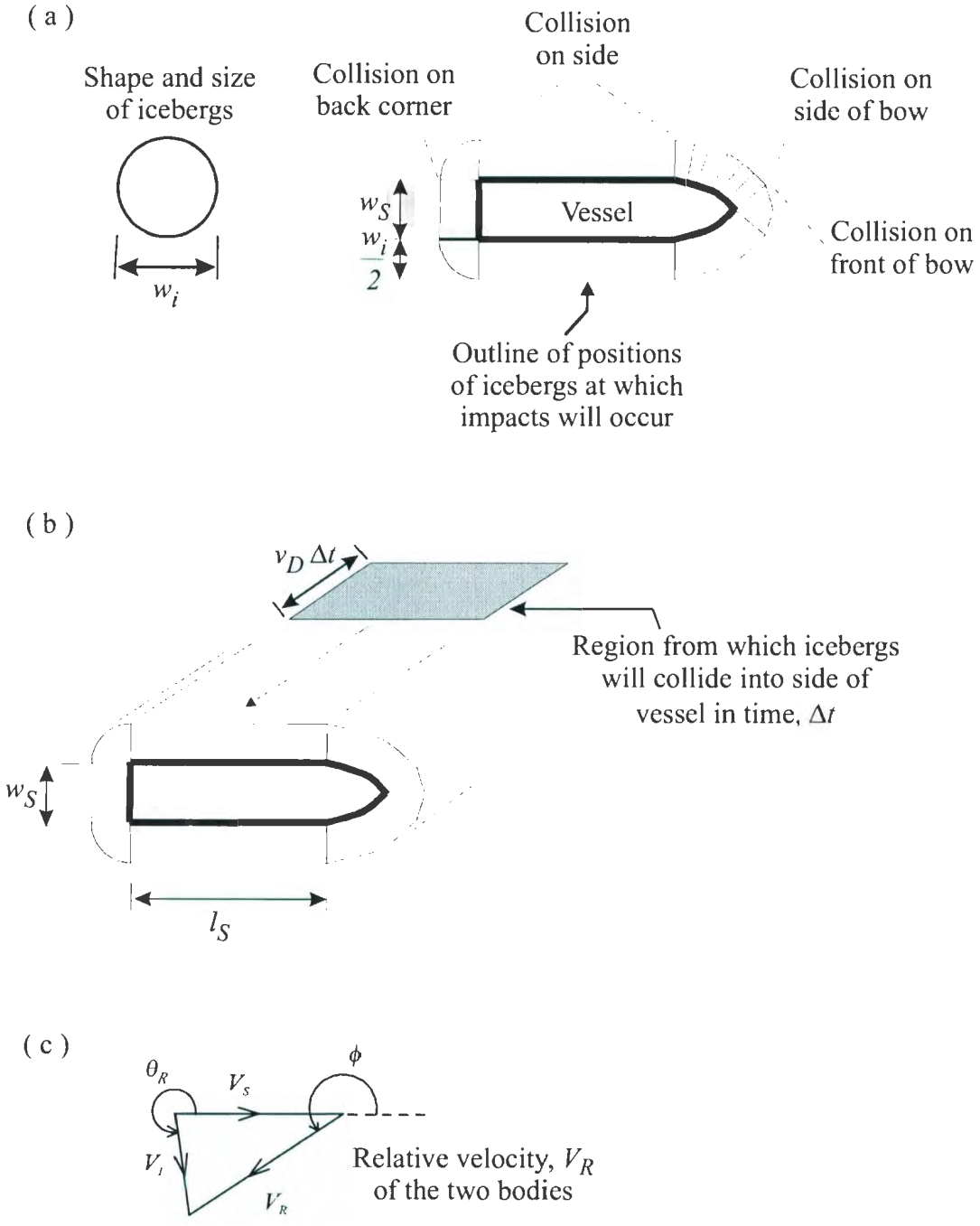

Figure 2.8: Illustration of expected number of iceberg encounters with a FPSO

number of collisions with the bow is given by

$$\eta_E = \rho_D \left(w_s + w_i\right) v_s T = \rho_D \left(w_s + w_i\right) d_s, \tag{2.18}$$

where d_s is the distance traveled. For a turret-moored or dynamically positioned ship, it is assumed that the bow of the vessel faces into the prevailing weather conditions. Also, assuming that this is the direction from which icebergs will be approaching, the expected number of collisions with the bow is given by

$$\eta_E = \rho_D \left(w_s + w_i\right) v_D K, \tag{2.19}$$

where K is the number of seconds per year.

2.3.3 Iceberg Detection and Management

Iceberg detection and management may be employed to mitigate impact risk. For fixed structures, iceberg detection and physical management are used. For floating structures, such as an FPSO, avoidance or disconnection provides an additional level of mitigation. Both iceberg detection and physical management models are based on iceberg size and drift speed, significant wave height, and range from the structure. McKenna et al. (2003) provide an overview of iceberg detection and management strategies.

The influence of iceberg detection and management on the probability of an iceberg impacting an installation is illustrated in Figure 2.9. Of the approaching icebergs, only those remaining undetected and unmanaged pose a risk to the facility. If the facility has the ability to disconnect, such as an FPSO, the risk is from those icebergs that remain undetected, that are detected but cannot be managed or that

are detected, but can not be managed and the structure can not disconnect in time to avoid an impact.

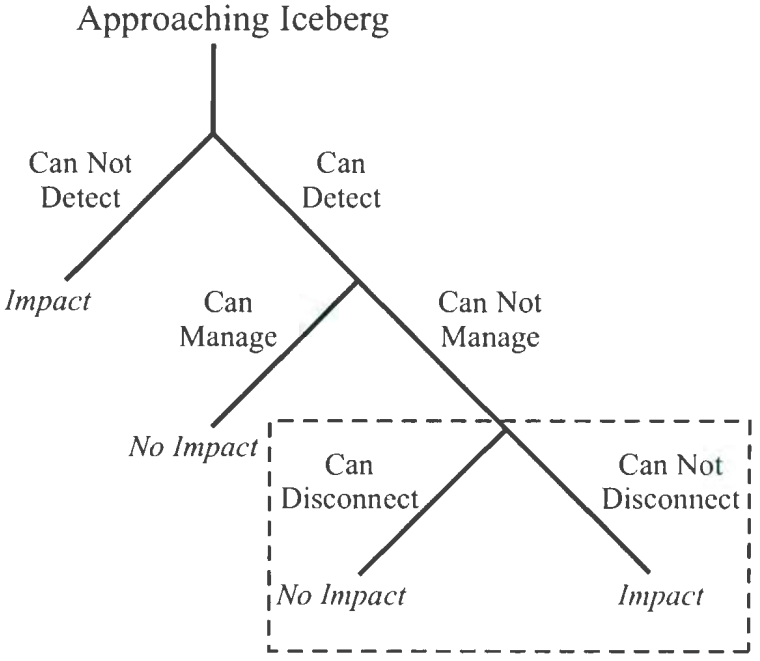

Figure 2.9: Iceberg detection and management decision tree (from McKenna et al. 2003)

Iceberg Detection

Icebergs on the Grand Banks are typically detected and monitored by means of aerial surveillance, supply vessels, marine radar located high on the platforms, HF radar and satellite-based radar. However, for the present study, the structure under consideration is providing the only means of iceberg detection; that is, the marine radar, one of the better sources of information at close range and during higher sea states.

The detection model is primarily a function of the iceberg size, the significant wave height and the range from the structure. The probability of detection, given a specific iceberg waterline length and significant wave height, is based on a model of marine radar performance developed by Johnson and Ryan (1991). Figure 2.10

illustrates the radar performance.

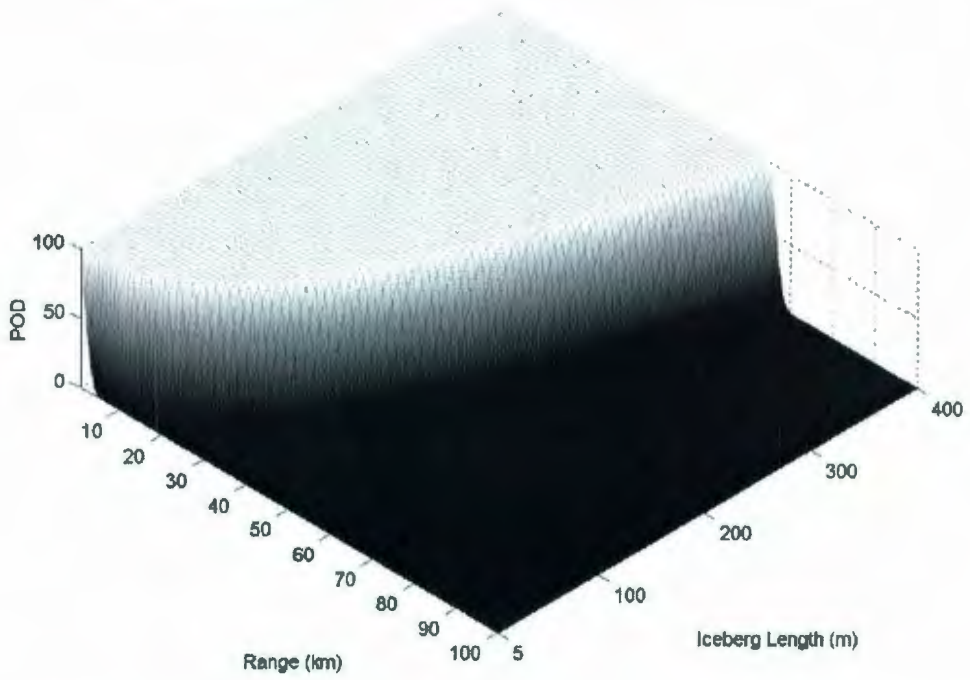

Figure 2.10: Illustration of a marine radar performance model for a 25 m radar height and a significant wave height of 4.5 m

Iceberg Management

The risk of impact due to threatening icebergs may be reduced by utilizing ice management procedures, which range from the use of a water cannon or prop-washing for bergy bits and growlers to towing icebergs using multiple vessels. For the purposes of modelling ice management in the design load methodology, a tow is deemed successful if a change in free drift course was achieved, and the towed iceberg maintained a Course Made good (CMG) with one or multiple attempts.

A two-dimensional probability of tow success matrix is defined as a function of iceberg waterline length and significant wave height. Data from the PERD Comprehensive Ice Management Database (PERD 2003) is used to develop the matrix.

Tow success is based on iceberg towing operations involving a single tow line only. Other towing methods involving the towing net or tow lines, or other methods such as water-cannon and prop-wash, are not considered.

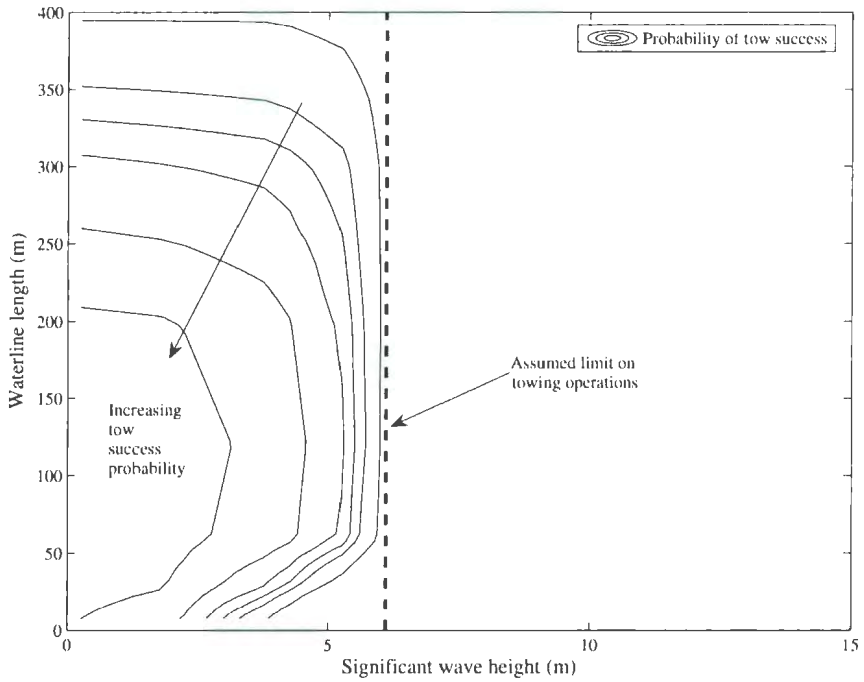

Figure 2.11: Schematic illustration of a typical tow success matrix

Figure 2.11 illustrates a typical tow success matrix for significant wave heights ranging from 0.25 m to 14 m and waterline lengths from 7.5 m to 400 m. The contour lines represent the probability of a successful tow operation for the given iceberg size and significant wave height. Iceberg towing operations are practically limited by the significant wave height. It has been assumed for this work that wave heights greater than 6 m may create hazardous operating conditions on the stern of the supply vessels, and is used as a cutoff for modelling ice management performance. This cutoff depends on the towing vessels used. Newer and larger vessels have improved sea keeping performance in higher sea states, which may lead to an increase in this limit.

FPSO Disconnection

Should efforts to manage an encroaching iceberg fail, an FPSO may disconnect from its riser system. The Terra Nova and Whiterose FPSOs, presently operating on the Grand Banks, were designed for emergency disconnection. A controlled disconnection process, including production shutdown, will take approximately 4 to 8 hours. Emergency disconnection may be achieved in approximately 15 minutes.

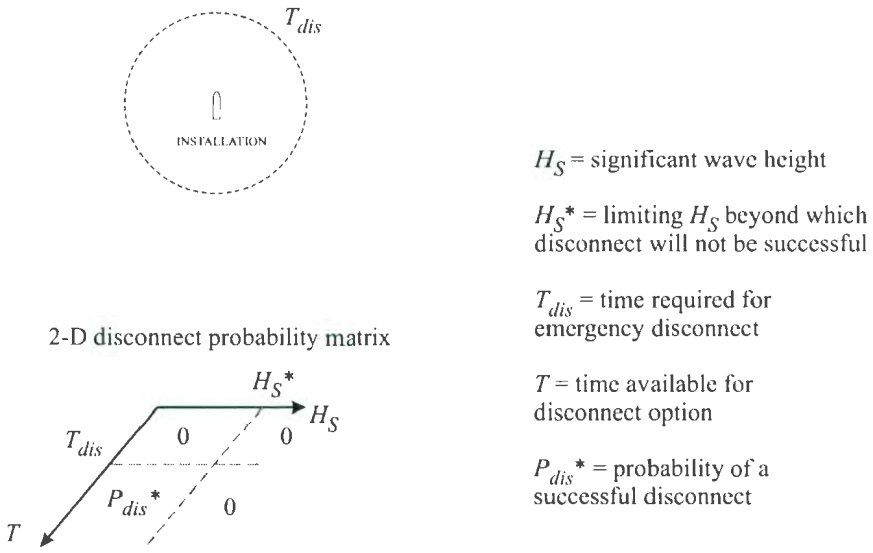

Figure 2.12: FPSO disconnection strategy (from McKenna et al. 2003)

The disconnect strategy is illustrated in Figure 2.12. Factors considered in the disconnect model include:

- the critical significant wave height H_S*, above which disconnection may not be achieved;
- the emergency disconnect time T_{dis}; and
- reduced disconnection success (i.e. disconnection success less than 100 percent) resulting from other operational control features such as mechanical failure,

power failure, etc, such that $P_{dis}{}^{*}$ is the maximum probability of successful disconnect operation.

These variables may be considered specific to each FPSO being analyzed, or each specific location. When FPSO disconnection is considered in the design load methodology, a 98% success rate is typically used.

2.3.4 Updating of Distributions

The iceberg encounter model determines the probability of encounter for the **generic** iceberg population and the environmental conditions for all combinations of L and H_S. The detection and management model uses the same $\{L, H_S\}$ combinations to determine which icebergs will not be detected and those that will be detected but not managed. The matrices are then combined to give the resulting probability of collision for all $\{L, H_S\}$ combinations, for the specified detection and management assumptions.

Following the assumptions made in the iceberg encounter model, the **updated** population of icebergs impacting a structure will be larger and moving faster than the generic iceberg population. Larger icebergs sweep out more area in a given time period due to the increased swath. The faster icebergs sweep out more area during the time period. Similarly, since ice management is a function of iceberg size, the distribution of icebergs that collide will also differ from the generic distribution.

To account for the variation in the impacting or colliding distributions, Bayes' Theorem is adopted which relates the conditional and marginal probability distributions of random variables. Bayes' Theorem is written as

$$P(A_i|B) = \frac{P(B|A_i)\,P(A_i)}{\sum_{j=1}^{n} P(B|A_j)\,P(A_j)}, \tag{2.20}$$

where $P(A_i|B)$ denotes the probability of event A_i conditional on event B. In the case of updating iceberg size distribution, A_i represents a certain combination of iceberg size and sea state, whereas B represents collision between the iceberg and structure. Thus, $P(A_i|B)$ represents the joint probability distribution of the iceberg size and sea state given collision, $P(B|A_i)$ represents the encounter rate for a given iceberg and sea state, $P(A_i)$ is the generic joint probability distribution of iceberg size and sea state. The denominator in Equation 2.20 serves as a normalizing constant to ensure the overall probability equals one.

Bayes' Theorem is used to generate the size distribution of impacting icebergs by updating the generic iceberg length distribution. The iceberg length distribution updated simultaneously with the distribution of the significant wave heights, H_S. By assuming that L and H_S are independent of each other, the generic joint probability distribution of L and H_S, $p_{L,H_S}(l, h_S)$, can be written as

$$p_{L,H_S}(l, h_S) = f_L(l) \times f_{H_S}(h_S), \tag{2.21}$$

where $f_L(l)$ is the generic iceberg length distribution described in Section 2.2.1 and $f_{H_S}(h_S)$ is the significant wave height distribution described in Section 2.2.2. The updated joint probability distribution of L and H_S (including the effects of iceberg detection/management) is written as follows

$$p'_{L,H_S}(l, h_S) = p_{L,H_S}(l, h_S) \times (w_S + L) \times p_{v_D}(L, H_S) \times (1 - p_{DM}(L, H_S)), \tag{2.22}$$

where $p_{v_D}(L, H_S)$ denotes that the iceberg drift speed is a function of

L and H_S and $p_{DM}(L, H_S)$ is the probability of successful iceberg detection/management/disconnection (if applicable). The updated iceberg length distribution is obtained from

$$F_L(l) = \int p'_{L,H_S}(l, h_S)\, dH_S. \tag{2.23}$$

2.4 Iceberg Impact Module

The iceberg impact module consists of three components; data simulation, iceberg hydrodynamics, and ice mechanics. Input variables, such as iceberg waterline length, draft, mass, and drift speed are simulated from the distributions and relationships described in the previous sections. The iceberg impact speed is calculated using components of iceberg drift and wave induced orbital motions. Finally, the impact force is calculated accounting for the relationships between pressure and area, area and penetration, and iceberg rotational effects.

2.4.1 Data Simulation

Using a Monte Carlo simulation approach, a large number of iceberg waterline length and significant wave height data are simulated. Using the waterline length, other iceberg characteristics are estimated, such as the iceberg draft and mass. The iceberg drift speed is calculated using both the waterline length and significant wave height distributions as inputs.

2.4.2 Hydrodynamics Model

The hydrodynamics model consists of the iceberg collision speed and added mass calculations. For the present study, the added mass of the iceberg is assumed to be 50% of the iceberg mass.

Iceberg Collision Speed Model

In a similar manner as described in Section 2.3.4, the iceberg drift speed is updated to give the collision speed. Two assumptions are inherent in the collision speed model. First, only the surge component of the wave-induced motion was included in the iceberg collision velocity. For a cylindrical GBS piercing the water surface, ignoring iceberg heave and pitch has no impact on the design load, as these motions are tangential to the structure surface and do not result in additional contact force under the zero friction assumption adopted in the methodology. Second, the wave induced velocity follows a Gaussian process, with a mean of zero and a variance of σ, the zeroth moment of the open water velocity spectrum.

In order to properly capture the random wave-induced motions for collision velocities, a new method was been developed. Fuglem (1997) enhanced the approach by Lever et al. (1988), in order to consider the forward drift of the iceberg. The wave induced collision speed is approximated using the following "Special Rayleigh" distribution

$$F_{SR} = \frac{s(\sigma)\left[F_R(u-k,\sigma) - F_R(k,\sigma)\right] + k\left[F_N(u-k,0,\sigma) - F_N(-k,0,\sigma)\right]}{s(\sigma)\left[1 - F_R(k,\sigma)\right] + k\left[1 - F_N(-k,0,\sigma)\right]}. \quad (2.24)$$

where s is a normalization constant, F_R is the cumulative Rayleigh distribution, u is the iceberg collision velocity, k is the forward drift speed of the iceberg, σ is the variance of the iceberg surge velocity, and F_N is the cumulative normal distribution.

The full derivation is provided in Fuglem (1997).

2.4.3 Ice Mechanics Model

The iceberg impact model is based on the work of Matskevitch (1996, 1997a, 1997b). The model accounts for the inertial properties of the iceberg during impact. A small angle of rotation assumption is adopted in the model. As well, any secondary impacts with other locations on the iceberg are ignored. The degrees of freedom considered in an iceberg-structure impact include translation in the x direction and rotation about the three principal axes of the iceberg.

2.4.4 Iceberg Rotational Effects

Upon impact, a portion of the initial kinetic energy of the iceberg is converted into rotational energy. This results in less energy available for ice crushing. The effects of iceberg rotation are incorporated through the use of a non-dimensional eccentricity parameter, G.

Consider an iceberg impacting a vertical walled structure, as shown in Figure 2.13. The eccentricities about the three global axes (x, y, z) are

$$\epsilon_x = x_{CP} - x_{CM}, \tag{2.25}$$

$$\epsilon_y = y_{CP} - y_{CM}, \tag{2.26}$$

$$\epsilon_z = z_{CP} - z_{CM}, \tag{2.27}$$

where the subscripts CM and CP denote iceberg center of mass and contact point respectively.

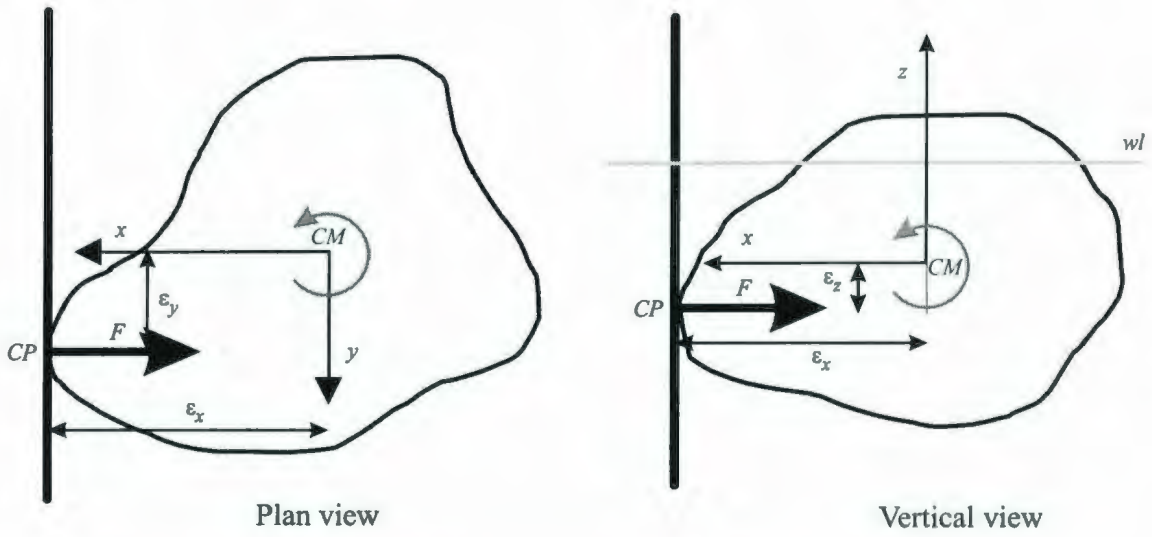

Figure 2.13: Illustration of iceberg contact mechanics and eccentricity

The maximum and minimum moments of inertia for the iceberg are given by

$$\pm I_{max,min} = \frac{I_x + I_y}{2} \pm \sqrt{\left(\frac{I_x - I_y}{2}\right)^2 + I_{xy}^2}, \tag{2.28}$$

and the angle between the maximum and the x-axis is calculated using

$$\beta_0 = \frac{1}{2}\tan^{-1}\left(\frac{-I_{xy}}{I_x - I_y/2}\right). \tag{2.29}$$

The iceberg is assumed to rotate about three principal axes of inertia, l_1, l_2, and l_3. The first two principal axes lie in the xy plane and the third principal axis is assumed to point upwards, as illustrated in Figure 2.14. The three axes can be described using the following unit vectors

$$l_1 = l_{xymax} = [\cos\beta_0 \quad \sin\beta_0 \quad 0], \tag{2.30}$$

$$l_2 = l_{xymax} = [-\sin\beta_0 \quad \cos\beta_0 \quad 0], \tag{2.31}$$

$$l_3 = l_{xymax} = [0 \quad 0 \quad 1]. \tag{2.32}$$

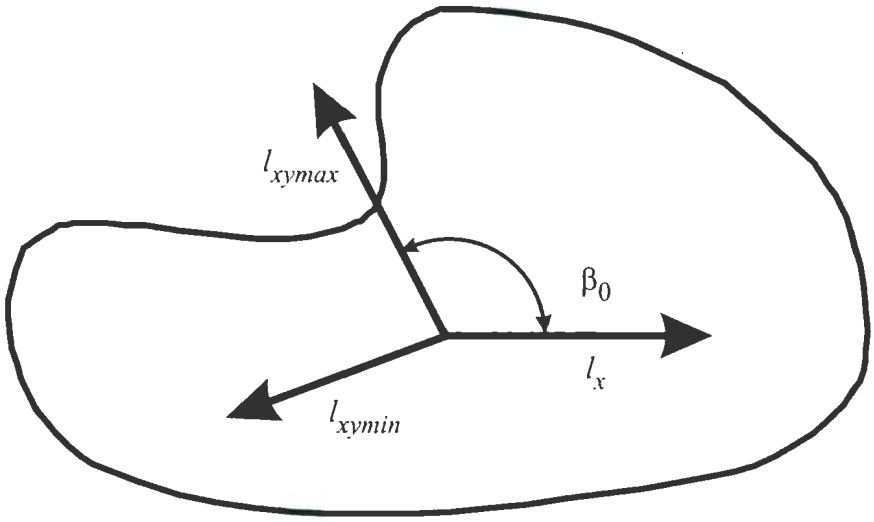

Figure 2.14: Illustration of iceberg principal axes

2.4.5 Iceberg Radius of Gyration

The radius of gyration for the iceberg is calculated as

$$r_{g_i} = \sqrt{\frac{I_i}{\tilde{m}}}, \tag{2.33}$$

where I_i is the inertia about the ith axis and $\tilde{m}$ is the iceberg mass (including added mass).

2.4.6 Eccentricities About the Axes of Inertia

The eccentricities ϵ_i are defined as the shortest distance between the force F and the ith axis of inertia and are calculated as

$$\epsilon_i = k_i \cdot [\epsilon_x \epsilon_y \epsilon_z], \tag{2.34}$$

where

$$k_i = \frac{\mathbf{F} \times l_i}{|\mathbf{F} \times \mathbf{l}|}, \tag{2.35}$$

represents the unit vector normal to the plane containing F and l_i

2.4.7 Equations of Motion

The ice force vector F is assumed to act normal to the surface of the structure. For a flat vertical structure then, the force only acts in the x-direction

$$\mathbf{F} = [F\ 0\ 0]\,. \tag{2.36}$$

Translational and rotational motions are accounted for using the standard equations of motion (translation and rotation, respectively)

$$\ddot{x} = -\frac{F}{\tilde{m}}, \tag{2.37}$$

and

$$\ddot{\theta}_i = \frac{M_i}{I_i} = \frac{(q_i\mathbf{F}) \cdot \epsilon_i}{\tilde{m} \cdot r_{g_i}^2}, \tag{2.38}$$

where F is the impact force acting in the x-direction, M_i is the moment developed about the *ith* axis, q_i is the proportion of force acting perpendicular to the ith axis and is calculated as

$$q_i = \frac{|\mathbf{F} - (F_i)\, l_i|}{|\mathbf{F}|}. \tag{2.39}$$

2.4.8 Penetration

Given the assumption of small angle rotation, the penetration δ normal to the surface may be approximated using

$$\delta = x - \epsilon_1\theta_1 \sin\beta_0 - \epsilon_2\theta_2 \cos\beta_0 - \epsilon_3\theta_3. \tag{2.40}$$

The second derivative of penetration, with respect to time, results in

$$\ddot{\delta} = \ddot{x} - \epsilon_1 \ddot{\theta}_1 \sin\beta_0 - \epsilon_2 \ddot{\theta}_2 \cos\beta_0 - \epsilon_3 \ddot{\theta}_3. \tag{2.41}$$

Substituting Equations (2.37) and (2.38) into equation (2.41) results in

$$\ddot{\delta} = -\frac{F}{\tilde{m}} \left[1 + (\sin\beta_0)\, q_1 \frac{{\epsilon_1}^2}{{r_{g_1}}^2} + (\cos\beta_0)\, q_2 \frac{{\epsilon_2}^2}{{r_{g_2}}^2} + q_3 \frac{{\epsilon_3}^2}{{r_{g_1}}^3} \right], \tag{2.42}$$

or

$$\ddot{\delta} = -\frac{F}{\tilde{m}} G, \tag{2.43}$$

with the non-dimensional eccentricity factor G defined as

$$G = 1 + (\sin\beta_0)\, q_1 \frac{{\epsilon_1}^2}{{r_{g_1}}^2} + (\cos\beta_0)\, q_2 \frac{{\epsilon_2}^2}{{r_{g_2}}^2} + q_3 \frac{{\epsilon_3}^2}{{r_{g_1}}^3}. \tag{2.44}$$

2.4.9 Maximum Impact Force

The maximum impact force occurs at the point of maximum penetration. Substituting equation 2.43 into 2.6, rearranging and multiplying by the penetration velocity $\dot{\delta}$ results in

$$\frac{\tilde{m}\dot{\delta}\ddot{\delta}}{G} = -k\delta^{\gamma}\dot{\delta}. \tag{2.45}$$

Integrating Equation (2.45) with respect to time, from the time of initial contact to the time at which the iceberg comes to a complete rest, t_f, where $\dot{\delta} = 0$, results in

$$\left. \frac{\tilde{m}\dot{\delta}^2}{2G} \right|_{t_0}^{t_f} = \int_0^{\delta_{max}} \left[-k\delta^{\gamma} \right] d\delta. \tag{2.46}$$

The iceberg design load methodology is based on the assumption that the initial kinetic energy of the iceberg must be dissipated through ice crushing or converted to rotational potential energy. Since $\dot{\delta}(0) = \dot{x}(0)$ and $\dot{\delta}(t_f) = 0$, the left side of the equation represents the component of the initial kinetic energy dissipated through crushing and the right hand side represents the amount of crushing work required to reach maximum penetration. Equation (2.46) simplifies to

$$\frac{KE_0}{G} = -\frac{k}{\gamma+1}{\delta_{max}}^{\gamma+1}. \tag{2.47}$$

Solving for the maximum penetration results in

$$\delta_{max} = \left[\frac{KE_0}{G}\frac{\gamma+1}{k}\right]^{\frac{1}{\gamma+1}}. \tag{2.48}$$

Substituting δ_{max} into Equation (2.6) results in

$$F_{max} = k\left[\frac{KE_0}{G}\frac{\gamma+1}{k}\right]^{\frac{\gamma}{\gamma+1}}. \tag{2.49}$$

2.5 Probabilistic Design Loads Module

Iceberg impacts with an offshore structure on the Grand Banks are rare – on the order of 1 impact in 10 years when considering all icebergs. The number of impacts, or arrival rate of icebergs, may be treated as random and modelled using a Poisson process, as described in Jordaan (2005). It can be shown that the extremal distribution corresponding to n = 100, 1000 or 10,000 is given as

$$F_Z(z) = \exp\left\{-\nu\left[1 - F_X(x)\right]\right\}, \tag{2.50}$$

where $F_Z(z)$ is the extreme distribution of impact forces, $F_X(x)$ is the distribution of all impact forces, and ν is the expected number of impacts per year.

2.6 Application of Methodology

The iceberg design load methodology can be used to analyze a variety of structure types, ranging from a fixed GBS type, to a floating vessel capable of disconnecting to avoid an impact. Two typical structures operating in the Jeanne d'Arc Basin, a GBS and a FPSO, are analyzed using the methodology. The output results include global impact forces applicable to the entire structure, and a summary of parameters contributing to the design loads.

2.6.1 GBS Analysis

Consider a GBS located at the center of a degree square in the Jeanne d'Arc Basin. The GBS has diameter of 100 m and extends above the water surface. The water depth is 100 m. Iceberg design loads are estimated using the methodology described in this chapter. The main result or output from the methodology is a distribution of impact forces.

Figure 2.15 shows the exceedence distribution of horizontal impact forces. The dashed line represents the distribution of forces, assuming an impact has occurred, and will be referred to as the per impact distribution. However, iceberg impacts are a rare occurrence. To account for rare the occurrence of iceberg impacts, the probability of exceedence is multiplied by the impact frequency. The result is a vertical shift in the force distribution, as shown by the solid line in Figure 2.15. The 100, 1000, and 10,000-year design loads can be read directly from the figure, as indicated.

Table 2.1 summarizes the results from the GBS analysis. The overall impact force

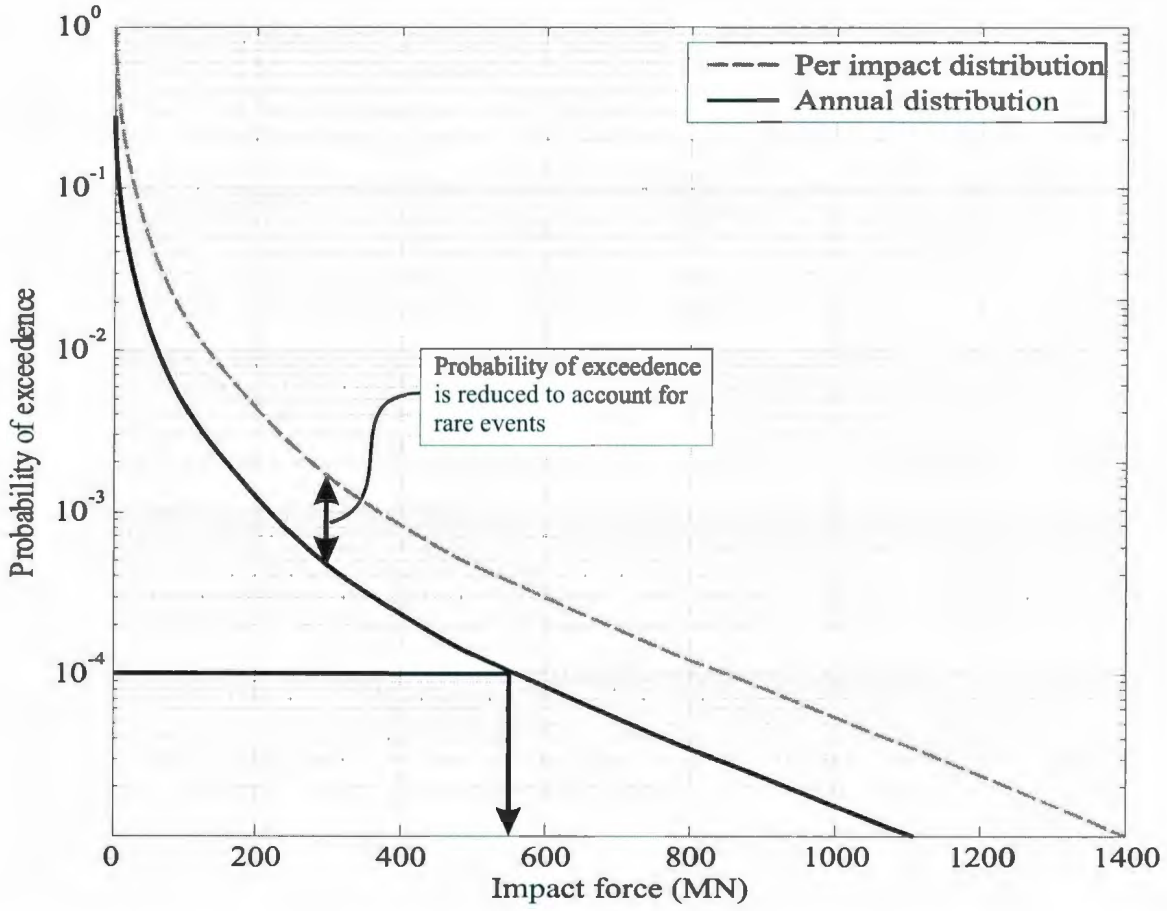

Figure 2.15: Per impact and annual force distributions; no ice management modelled

Table 2.1: Summary of generic GBS results; no ice management modelled

	Exceedence Probability		
	10^{-2}	10^{-3}	10^{-4}
Horizontal impact force (MN)	77	240	552
Overturning moment (GN·m)	6	18	40
Contributing iceberg length (m)	108	135	152
Contributing significant wave height (m)	4.5	5.5	6.0
Contributing iceberg drift speed ($m\,s^{-1}$)	0.68	0.77	0.81
Contributing iceberg collision speed ($m\,s^{-1}$)	0.65	0.77	0.87
Contributing iceberg mass (1000 tonne)	538	1111	1628
Contributing kinetic energy (MJ)	135	417	807

and overturning moment for the 100, 1000, and 10,000-year events are given in the first two rows of the table. A summary of the mean values of the parameters that contribute to the design load is given in the lower portion of the table. Contributing parameters are defined as the mean of the values that correspond to the forces that lie within a ±10% band around the design load.

When ice management is used to mitigate the risk of impact from icebergs, the design load reduces from 552 MN to 496 MN, a reduction of 10%.

2.6.2 FPSO Analysis

Consider a FPSO with a length of 250 m and a width of 40 m. The FPSO is assumed to be able to disconnect, in a controlled manner, and move offsite, if necessary. The FPSO is located at the same location as the GBS in the above example. Iceberg design loads are estimated using the methodology described above.

Table 2.2 summarizes the results of the analysis for the case with no ice management or disconnection options modelled. The 10,000-year design load is 518 MN.

Table 2.2: Summary of generic FPSO results; no ice management modelled

	Exceedence Probability		
	10^{-2}	10^{-3}	10^{-4}
Horizontal impact force (MN)	63	215	518
Contributing iceberg length (m)	107	133	148
Contributing significant wave height (m)	4.4	5.2	6.0
Contributing iceberg drift speed ($m\,s^{-1}$)	0.67	0.74	0.81
Contributing iceberg collision speed ($m\,s^{-1}$)	0.62	0.75	0.88
Contributing iceberg mass (1000 tonne)	520	1040	1487
Contributing kinetic energy (MJ)	126	402	814

Incorporating ice management reduces the 10,000-year design load to 415 MN, a reduction of 20%. The load is further reduced to 105 MN when FPSO disconnection is included in the analysis.

2.7 Review of Drift Speed Modelling

Modelling the drift speed of icebergs requires a knowledge of all the different forces acting on the iceberg. This requires an understanding of the environmental conditions of the regions as well as knowledge of the iceberg characteristics, such as the size and shape. Various types of iceberg drift models have been developed during the past couple of decades. The models range from very basic empirical models when little data is available, to complex dynamic models based on detailed environmental information and iceberg characterization.

Icebergs reaching the Grand Banks usually originate from the glaciers on the eastern side of Greenland. Figure 2.16 illustrates the general current patterns which carry icebergs from the northern regions of Greenland. Icebergs calve from the glaciers and

tend to drift south following the Eastern Greenland Current. The Western Greenland Current then carries the icebergs in a northerly direction, along the western shores of Greenland, into Baffin Bay. The Baffin Island Current then tends to move the icebergs in a southerly direction, along Baffin Island. The Labrador Current continues to carry the icebergs south past the coast of Labrador and down through "Iceberg Alley" until it reaches the Grand Banks. Here the current splits into two parts. The eastern portion carries icebergs close to shore, through the Avalon Channel. The offshore portion carries the icebergs through the Flemish Pass. Icebergs are normally disintegrated before reaching any significant distances south or west of the Grand Banks.

Near the Grand Banks, the south flowing Labrador Current meets the north flowing Gulf Stream, and the ocean current conditions become quite complex. The region is not dominated by a single definite ocean current, however the general drift direction appears to be toward the southeast. With the increased amount of exploration, development and production activities taking place on the Grand Banks, accurate information concerning iceberg drift is required. Estimates using the general drift trends are not sufficient to use in the iceberg design load methodology.

During the past few decades, many authors have published iceberg drift models to predict the different aspects of the iceberg drift process. The models have been developed based on the needs of the authors at the time as well as the available data. These models can be classified into three major categories based on the spatial and temporal scales to which the models apply.

1. *Short term models.* These models can be used to predict iceberg trajectories over periods of up to one day and for distances within close proximity of the structure. The most common application of these types of models is to determine a drift

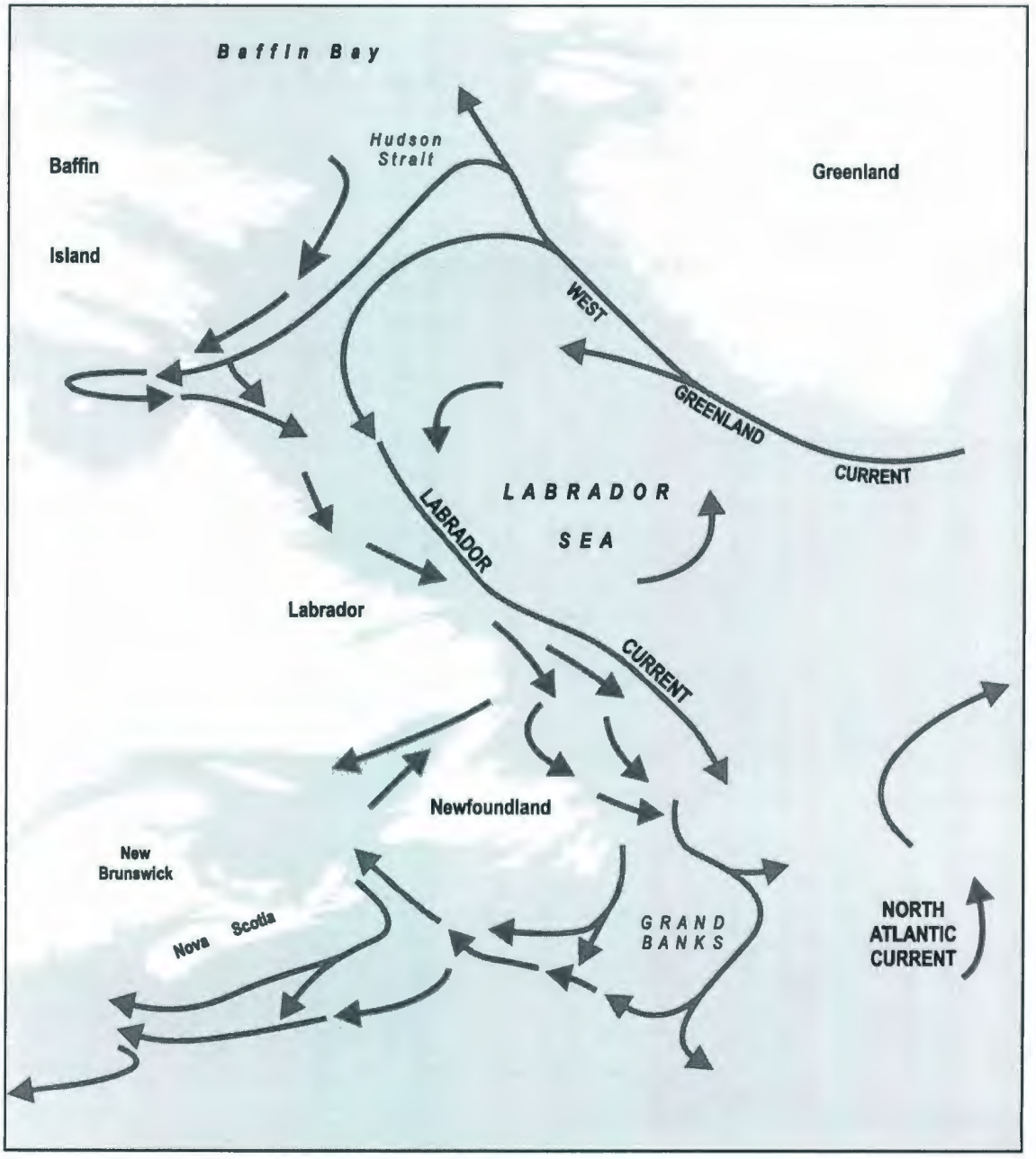

Figure 2.16: Ocean current patterns

speed input for iceberg load estimation, or detection and physical management algorithms.

2. *Intermediate term models.* Intermediate drift speed models are similar to the short term models, however with larger spatial and temporal ranges. These models are used to estimate trajectories for periods of up to 14 days and may cover regions as great as several hundred square kilometers. Iceberg drift models used by the International ice Patrol (IIP) and the Canadian Ice Service (CIS) may be classified as intermediate models.

3. *Long term models.* These models are used to predict iceberg trends over longer periods, on the order of several months to a year. The objectives of long term drift models are to capture the trends regarding the numbers and general locations of icebergs, and not specific trajectories.

The majority of the iceberg drift models can be classified as short term models, with a few intermediate types. The following sections describe some of the iceberg drift models developed during the last couple of decades. In addition, models presently used by the IIP and the CIS are described.

2.7.1 Short Term Drift Models

The main objective of short term iceberg drift models is to predict the drift trajectory of an iceberg within close range of a structure. Depending on the forecast trajectory, physical management procedures, such as towing, may be initiated. In addition, short term models may be used to estimate near instantaneous iceberg drift speeds, which are particularly important in modelling the expected impact force from an iceberg colliding with a structure.

Short term models can be divided into three categories depending on the approach adopted when deriving the model. The simplest type is the *kinematic* drift speed model which bases the iceberg drift speed on basic empirical relationships. The dynamics of the iceberg are not considered. For example, Garrett et al. (1985a) state that the drift speed is approximately 2% of the current speed. *Statistical* models make predictions of iceberg drift speed (and sometimes direction) based on spatial and temporal correlations of present and historical drift data. The results are based on the analysis of data, and generally do not consider any physical processes acting on the iceberg. The drift speed is estimated using empirical relationships derived using data collected from other iceberg tracks. *Dynamical* models follow Newton's equations of motion to determine the new position of the iceberg based on the iceberg mass and all the significant forces acting on the iceberg. Most of the iceberg models in literature are of this type. Both the CIS and the IIP use dynamical drift speed models.

Kinematic Models

Kinematic iceberg drift speed models predict iceberg movement using empirical relationships involving some of the environmental parameters, including wind speed, direction and duration, current speed and direction, as well as iceberg shape and size.

Murray (1969) stated that the IIP estimated iceberg drift as a percentage of the wind speed (knots), $v_d = f v_w$. The coefficient f ranged from 0.0012 to 0.0015, and the iceberg direction was assumed to be 30 degrees to the right of the wind.

Dempster (1974) stated that the drift speed could be estimated using a vector summation of the difference parameters acting on the iceberg, as shown

$$\vec{v} = k_i v_i cos\theta, \tag{2.51}$$

where v_i is the velocity of the ith influence, θ is the phase angle and k_i is an empirical coefficient.

Other authors have presented statistical relationships for iceberg drift speed. Ainslie and Duval (1974) stated that present drift speed was correlated with past drift speed values. Soulis (1976) stated that iceberg drift was correlated with environmental parameters such as wind and current velocities. Garrett et al. (1985a) stated that the iceberg drift speed could be estimated as 1.8 ± 0.7 percent of the wind speed.

Kinematic models can be used to estimate iceberg drift speeds when there is insufficient detailed information available for modelling purposes. However, in the present study, kinematic models do not adequately capture the variation in the drift speed process over the full range of iceberg sizes and significant wave heights.

Statistical Models

Statistical models are generally based on the analysis of a collection of iceberg drift tracks. Spatial and temporal variations in parameters such as the mean and standard deviation of drift speed are the basis for such models. Statistical models do not rely heavily on descriptive physical parameters such as the iceberg shape and size, wind and water drag coefficients and the significant wave height.

One of the early statistical models is described in Intera (1980). In this work a model is described in which predicted iceberg velocities are the summation of historical mean velocities plus weighted residuals from the mean. The weighting algorithm was based on the auto- and cross-correlation coefficients derived using historical data in the region. Poor results were obtained using this approach.

Garrett (1985) took the approach a step further in utilizing historical data and the Gauss-Markov theorem to obtain optimal linear estimates of both iceberg velocity

and position. The future velocity of an iceberg (other than the predictable parts due to wind, mean current flow or tides) is a weighted sum of previous measured velocities. The Garrett model uses a Lagrangian velocity auto-correlation function, based on one predictor, the previous velocity point. Little value was gained in using more than one predictor. However, it was noted that the rapid decay of the cross-correlation function with distance was one limitation to the model. Garrett et al. (1985b) extended the model to two dimensions, increasing performance by including the presence of noise as well as tidal-, inertial- and wind-driven components in the observed velocity data. Given sufficient historical data, optimum (meaning the minimization of the overall iceberg ensemble predictions) iceberg velocity and position predictors can be obtained. However, uncertainty in the iceberg position predictor was still large.

Moore (1985) adopted a multiple time series approach to modelling iceberg drift. The future trajectory of the iceberg was predicted using historical data and an autoregressive integrated moving average (ARIMA) algorithm. ARIMA models are used to model time series data and to predict future points within the series. Random-walk, autoregressive models, and exponential smoothing models are all special cases of ARIMA models. Moore (1985) uses this approach to generate elliptical confidence contours for each predicted iceberg position. Moore states that the approach adequately captures the velocity time series, but he does not provide any comparisons with observed data to support the statement. In subsequent work, Moore (1987) proposed using another ARIMA type model, a double exponential smoothing approach, to predict iceberg displacements. The approach required little computational effort, limited data, and could be updated with the availability of new data. Historical time series data are averaged using an exponentially decreasing weighting function. Forecasts obtained using this approach were shown to be as good as results from the more detailed statistical approaches described above.

In general, statistical models are useful when the required environmental data or physical iceberg characteristics are not available. Limited information may be used to predict iceberg drift speed by estimating drift speed parameters (mean and standard deviation) as functions of other parameters such as iceberg size.

Dynamic Models

Dynamic iceberg drift speed models have been proposed, among others, by Mountain (1980), Sodhi and El-Tahan (1980) and Smith and Banke (1981). The environmental forces considered by these models included the Coriolis force, water and air drag forces and geostrophic current forces. The wave drift force was omitted in the early drift models. However, Isaacson (1988) shows that wave drift force may be significant, and later models have included it.

Dynamic iceberg drift models are based on Newton's Second Law of Motion, stated as: "The rate of change of momentum of a body is proportional to the resultant force acting on the body and is in the same direction." Both the IIP and the CIS have developed iceberg drift models using a dynamic approach. Some of the common features and differences between the two models are discussed in the following sections.

IIP Drift Model

The IIP have incorporated an iceberg drift model as part of daily operations. All relevant information pertaining to icebergs observed by, and reported to, the IIP are entered into the drift model. The model has two primary purposes. It is used to estimate the future position of the iceberg, which provides an estimate of the iceberg location if it is not spotted on subsequent flights. The model is also used to determine if a observed iceberg was sighted during a previous flight or if it is a new observation.

The IIP drift model is based on the model developed by Mountain (1980), which

was derived by balancing forces acting on the iceberg. These forces include water and air drag forces, a Coriolis term, and a sea slope term. The effects of wave drift on the iceberg and the added mass are not included. The equation of motion for the IIP model is given as

$$M\ \vec{a}=\vec{F_A}+\vec{F_W}+\vec{F_C}+\vec{F_P}, \tag{2.52}$$

where M is the mass of the iceberg, $\vec{a}$ is the acceleration, $\vec{F_A}$ is the air drag force, $\vec{F_W}$ is the water drag force, $\vec{F_C}$ is the Coriolis force, $\vec{F_P}$ is the pressure gradient force.

The air drag force $\vec{F_A}$ is calculated using the standard drag equation, defined as

$$\vec{F_A}=\frac{1}{2}C_a\rho_A A_A U_A^2, \tag{2.53}$$

where C_a is the air drag coefficient, ρ_A is the density of air, A_A is the above water projected area of the iceberg sail (above water portion) and U_A is the velocity of the air relative to the iceberg.

Similarly, the water drag force $\vec{F_W}$ is calculated as

$$\vec{F_W}=\frac{1}{2}C_w\rho_W A_B {U_W}^2, \tag{2.54}$$

where C_w is the drag coefficient, ρ_W is the density water, A_B is the cross sectional area of the iceberg keel (below water portion) and U_W is the velocity of the water relative to the iceberg. Given that the water velocity varies with depth, the water drag expression should be integrated over the draft of the iceberg. This approach is approximated by dividing the iceberg draft into four layers. The water velocity for each layer is approximated as the sum of the geostrophic current which is considered to be constant with depth, and the time dependent Ekman current. This approach provides for variation in the water drag for icebergs with different shapes and sizes.

In 1981, an addition was made to the model to allow the mean current field to be modified by real time satellite tracked drifter data (IIP 2007).

The Coriolis effect may be defined as the apparent deflection of an object from its path in a rotating coordinate system. The Coriolis force, $\vec{F_C}$, is given as

$$\vec{F_C} = 2m\Omega \left(\hat{k} \times \vec{u}\right) \sin\phi, \tag{2.55}$$

where m is the iceberg mass, $\Omega = 7.27 \times 10^{-5}$ rad/s, $\hat{k}$ is a vertical unit vector, u is the velocity of the iceberg relative to the water and ϕ is the latitude.

The pressure gradient force $\vec{F_P}$ is determined using the following expression

$$\vec{F_p} = m \left(\frac{d\,\vec{V_{mw}}}{dt} + \vec{f} \times \vec{V_{mw}} \right), \tag{2.56}$$

where $\vec{V_{mw}}$ is the mean current velocity, and $\vec{f}$ is the Coriolis parameter.

CIS Drift Model

The CIS has developed an iceberg drift and deterioration model which is documented in Savage (1999), Sayed (2000) and Carrieres et al. (2001). The deterioration is modelled using thermal processes and calving, with details given in Savage (2001). The drift component of the model is based on the work of Smith and Banke (1981), El-Tahan et al. (1983) and Eigg et al. (1997). Several enhancements and new features are also incorporated into the model. One of the significant features is an improved environmental forcing algorithm and associated inputs. The model relies on input from the Community Ice Ocean Model (CIOM), which is an implementation of the Princeton Ocean Model (Mellor 1997). The CIOM provides predicted ocean currents at 16 sigma depths, which are then in turn interpolated to 10 m layers. The governing

equation of motion for the CIS drift model is given as

$$m\left(\frac{d\vec{V}}{dt}+\vec{f}\times\vec{V}\right)=\vec{F_A}+\vec{F_W}+\vec{F_R}+\vec{F_P}+\vec{F_{am}}, \tag{2.57}$$

where $\vec{V}$ is the iceberg velocity.

The air drag force is calculated using the same format as in the IIP model (Equation (2.53)). However, since the iceberg velocity is usually much smaller than the wind velocity, the relative velocity U_A is replaced with the wind velocity (Kubat and Sayed 2005).

The water drag force $\vec{F_w}$ is estimated using

$$\vec{F_w}=\frac{1}{2}\rho_W C_w \sum_k A_w(k)\left|\vec{u_w}(k)-\vec{V}\right|\left(\vec{u_w}(k)-\vec{V}\right), \tag{2.58}$$

where ρ_W is the density of water and C_w is the water drag coefficient, and A_W is the cross-sectional area of each layer. The draft of the iceberg is divided into 10 m layers, as suggested by Smith and Donaldson (1987). The current velocity at each layer is $\vec{u_w}(k)$. This is an improvement on the IIP model which uses four unequal layers to represent the iceberg keel.

The wave radiation stress force $\vec{F_R}$ is given as

$$\vec{F_R}=\frac{1}{2}\rho_W C_{wf} g L a^2\left|\vec{u_a}\right|\vec{u_a}, \tag{2.59}$$

where C_{wf} is the wave drift coefficient, g is the acceleration due to gravity, L is the iceberg waterline length, a is the wave amplitude, and $\vec{u_a}$ is the wind velocity.

Previous models, such as Smith and Banke (1981), have assumed the ocean is in

steady, geostrophic equilibrium, and that the pressure gradient force $\vec{F_P}$ is proportional to $fk \times V_w$. Bigg et al. (1997) have shown that the pressure gradient force $\vec{F_p}$ is better defined as

$$\vec{F_p} = m \left(\frac{d\,\vec{V_{mw}}}{dt} + \vec{f} \times \vec{V_{mw}} \right), \tag{2.60}$$

where $\vec{V_{mw}}$ is the mean current velocity, and $\vec{f}$ is the Coriolis parameter.

The CIS model takes into account the added mass of the iceberg. This is incorporated throughout the model as $m = (m + m_{am})$.

Chapter 3

Dimensional Analysis of Iceberg Drift Speed

3.1 Introduction

Sometimes it is difficult to obtain complete solutions to engineering problems. Some problems contain a large number of variables and calculations may become too long to solve by hand or even by computer. Other times, there is just not enough information known to determine a complete solution. In cases like this, partial solutions may provide enough information to resolve the problem. One method of obtaining partial solutions is through the use of dimensional analysis.

Dimensional analysis involves studying the dimensions of each variable involved in the problem and combining them to form new parameters. The new parameters all have the same dimensions (normally zero dimension or dimensionless). By combining the variables, any extra or redundant variables are removed and the problem is simplified. The result of dimensional analysis is a set of non-dimensional terms which may be used as building blocks for experimental work.

Fourier's principle of dimensional homogeneity forms the basis of dimensional analysis. Fourier stated that each and every term of an equation must have the same dimensions. Since Fourier, many other mathematicians have developed methods to solve partial analysis problems. Amongst the first were Buckingham (1914) and Rayleigh (1915).

In this chapter, the theory of dimensional analysis is applied to the drift speed of icebergs on the Grand Banks. Several dimensional analysis methods are introduced briefly. The matrix method is explained in detailed and is applied to the drift speed problem. Results are then compared with the deterministic drift speed model described in Chapter 4.

3.2 Methods of Dimensional Analysis

Buckingham (1914) was the first to develop a rule regarding the number of dimensionless parameters required properly to represent a phenomenon. Buckingham's Law states that for a problem with m variables, involving n dimensions, the correct solution to the partial analysis would involve $(m-n)$ parameters. Buckingham called these dimensionless terms π-terms. Buckingham also developed a method in which each π-term could be developed based upon $(m-n)$ repeating variables. Repeating variables are chosen such that the set of all repeating variables contains all the relevant dimensions to the problem. Each remaining variable is then combined with the set of repeating variables in such a manner that the result is a new dimensionless parameter.

Lord Rayleigh (1915) developed an approach to solving dimensional analysis problems using three steps. The first step involved developing a functional equation describing the phenomenon in question. Each dimension must be included in the equation. The next step was to expand the functional equation into the 'fundamental' dimensions of each variable. The final step involved equating the exponents of each dimension, resulting in dimensionless parameters.

There are several other methods which may be applied to dimensional analysis. They include the matrix method, the method of governing equations, and the method of synthesis.

3.2.1 Matrix Method

The matrix method, first introduced by Barr (1985) and later refined by Sharp and Moore (1988), is a very powerful method for determining the non-dimensional terms associated with a particular phenomenon. It is especially powerful when there is a large number of variables involved. The steps involved are straight forward and mechanical in nature. However, the user has limited flexibility in guiding the solution when choosing the repeating variables. The following steps outline the procedure followed when using the matrix method.

1. Formulate the dimensional matrix. This is a matrix in which the column headings are the variables involved in the problem and the row headings are the basic dimensions (i.e. length, mass time). Each matrix entry represents the exponent of the dimension for that particular variable.

2. Determine the rank, m, of the dimensional matrix. The rank is calculated as the number of variables required to completely describe the problem. The number of basic dimensions required to completely describe the problem is given by n.

The number of π-terms, k, required to completely describe the problem is then given by $k = n - m$.

3. Choose the repeating variables for the calculations. The repeating variables must contain all of the dimensions involved in the problem and should be chosen from the set of governing (or independent) variables.

4. Divide the dimensional matrix into two submatrices, A_1 and A_2. A_1 is an $m \times m$ matrix containing the dimensions of the repeating variables. A_2 is the remaining portion of the dimensional matrix.

5. Solve the equation $B = A_1^{-1} A_2$.

6. Form the solution matrix by combining an $m \times m$ identity matrix and B. Extract the k π-terms from the resulting matrix.

3.3 Formulation of Functional Equation

The first step of any dimensional analysis problem is to select the variables to include in the analysis. There is no set of rules or guidelines for this procedure. However, a complete understanding of the phenomenon will greatly assist in the matter.

The variables involved in the drift speed of icebergs can be divided into five categories:

- the geometric properties of the iceberg,
- the physical properties of the iceberg,
- the physical properties of the sea water,
- the environmental conditions, and

- the location of the iceberg.

The geometric properties of the iceberg include variables such as the shape and size of the iceberg. An iceberg with a large waterline length will be affected by wind and currents in a different manner than an iceberg with a smaller waterline length. Variables in this category include the iceberg waterline length L, iceberg draft D, and sail height H_I. The above (A_A) and below (A_B) water projected areas are also important since these are directly proportional to the environmental driving forces. Iceberg shape is another important factor. Icebergs can be classified into different shape categories which include: blocky icebergs, tabular icebergs, domed icebergs, and dry-docked icebergs. A qualitative variable, IS, will be assigned to the iceberg shape.

The second category of factors include the physical properties of the iceberg. The mass and the density of the iceberg are two important variables, and are included in the list.

The third category includes the physical properties of the ocean. The viscosity and the density of the water may play a role in the drift speed model. The viscosity of the water may be omitted from the analysis since the viscous effects are considered negligible in this problem.

The fourth category consists of the environmental conditions. Factors such as the wind speed, the wave height, the current speed must be considered. The acceleration due to gravity must be considered since it affects currents and waves.

The last category contains factors concerning the location of the iceberg. The latitude and longitude, and the water depth must be considered. Since this study is concerned with icebergs on the Grand Banks, the latitude and longitude will remain relatively constant for the Grand Banks area, and can be removed from the analysis.

Table 3.1 lists all the relevant variables and dimensions. The total number of variables required to completely describe the drift speed problem is $m = 14$. These variables contain three dimensions ($n = 3$); length $\mathbf{L}$, mass $\mathbf{M}$, and time $\mathbf{T}$. Therefore, the number of dimensionless parameters required to completely describe the problem is $m - n = 11$.

Table 3.1: List of variables applicable to iceberg drift speed modelling

Variable	Dimensions
Iceberg waterline length, L	$[\mathbf{L}]$
Iceberg height, H	$[\mathbf{L}]$
Iceberg draft, D	$[\mathbf{L}]$
Iceberg above water projected area, A_A	$[\mathbf{L}^2]$
Iceberg below water projected area, A_B	$[\mathbf{L}^2]$
Iceberg shape number, IS	[-]
Iceberg mass, M	$[\mathbf{M}]$
Density of ice, ρ_I	$[\mathbf{L}^{-3}\mathbf{M}]$
Density of water, ρ_W	$[\mathbf{L}^{-3}\mathbf{M}]$
Wind speed, U_W	$[\mathbf{L}\mathbf{T}^{-1}]$
Current speed, U_C	$[\mathbf{L}\mathbf{T}^{-1}]$
Significant wave height, H_S	$[\mathbf{L}]$
Water depth, W_D	$[\mathbf{L}]$
Gravitational acceleration , g	$[\mathbf{L}\mathbf{T}^{-2}]$

Using the variables listed in Table 3.1, the following functional equation can be created

$$v_D = (L, H, D, A_A, A_B, IS, M, \rho_I, \rho_W, U_W, U_C, H_S, W_D, g)\,. \tag{3.1}$$

Equation 3.1 can be rewritten with the dependent variable, v_D, placed inside the

functional, as shown

$$\phi\left(v_D, L, H, D, A_A, A_B, M, \rho_I, \rho_W, U_W, U_C, H_S, W_D, g\right). \tag{3.2}$$

Repeating variables are chosen from the entire set of variables such that the set of repeating variables contains all the dimensions involved in the problem. Choosing the variables L, M and g meets this requirement.

The dimensional matrix is constructed using the variables in Equation 3.2. Each entry in the matrix contains the exponent for the dimensions (row) of each variable (column). The resulting dimensional matrix is shown in Table 3.2).

Table 3.2: Tabulated dimensions of variables included in the analysis

	L	M	g	V_D	H	D	A_A	A_B	IS	ρ_I	ρ_W	U_W	U_C	H_S	W_D
L	1	0	1	1	1	1	2	2	0	-3	-3	1	1	1	1
M	0	1	0	0	0	0	0	0	0	1	1	0	0	0	0
T	0	0	-2	-1	0	0	0	0	0	0	0	-1	-1	0	0

The dimensional matrix is then divided into two sub-matrices A_1 and A_2 as shown. The first matrix A_1 is a $m \times m$ matrix containing the dimension exponents for each repeating variable

$$A_1 = \begin{vmatrix} 1 & 0 & 1 \\ 0 & 1 & 0 \\ 0 & 0 & -2 \end{vmatrix}. \tag{3.3}$$

The second matrix A_2 contains the exponent for the remaining variables.

$$A_2 = \begin{vmatrix} 1 & 1 & 1 & 2 & 2 & 0 & -3 & -3 & 1 & 1 & 1 & 1 \\ 0 & 0 & 0 & 0 & 0 & 0 & 1 & 1 & 0 & 0 & 0 & 0 \\ -1 & 0 & 0 & 0 & 0 & 0 & 0 & 0 & -1 & -1 & 0 & 0 \end{vmatrix}. \tag{3.4}$$

Solving the equation $B = A_1^{-1}A_2$ results in

$$D = \begin{vmatrix} 0.5 & 1 & 1 & 2 & 2 & 0 & -3 & -3 & 0.5 & 0.5 & 1 & 1 \\ 0 & 0 & 0 & 0 & 0 & 0 & 1 & 1 & 0 & 0 & 0 & 0 \\ 0.5 & 0 & 0 & 0 & 0 & 0 & 0 & 0 & 0.5 & 0.5 & 0 & 0 \end{vmatrix} \tag{3.5}$$

The final solution is formed by combining an $m \times m$ identity matrix with B. The result is shown in tabulated in Table 3.3:

Table 3.3: Tabulated solution

	L	M	g	V_D	H	D	A_A	A_B	IS	ρ_I	ρ_W	U_W	U_C	H_S	W_D
L	1	0	0	0.5	1	1	2	2	0	-3	-3	0.5	0.5	1	1
M	0	1	0	0	0	0	0	0	0	1	1	0	0	0	0
g	0	0	1	0.5	0	0	0	0	0	0	0	0.5	0.5	0	0

The π-terms are formed by combining each of the variables starting with column four with the repeating variables (columns one to three). For example, the first π-term is formed using the variables v_D, L, M and g. The numerator is the variable at the top of the column, v_D. The denominator is formed using the three repeating variables and the associated exponents in the matrix, $L^{0.5} \times M^0 \times g^{0.5} = \sqrt{gL}$. Repeating this procedure for each of the remaining variables (columns 4 through to 14) results in the following parameters

$$\begin{aligned} &\pi_1 = \tfrac{v_D}{\sqrt{gL}}, \quad \pi_2 = \tfrac{H}{L}, \quad \pi_3 = \tfrac{D}{L}, \quad \pi_4 = \tfrac{A_A}{L^2}, \\ &\pi_5 = \tfrac{A_B}{L^2}, \quad \pi_6 = IS, \quad \pi_7 = \tfrac{\rho_I L^3}{M}, \quad \pi_8 = \tfrac{\rho_W L^3}{M}, \\ &\pi_9 = \tfrac{U_W}{\sqrt{gL}}, \quad \pi_{10} = \tfrac{U_C}{\sqrt{gL}}, \quad \pi_{11} = \tfrac{H_S}{L}, and \quad \pi_{12} = \tfrac{W_D}{L}. \end{aligned} \tag{3.6}$$

The π-terms can be rearranged to form the following functional equation which can

be used to model the drift speed of icebergs on the Grand Banks

$$v_D\sqrt{gL} = \phi\left(\frac{H}{L}, \frac{D}{L}, \frac{A_A}{L^2}, \frac{A_B}{L^2}, IS, \frac{\rho_I L^3}{M}, \frac{\rho_W L^3}{M}, \frac{U_W}{\sqrt{gL}}, \frac{U_C}{\sqrt{gL}}, \frac{H_S}{L}, \frac{W_D}{L}\right). \quad (3.7)$$

3.4 Discussion of Dimensional Analysis Results

The results shown in Equation 3.7 show the dimensionless parameters required to properly model the iceberg drift speed phenomenon. These twelve π-terms can be grouped into 3 categories.

The first category of π-terms relates to physical models. If a model iceberg were to be constructed and tested in a wave tank, geometric similarity must exist between the model iceberg and the real iceberg. All dimensions must be scaled accordingly. The parameters π_2, π_3, π_4, and π_5, ensure that geometric similarity is achieved between the model and the actual iceberg. The parameters, π_{11} and π_{12}, ensure that there is geometric similarity between the iceberg and its surroundings.

The second category of parameters deal with gravitational forces. Gravitational forces play a large role in iceberg drift. The Froude number, a ratio between the inertial forces and the gravitational forces, must be present and remain constant. In this case, the Froude number is directly given by parameters, π_1, π_9, and π_{10}.

The final category includes the remaining π-terms. The first, π_6, is a qualitative variable describing the iceberg shape characteristics. The variable may be an integer value from 1 to k, where k is the number of different iceberg shapes. The parameters, π_7 and π_8, is a ratio between the volume/density of the iceberg (or water) and its mass.

The iceberg drift speed model is compatible with the results from the dimensional analysis. Several of the π-terms formulated above are directly or indirectly found

in the deterministic model. The parameter, π_{11} is the building block of the entire analytical model. The model is set up as a function of L and H_S, only. All other variables have been determined to be functions of these two variables.

Chapter 4

Deterministic Iceberg Drift Speed Model

4.1 Introduction

The iceberg drift speed model is a fundamental component of the design load methodology. The model is based on a balance of environmental forces acting on an iceberg in a steady state environment (Fuglem 1997). The physical properties of the iceberg are represented by the iceberg waterline length, L. The environmental conditions are modelled as a function of the significant wave height, H_S. All other variables are modelled as functions of either L, H_S, or both L and H_S. The model is deterministic in nature. Given a specific iceberg waterline length and significant wave height, the model will always return the same iceberg drift speed.

The present chapter reviews the approach of the deterministic drift speed model. Formulations for the wind and water drag forces, the wave drift force and the current forces are described in detail. The summation of vectors and the resulting drift speed are explained as well. A comparison between observed and modelled data is presented.

4.2 Model Components

Since the environmental conditions change relatively slowly, the iceberg is considered to be moving at or near the equilibrium speed. Therefore, the external forces are assumed to be in equilibrium and the inertial forces are ignored. Coriolis forces and pressure gradients are not included in the model.

The external forces in the present model include the wind drag, the water drag, the wave drift, and the local current drag forces. Figure 4.1 illustrates the forces acting on the iceberg. The wind will create a drag force on the iceberg acting in the direction of the wind. Waves will cause diffraction and result in a wave force acting in the direction of the waves. Local currents will also influence iceberg motion. In addition to these forces, there will be a water drag force acting against the forward motion of the iceberg.

The wind drag and the wave drift forces are calculated using standard fluid drag equations. The velocity of the iceberg relative to the local current is then determined such that the water drag force is in equilibrium with the wind drag and wave drift forces. The drift velocity is then calculated using a vector summation of the remaining velocity components. Only the speed component (i.e. the magnitude of the drift velocity vector) is required for the design load methodology.

4.2.1 Local Current Forces

An estimate of local current force is required for the drift speed model. The approach is to model the current as a function of the local winds. This approach is suitable because the wind speed is readily calculated as a function of the significant wave height. In addition, the local wind generated current component dominates iceberg drift during storm conditions. An estimate of the local wind generated current was

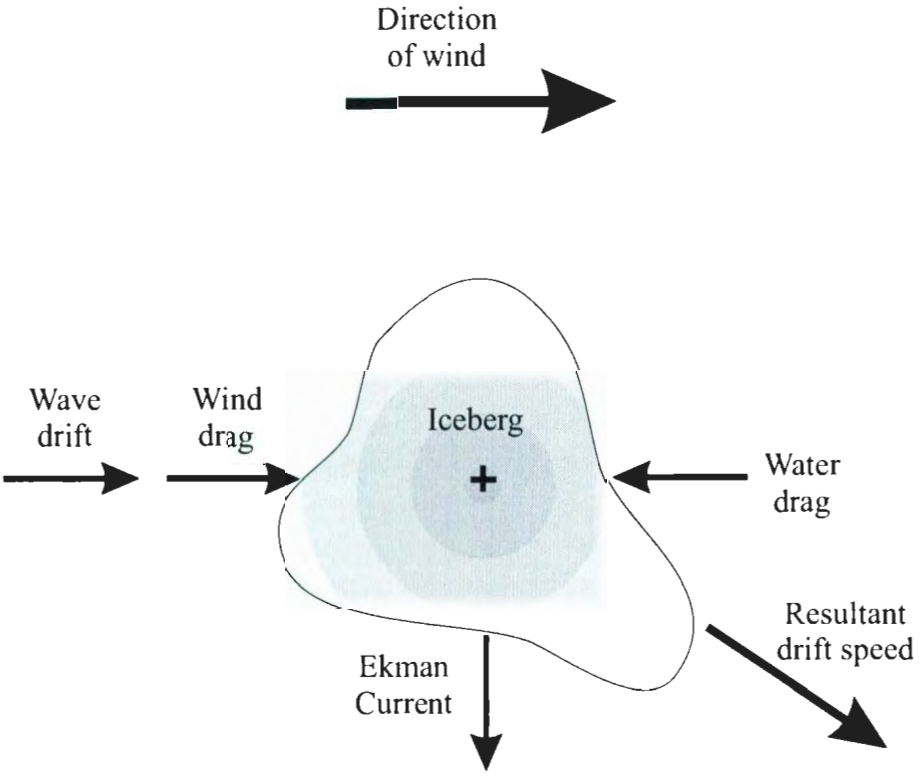

Figure 4.1: Illustration of forces acting on an iceberg

obtained using Ekman's current theory.

Wind blowing across the ocean surface will create a drag force on the surface layer of water causing a thin layer of water to move in the direction of the wind. The magnitude of this surface layer current is given by (Pond and Pickard 1983)

$$\frac{V_0}{U_W} = \frac{0.0127}{\sqrt{\sin|\phi_{lat}|}}. \tag{4.1}$$

where V_0 is the surface current speed, U_W is the wind speed, and ϕ is the latitude in degrees.

Due to the Earth's rotation and the Coriolis effect, the surface current is deflected 45° to the right (in the Northern Hemisphere) of the direction of the wind. The layer of water at the surface, in turn, exerts a stress on, and thus produces motion in, a layer of water immediately below it. The sub-surface motion is deflected even farther to the right of the wind by the Coriolis effect. The transfer of momentum between layers is inefficient and energy is lost between each layer. The overall effect is a deflection to the right, increasing with depth. This creates a spiral pattern. The magnitude of the current varies with depth exponentially as shown by

$$U_C = V_0 \exp\left(\frac{\pi z}{D_E}\right), \tag{4.2}$$

where V_0 is the surface current speed, z is the depth, and D_E is the Ekman depth. The Ekman depth is the depth at which the magnitude of the current is 0.04 times the magnitude of the surface current, and is given as

$$D_E = \frac{4.3U_W}{\sqrt{\sin|\phi|}}. \tag{4.3}$$

The net movement of water through to the Ekman depth is 90° to the right of

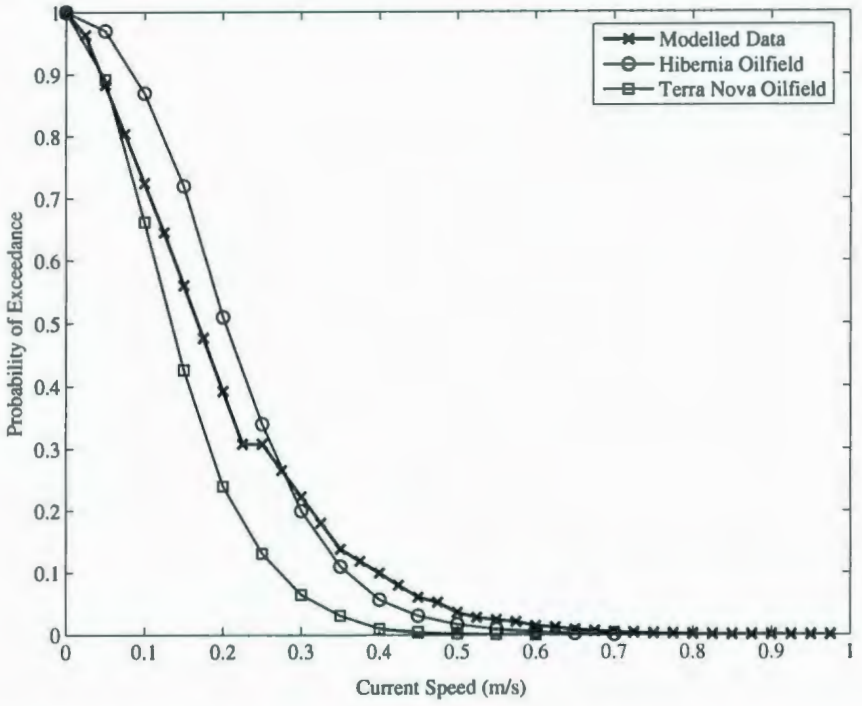

Figure 4.2: Comparison between modelled and measured currents

the wind direction. Figure 4.2 compares the modelled wind generated current with two measured current distributions. The first observed distribution is based on measurements from the Hibernia oilfield (Petrie 1982). The second observed distribution is calculated from a three-month data set collected at the Terra Nova oilfield (Seaconsult 1988). Both observed data sets contain residual currents after tidal currents have been removed. The comparison shows that the current modelled using Ekman Theory is comparable to observed ocean currents recorded at two different locations on the Grand Banks, and can be used to estimate local wind driven currents for the region.

4.2.2 Wind Drag Force

Wind blowing across the face of an iceberg will cause a drag force acting in the same direction as the wind. This force depends on the density, velocity, viscosity and compressibility of the air, and the size and shape of the iceberg. The wind drag force acting on an iceberg can be calculated using the standard drag equation

$$F_A = \frac{1}{2} C_A \rho_A A_A U_W^2, \tag{4.4}$$

where F_A is the wind drag force acting on the iceberg, C_A is the wind drag coefficient for a given iceberg, ρ_A is the density of air, A_A is the projected area of the above water portion of the iceberg perpendicular to the direction of the wind, and U_W is the wind speed.

Irregular shaped objects can have a drag coefficients ranging from approximately 0.3 for smooth sloping objects to approximately 1.5 for sharp edged objects (Smith and Donaldson 1987). For icebergs, the wind drag coefficient C_A was chosen to be 1.0.

The above water portion of the iceberg is the only part of the iceberg influenced directly by the wind drag force. Smith and Donaldson (1987) performed a detailed survey of nine icebergs, obtaining profile measurements for each iceberg. Using the information from this survey, a relationship between the iceberg waterline length, L, and the above water projected area, A_A, was determined. The above water projected area may be estimated using $A_A = 0.115L^2$.

4.2.3 Wave Drift Force

Since the waterline length of icebergs is large relative to the wave length, the waves will scatter around them. This scattering creates a net force on the object due to the diffraction of the wave energy. Many iceberg drift models neglect this force. However, wave drift forces are significant when compared with the other forces acting on an iceberg (Hsiung and Aboul-Azm 1982). A good understanding of wave-body interactions is necessary when calculating wave drift forces acting on drifting icebergs. Wave drift forces can be divided into two parts:

(1.) First order wave forces which are linearly proportional to the wave amplitude. These forces have the same frequency as the waves, and are periodic in nature.

(2.) Second order wave forces. These forces are time averaged and vary slowly with the magnitude proportional to the square of the wave amplitude.

The wave drift force is the steady state component of the second order force and may be estimated using the following equation (Isaacson 1988)

$$F_D = \frac{1}{2} C_D \rho_W g D_I H^2, \tag{4.5}$$

where F_D is the wave drift force, C_D is the wave drift coefficient for a given iceberg, ρ_W is the density of water, g is the gravitational acceleration, D_I is the characteristic dimension of the iceberg, and H is the regular wave height.

Dimensional analysis reveals that the wave drift coefficient C_D is a function of D_I/L_W where L_W is the wave length. The wave drift coefficient is usually estimated using models based on potential flow theory. Figure 4.3 shows wave drift coefficients for three icebergs varying in shape. Isaacson (1988) provided two wave drift curves, representative of tabular icebergs with steep sides. The first curve is based on a

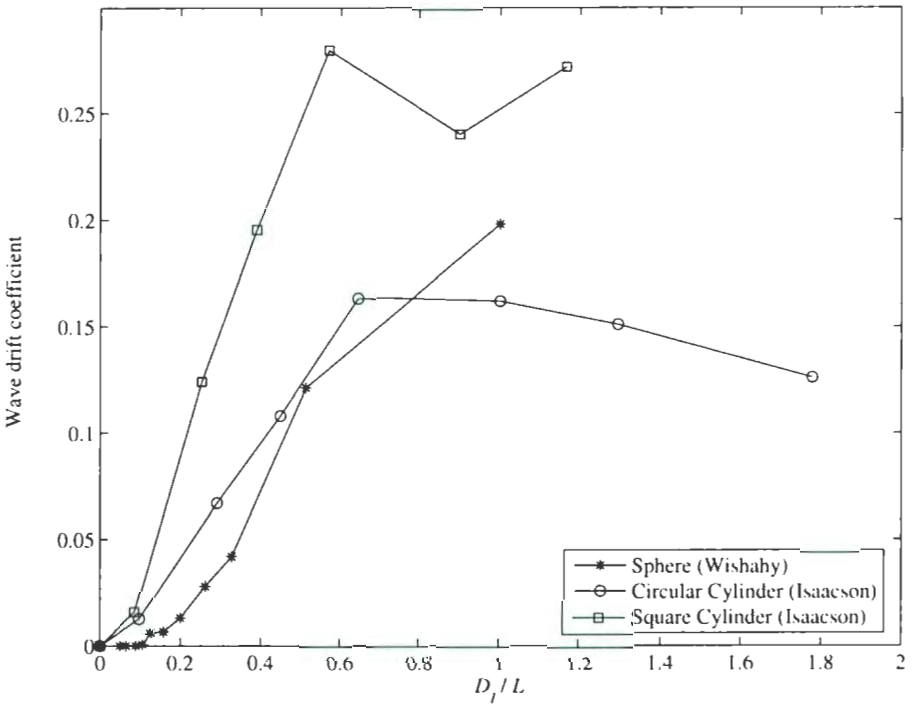

Figure 4.3: Wave drift coefficients

circular cylinder with a draft to diameter ratio of 0.5 and the second curve is based on a square cylinder with a draft to diameter (side) ratio of 0.5. A spherical iceberg was used to represent wave forces on domed icebergs, growlers, and bergy bits (Cammaert et al. 1992). A spherical iceberg is most representative of icebergs found on the Grand Banks.

The characteristic dimension of the iceberg, D_l is set equal to the waterline length for all icebergs. The regular wave height is represented using the root-mean-square of the wave height. This variable gives results that best represent the random sea state.

4.2.4 Water Drag Force

Icebergs moving through water will develop a drag force acting in the opposite direction of the movement. This drag force is calculated using the standard drag equation

$$F_W = \frac{1}{2} C_W \rho_W A_B U_W^2, \tag{4.6}$$

where F_W is the water drag force, C_W is the water drag coefficient, ρ_W is the density of water, A_B is the below water projected area perpendicular to the direction of motion of the iceberg, and U_W is the velocity of the water relative to the iceberg.

The below water projected area is based on iceberg measurements by Smith and Donaldson (1987) and is given as $A_B = 0.612L^2$. The water drag coefficient C_W is set to 1.0. Single values for both C_W and A_B were chosen for the model instead of depth dependent values. Depth dependent values would require a more detailed underwater iceberg profile as well as drag coefficient data for various depths. This was deemed unnecessary since the local current is approximated using Ekman theory, and the forces are averaged over the entire draft of the iceberg.

4.3 Resultant Drift Velocity

The resultant drift velocity is determined as a vector addition of the velocity components calculated using the above equations. The wind drag force F_A and the wave drift force F_D are assumed to act in the same direction and are set equal to the water drag force F_W. Using Equation 4.6, the velocity of the water relative to the iceberg, U_W, is determined. The resultant iceberg drift velocity V_D is then calculated by adding U_W and the current velocity U_C. The Ekman current is assumed to be acting 90° to the right of the wind direction.

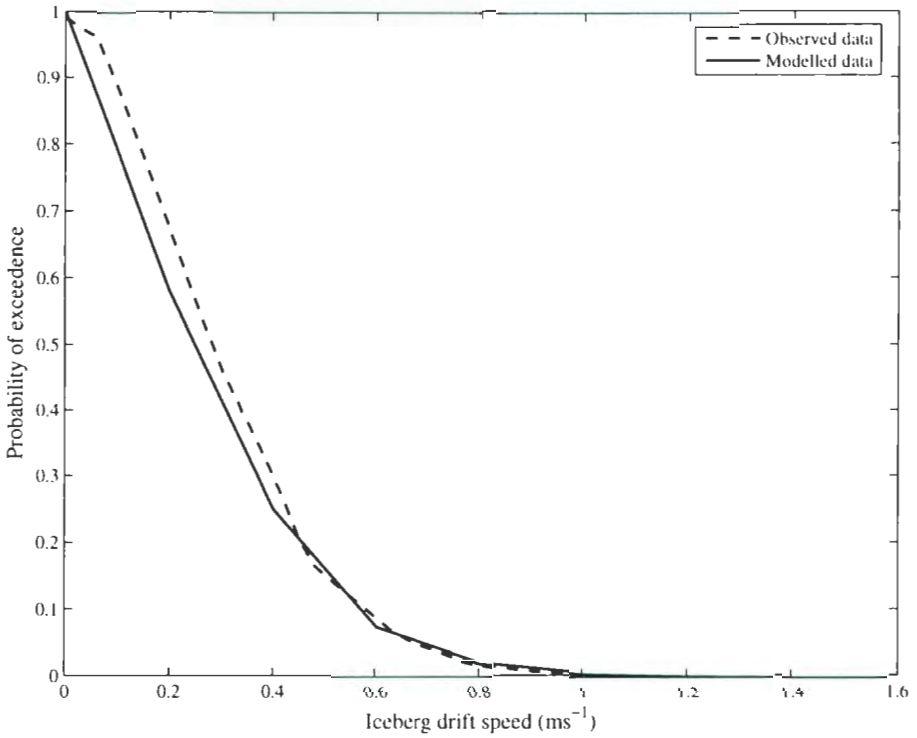

Figure 4.4: Comparison between modelled and observed drift speed distributions

The model output drift speed data were compared with a drift speed distribution developed by Seaconsult (1988). The distribution was developed based on onshelf observations from 100 icebergs covering three different years. The comparison is shown in Figure 4.4. The deterministic model is in good agreement with the observed data, especially for drift speed values greater than 0.4 m/s.

Chapter 5

Comparison Between Observed and Modeled Drift Speed

5.1 Introduction

The present chapter compares iceberg drift speed data calculated using the deterministic model described in Chapter 4 with observed data. The purpose is to determine if the existing drift speed model represents well the observed data, and if any correlations exist between the drift speed and either the waterline length or significant wave height. At the time the deterministic model was developed, there was a limited number of drift speed data available for comparison purposes. During the past decade, much more data have become available.

Section 5.2 discusses each of the data sets collected for the study. Several data sets were available for the iceberg drift speed observations, and one data set was available for the sea state conditions. Sections 5.3 and 5.4 discuss the calculation of the observed and modeled drift speed, respectively. The observed drift speed data are calculated directly from recorded iceberg drift tracks. The modeled drift speed

data are calculated using the deterministic speed model, with the observed L and H_S values used as inputs. Section 5.5 discusses in detail the comparisons made between the two data sets.

Figure 5.1 illustrates the study region chosen for the study. The study region was chosen such that the majority of the iceberg drift tracks were included as well as all of the major oilfields in the Jean d'Arc Basin. This region is bounded by 48.5°N latitude, 47°W longitude, 45.5°N latitude and 49.67°W longitude, and covers an area of approximately 52,000 square kilometers. Within this region two smaller regions were defined; namely the onshelf and offshelf regions, separated by the 100 m bathymetric contour.

5.2 Observed Data Sources

5.2.1 Iceberg Data Sources

Iceberg observations were collected from two sources. The first source was the Canadian Offshore Oil and Gas Environmental Data archive published by the Marine Environmental Data Service (MEDS 1997). This data set contains iceberg observations from drilling platforms operating on the Grand Banks during the 1980's. This data set was supplemented with data from the Provincial Airlines (PAL) Iceberg Detection and Reconnaissance Program (PAL 2000, PAL 2001, PAL 2002, PAL 2003, PAL 2004). These data were collected by PAL during routine flights over the Grand Banks during the 2000 to 2004 iceberg seasons. Both data sets were combined resulting in a total of 6146 data points.

Figure 5.2 shows the comparison between observed waterline length data and the distribution used in modelling for the Grand Banks region (see Section 2.2.1).

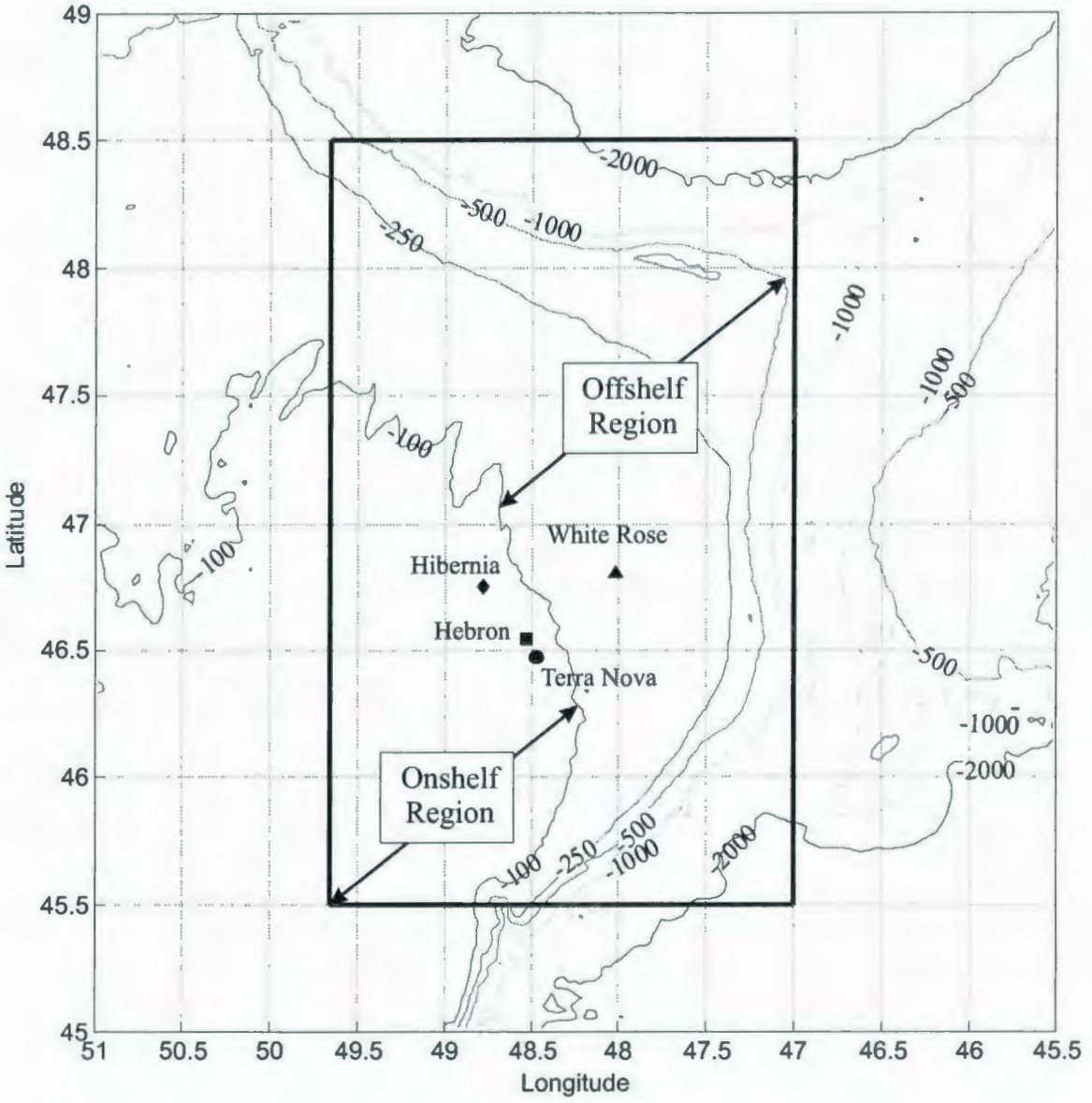

Figure 5.1: Study region

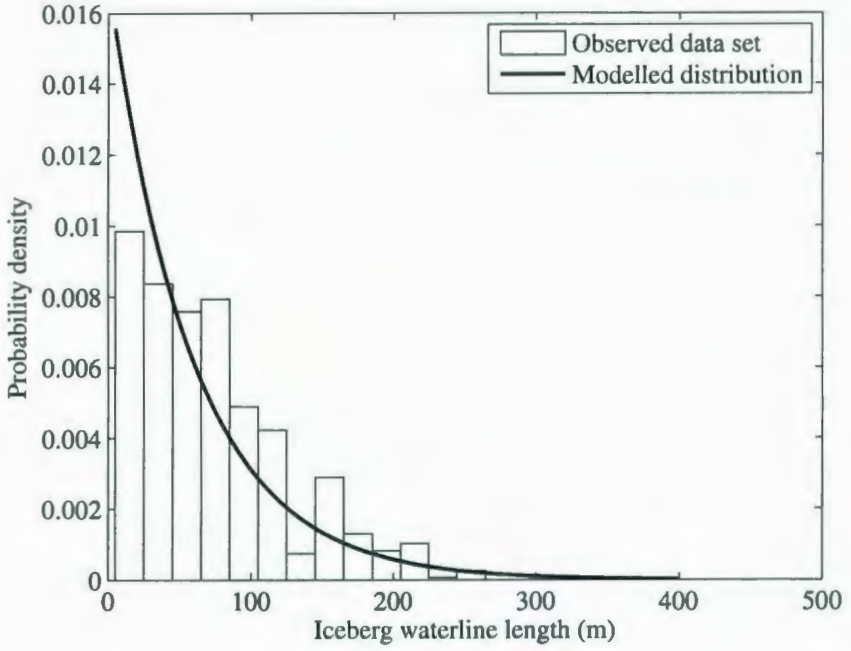

Figure 5.2: Observed and modelled iceberg waterline length distributions

The observed data set contains more icebergs in the 50 m to 150 m range than reflected in the modelled distribution. This is not a concern for the present study since comparisons are made on a one-on-one basis.

5.2.2 Environmental Data Sources

Environmental data, represented by the significant wave height, were extracted from the AES40 database (Swail et al. 2000). This database was developed by Oceanweather Inc. for the Meteorological Service of Canada, formerly known as the Atmospheric Environment Service (AES). The AES40 database contains 40-year wind and wave hindcasts referenced to several gridpoints for the North Atlantic. Data from two gridpoints were extracted for the present study.

In a similar manner, the modelled and observed significant wave height distributions are compared in Figure 5.3. The observed data set contains more data in the

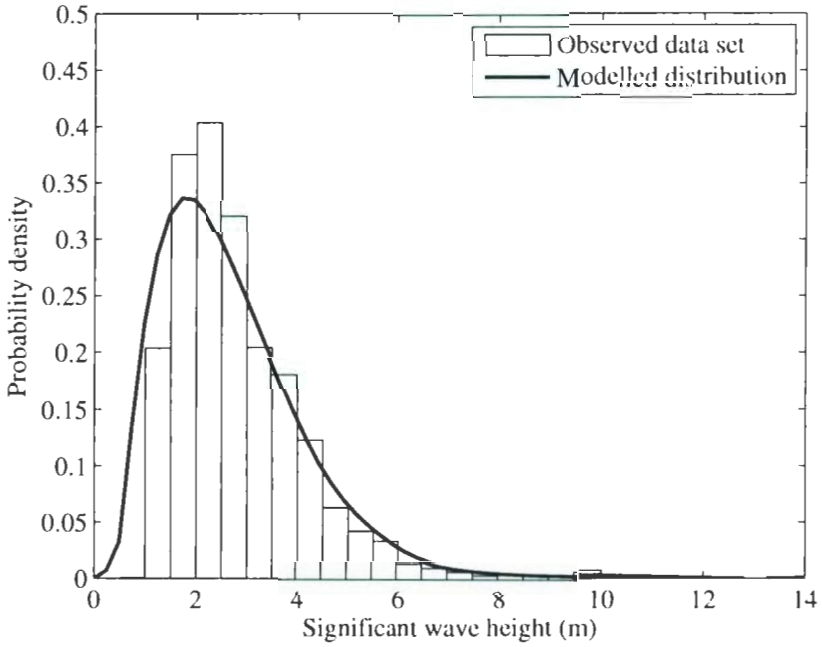

Figure 5.3: Observed and modelled significant wave height distributions

1 m to 3 m range. Overall, the iceberg drift data set is reasonably representative of the modelled waterline length and significant wave height distributions.

5.3 Calculation of Observed Drift Speed

The iceberg data were supplied in the form of iceberg drift tracks. These tracks contain data on the time and location of each observation of an iceberg. The observed drift speed was calculated as the ratio of the differences in position and time between two consecutive observations. Figure 5.4 illustrates this concept. The distance

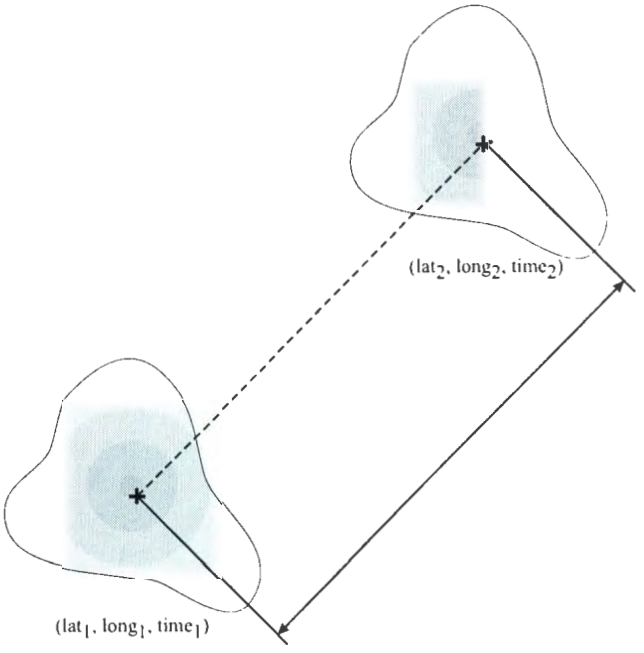

Figure 5.4: Calculation of iceberg drift speed using two consecutive data points

traveled between Point 1 and Point 2 is determined as

$$\begin{aligned} dist_x &= 111.1984 \times (long_2 - long_1) \times \cos\left(\tfrac{lat_1+lat_2}{2}\right) \times 1000 \\ dist_y &= 111.1984 \times (lat_2 - lat_1) \times 1000 \\ dist &= \sqrt{dist_x^2 + dist_y^2} \end{aligned} \tag{5.1}$$

where the constant 111.1984 km is the length of one degree of latitude (60 minutes or nautical miles). The length of one degree of longitude is a function of latitude; the length of one degree of longitude decreases with increasing latitude. The drift speed is calculated as the ratio between the distance travelled and the time difference between the two records

$$v_D = \frac{dist}{time_2 - time_1} \tag{5.2}$$

The drift speed data were then checked for any inconsistencies or anomalies. For

example, records with erroneous dates or missing information were excluded from the analysis. Each data point was checked using the following set of criteria:

- the iceberg waterline length must be known;
- the iceberg cannot be grounded or have a drift speed of zero;
- the iceberg can not be under tow by a supply vessel;
- the time interval between two consecutive track data points must be greater than 30 minutes and less than 8 hours; and
- the iceberg must be located within the study region indicated by Figure 5.1.

In addition, any duplicate iceberg tracks recorded in the database were removed.

5.4 Calculation of Modelled Drift Speed

In order to perform a one-on-one comparison between modelled and observed drift speed data, the modelled drift speed must be calculated for the same size iceberg experiencing the same environmental conditions as recorded in the observed data set. This is accomplished by using the observed data pairs $\{L, H_S\}$ as inputs in the drift speed model described in Chapter 4.

The result is a data set containing observed iceberg waterline lengths and significant wave heights, as well as observed and modelled drift speeds. In the following sections, the observed and modelled drift speed data are compared on a one-on-one basis in an attempt to identify any significant correlations that may exist.

5.5 Model-Data Comparisons

The modelled data were compared with the observed data in an attempt to identify any correlations between iceberg drift speed, iceberg size and significant wave height. Comparisons are made on the basis of:

- the entire data set;
- iceberg size categories;
- significant wave height categories;
- joint iceberg size and significant wave height categories; and
- water depth categories.

The observed and modelled data are divided into categories based on the above criteria. For each data subset, the following information is provided:

- summary statistics, such as the mean and standard deviation of the drift speed data;
- observed and modelled drift speed distributions; and
- one-to-one scatter plot, including a best fit regression line.

5.5.1 Entire Data Set

Figure 5.5 shows the comparison between the observed and modelled data sets, for all data. The figure contains histograms of observed (left) and modelled (right) data at the top of the figure. Each histogram contains the summary statistics for that data set. As well, cumulative (middle) and exceedence (bottom) probability distributions are provided.

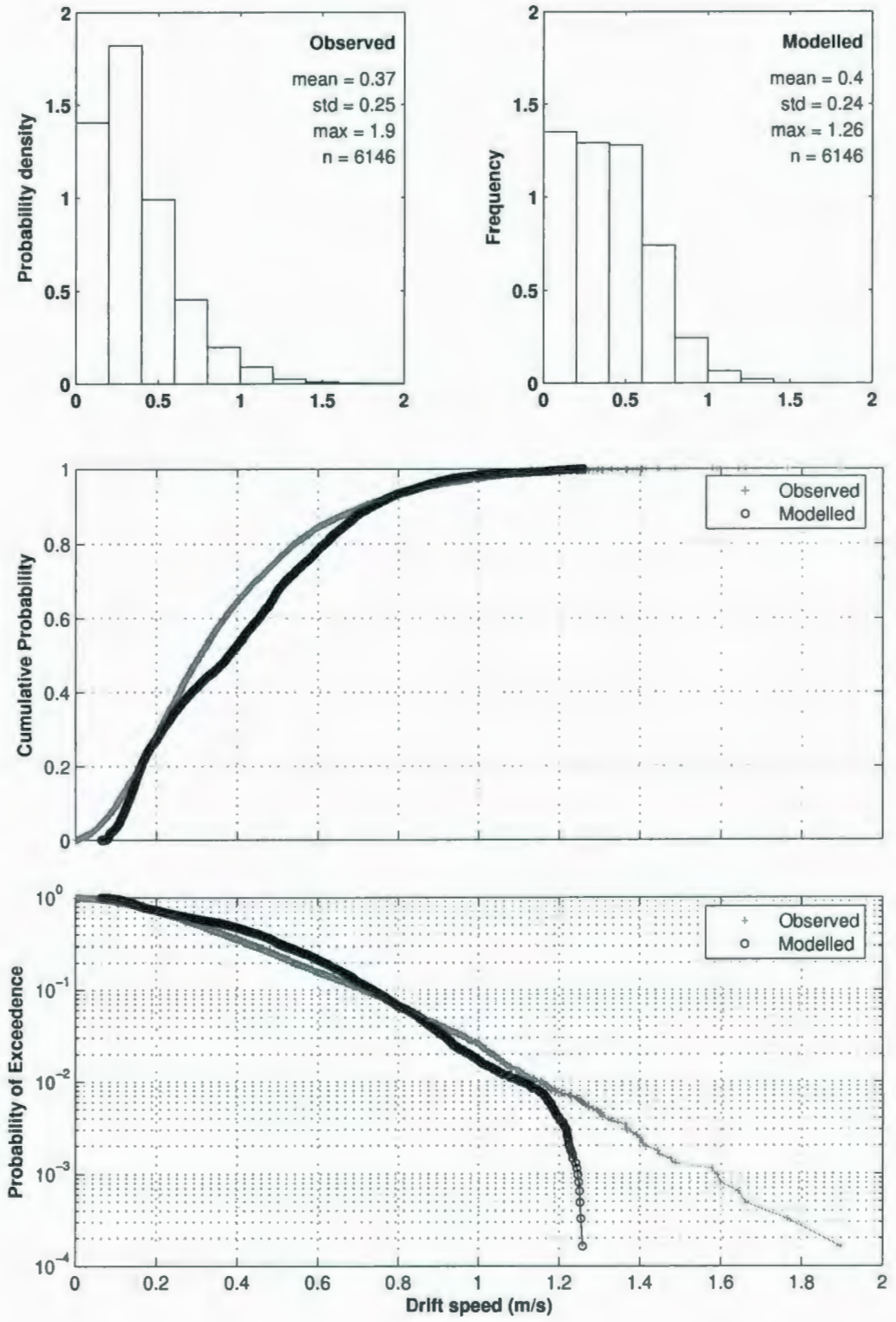

Figure 5.5: Overall comparison

The figure shows that the overall modelled drift speed distribution has a similar shape as the observed drift speed distribution, indicating the model predicts the drift speed well on average. The model underestimates the drift speed in the tail of the distribution (drift speed greater than 1 m/s). This may be important considering the tail of the distribution is significant in an extremal analysis.

Figure 5.6 shows the one-to-one comparison between the observed and modelled data sets. A least squares regression line and the r^2 value are included to indicate the correlation between the to data sets. For a "perfect" model, the regression line would indicate a one-to-one relationship, meaning the model would predict exactly the observed value for the same iceberg. The figure shows no significant correlation between the two data sets, as indicated by $r^2 = 0.42$. In addition, the deterministic model does not appear to generate any drift speeds less than 0.05 m/s while the observed data set does include speeds less than 0.05 m/s. Several reasons may contribute to this result. Overall, the deterministic model does not capture the randomness inherent in the observed drift speed data. First, the present drift speed model is based on a deterministic relationship with the significant wave height parameter. The observed data indicates that other factors add random components to the drift velocity. One such component may be ocean or tidal currents. Second, the deterministic model was developed based on the full distribution for both iceberg waterline length (5 m $< L <$ 400 m) and significant wave height (0 m $< H_S <$ 14 m). However, the observed data set does not cover the entire range for either waterline length or significant wave height. The joint distribution between the waterline length and significant wave height parameters is an integral part of the drift speed model and may not be fully captured by the observed data.

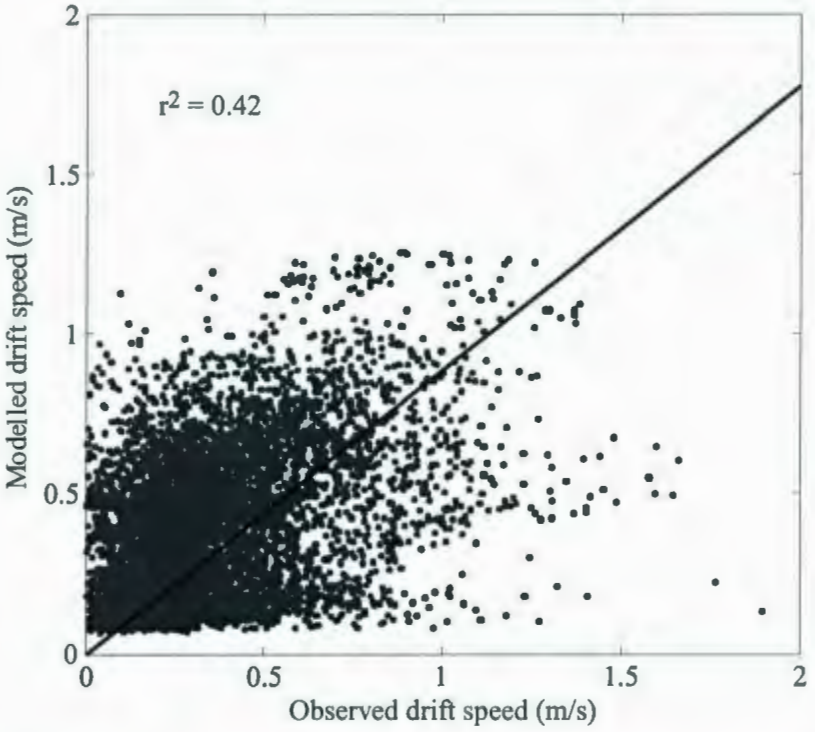

Figure 5.6: Correlation between observed and modelled iceberg drift speed

5.5.2 Comparison Based on Iceberg Size Categories

The observed and modelled data sets were divided into smaller subsets based on the observed waterline length to determine if there exists any correlation between iceberg size and drift speed. Iceberg size categories (Table 5.1), as defined by the International Ice Patrol (IIP), were used to divide the data into iceberg size categories. Large and extra-large icebergs were combined.

Table 5.1: Iceberg size categories as defined by the IIP

Size Category	Waterline Length Range
Growlers and bergy bits	< 16 m
Small icebergs	16 m to 60 m
Medium icebergs	60 m to 120 m
Large and extra-large icebergs	> 120 m

Table 5.2 summarizes the results for the comparisons for each iceberg size category. The results show that the mean observed drift speed remains relatively constant for all iceberg size categories. The modelled results show a slight decrease in the mean drift speed with increasing iceberg size. The highest correlation is obtained for the large and extra-large iceberg category.

The comparison figures for each size category are given in Appendix A. The observed and modelled distributions compare reasonably well for the medium and large iceberg size categories. For the smaller size categories, the model tends to over estimate the drift speed distribution.

Table 5.2: Summary statistics for observed and modelled data sets for iceberg size categories. Mean and standard deviation units are [m/s]

Iceberg Size	n	r^2	Observed		Modelled	
Category			Mean	Std	Mean	Std
Bergy bit/growler	703	0.40	0.36	0.22	0.45	0.17
Small	2302	0.44	0.36	0.24	0.42	0.24
Medium	2116	0.36	0.38	0.25	0.40	0.27
Large and extra-large	1025	0.55	0.35	0.27	0.36	0.24

5.5.3 Comparison Based on Significant Wave Height

Similarly, the observed and modelled data sets were divided into smaller subsets based on the associated significant wave height data, as indicated below:

- low sea state conditions ($H_S \leq 3$ m);
- medium sea state conditions (3 m $< H_S \leq 6$ m); and
- high sea state conditions ($H_S > 6$ m).

Table 5.3: Summary statistics for observed and modelled data sets for significant wave height categories. Mean and standard deviation units are [m/s]

Significant Wave Height Category	n	r^2	Observed		Modelled	
			Mean	Std	Mean	Std
$H_S < 3$ m	4006	0.22	0.31	0.21	0.26	0.13
3 m $< H_S <$ 6 m	1981	0.23	0.45	0.26	0.64	0.13
$H_S > 6$ m	159	0.18	0.77	0.27	1.06	0.12

Table 5.3 summarizes the results for each sea state category. The results show that the significant wave height has a more noticeable effect on the drift speed than the waterline length. Both the observed and modelled mean drift speeds increase with increasing significant wave heights. This trend is expected since the model is based on the summation of environmental forces, which are defined in terms of the significant wave height. A higher significant wave height will result in a higher drift speed. The highest correlation between the two data sets is obtained for the medium sea state conditions ($r^2 = 0.23$).

The comparison figures for each sea state category are given in Appendix B. The model fails to capture the shape of the drift speed distribution for all sea state categories. The model underestimates considerably the tails of the distributions for the low and medium sea state categories.

5.5.4 Joint Effect of Iceberg Size and Significant Wave Height

The deterministic model is based on the joint distribution between the iceberg waterline length and the significant wave height. To investigate this effect in the observed

data, and to make correlations between the two data sets, each of the sea state categories were further divided into the iceberg size categories.

Table 5.4 to Table 5.6 summarize the results. The comparison figures for the joint relationship categories are given in Appendix C. For all size categories, in all sea state conditions, the model failed to capture the shape of the observed drift speed distributions, and underestimated the tails of distributions considerably.

Table 5.4: Summary statistics for observed and modelled data sets for icebergs size categories in low sea states. Mean and standard deviation units are [m/s]

Iceberg Size	n	r^2	Observed		Modelled	
Category			Mean	Std	Mean	Std
Bergy bit/growler	484	0.36	0.32	0.21	0.36	0.11
Small	1637	0.19	0.31	0.21	0.30	0.13
Medium	1350	0.19	0.32	0.22	0.23	0.11
Large and extra-large	535	0.22	0.24	0.19	0.16	0.07

Table 5.5: Summary statistics for observed and modelled data sets for icebergs size categories in medium sea states. Mean and standard deviation units are [m/s]

Iceberg Size	n	r^2	Observed		Modelled	
Category			Mean	Std	Mean	Std
Bergy bit/growler	219	0.19	0.45	0.22	0.65	0.10
Small	602	0.17	0.47	0.25	0.68	0.09
Medium	706	0.16	0.45	0.26	0.66	0.14
Large and extra-large	454	0.42	0.44	0.30	0.54	0.14

Table 5.6: Summary statistics for observed and modelled data sets for icebergs size categories in high sea states. Mean and standard deviation units are [m/s]

Iceberg Size	n	r^2	Observed		Modelled	
Category			Mean	Std	Mean	Std
Bergy bit/growler	0	-	-	-	-	-
Small	63	0.09	0.83	0.25	1.10	0.09
Medium	60	0.24	0.73	0.33	1.11	0.10
Large and extra-large	36	0.20	0.73	0.17	0.92	0.07

5.5.5 Comparison Based on Water Depth

A comparison based on water depth was performed to assess the correlation between the two data sets. The onshelf region was defined as the portion of the study region which has a water depth less than 100 m. The offshelf region has a water depth greater than 100 m. The observed and modelled data sets were divided based on the water depth corresponding to each observation.

Table 5.7 summarizes the results of the comparison. For the onshelf region, the model over estimates the observed distribution. For the offshelf region, the model predicts well the observed drift speeds, for drift speeds less than 0.7 m/s. For data greater than 0.7 m/s, the model underestimates the observed drift speed. Appendix D contains details of the comparison.

5.6 Summary of Results

The deterministic drift speed model captures the overall trends of the observed drift speed data. Figure 5.5 shows that the model predicts well the observed data for drift speeds up to a maximum of 1.2 m/s. However, there is little correlation between

Table 5.7: Summary statistics for observed and modelled data based water depth. Mean and standard deviation units are [m/s]

Water Depth	n	r^2	Observed		Modelled	
Category			Mean	Std	Mean	Std
Onshelf (< 100m)	2023	0.52	0.34	0.25	0.46	0.26
Offshelf (> 100m)	4123	0.40	0.38	0.25	0.38	0.23

the observed and modelled data. This is evident through the model-data comparisons made based on various iceberg size and significant wave height categories. The following summarizes the results.

- Modelled drift speed decreases slightly with increasing iceberg size, whereas observed data appears to be independent of iceberg size.
- Both observed and modelled drift speed increase with increasing significant wave height.

Chapter 6

Development of a Probabilistic Drift Speed Model

6.1 Introduction

The results of the analysis presented in Chapter 5 indicate the deterministic model captures the overall trends in the iceberg drift speed data. The mean iceberg drift speed increases with increasing significant wave height, and decreases slightly with increasing iceberg size. However, the model does not capture well the correlation between the individual drift speed data points and the associated waterline lengths and significant wave heights. On a one-on-one basis, the model does not predict well the iceberg drift speed. Other random components, such as ocean or tidal currents, may contribute to the final drift speed.

In this chapter, a probabilistic iceberg drift speed model is presented. The model may be described as a *statistical* model, as outlined in Section 2.7. It is based on a joint distribution between the iceberg waterline length and the significant wave height. Since the results presented in Section 5.5.5 show that water depth has an

effect on drift speed, only onshelf drift speed data (water depth less than 100 m) are used to develop the probabilistic model. These data are considered representative of the drift speed of icebergs that may impact structures operating on the Grand Banks. However, given a sufficient data set, this type of model can be generated for any region.

Section 6.2 discusses the approach used to develop the probabilistic drift speed model using onshelf data. Section 6.4 summarizes a sensitivity analysis performed using the iceberg design load methodology. Iceberg design loads were estimated using both the deterministic and the new probabilistic drift speed models. Output design loads and mean contributing parameters are summarized.

6.2 Model Development

Ideally, a drift speed model should be developed using data from all the possible combinations of waterline lengths and significant wave heights. However, problems arise when the available data do not cover the entire range of the distributions. The approach adopted in this study is to identify the trends observed in the available data and to extrapolate those trends to the full range of the distributions. The results are reviewed carefully to ensure the extrapolation does not extend beyond what is believed to be true. The model framework is outlined in Figure 6.1

6.2.1 Model Framework

The mean iceberg drift speed is modelled as a function of the waterline length and significant wave height. Similarly, the scatter in the data is captured by the standard deviation which is also modelled as a function of the waterline length and significant wave height. Iceberg drift speed data from the available data sets described in Chapter

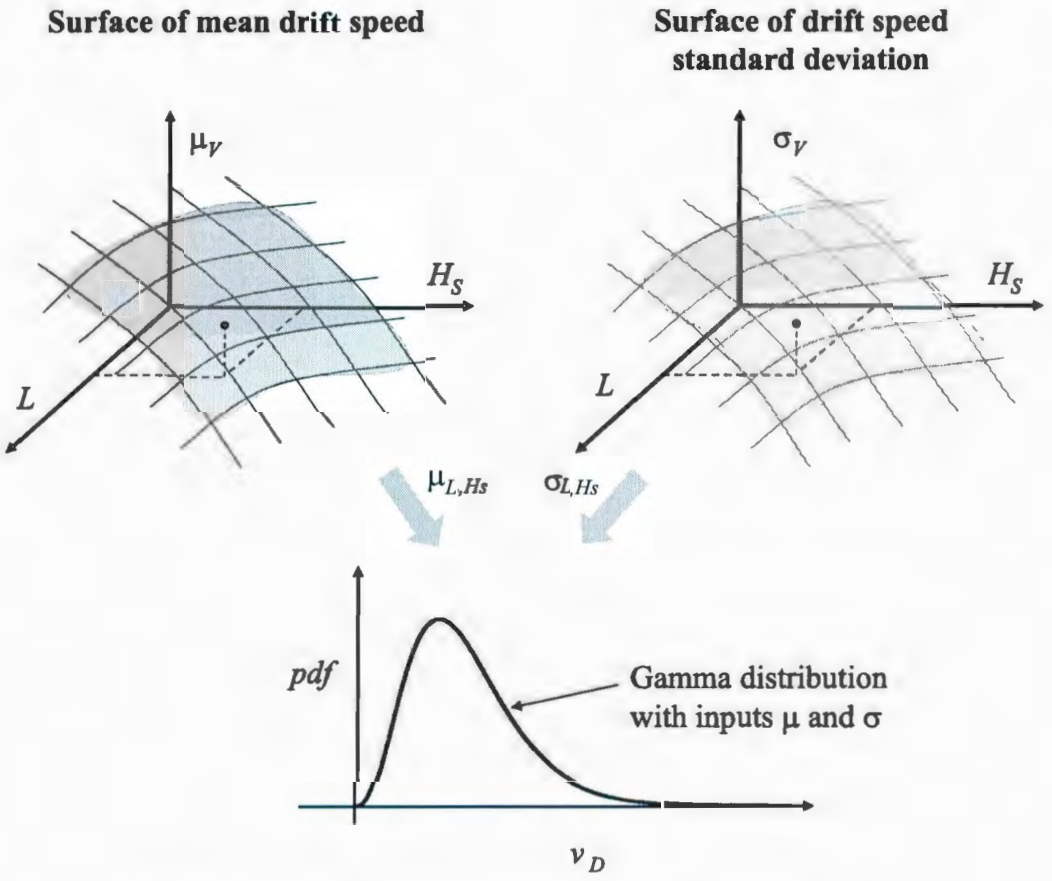

Figure 6.1: Overview of probabilistic drift speed model

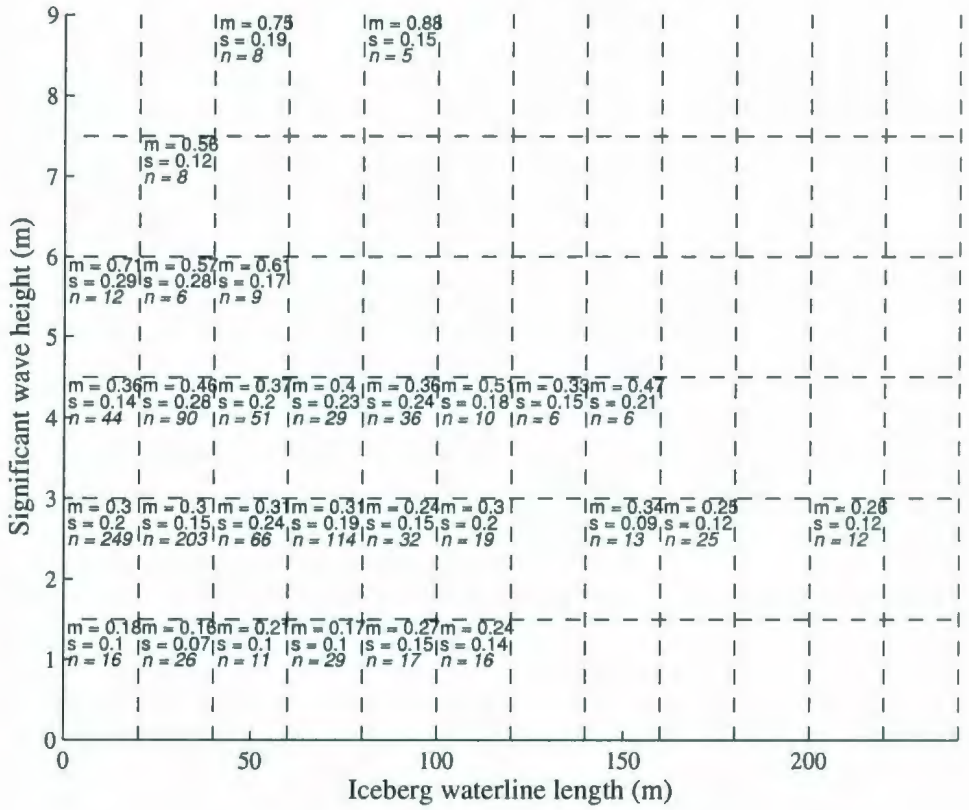

Figure 6.2: Binned drift speed data

5 are filtered to remove any iceberg observations occurring in a water depth greater than 100 m. This results in a total of 1212 data points available for modelling. These data are divided into two dimensional bins based on the waterline length and significant wave height. The waterline length data L are divided into 20 m bin sizes, and the significant wave height data H_S are divided into 1.5 m bin sizes. The mean, standard deviation and count of all drift speed data in each bin are determined. Figure 6.2 shows the range of data coverage and provides some basic descriptive statistics of the data in each bin. Several different types of distributions were fit to the data in each L, H_S bin. A gamma distribution was chosen as the best fit the data using a goodness of fit test.

The mean drift speed value from each bin shown in Figure 6.2 were extracted and plotted on a three-dimensional surface plot. At the lower iceberg waterline length range, a polynomial was fit through the data. A similar approach was followed for the upper range of waterline lengths, where a power law expression was chosen to model the drift speed as a function of the significant wave height. The two bounding curves were connected linearly, and extended to cover the full iceberg waterline length range (from 5 m to 400 m). The result is a smooth surface representing the mean iceberg drift speed as a function of L and H_S.

The best fit curves at the lower and upper waterline length ranges are expressed as

$$v_{D,L=7.5m} = -0.0042{H_S}^2 + 0.116H_S + 0.071 \tag{6.1}$$

$$v_{D,L=397.5m} = 0.173{H_S}^{0.404} \tag{6.2}$$

and shown in Figure 6.3. The resulting smooth mean drift speed surface is shown in Figure 6.4.

In a similar manner, a 3-dimensional surface was used to model the standard deviation as a function of L and H_S. Using a multi-variable regression technique, the standard deviation can be modelled using

$$\sigma\left(L, H_S\right) = 0.102 + 2.98 \times 10^{-5}L + 0.030H_S \tag{6.3}$$

The resulting surface is shown in Figure 6.5

The application of the model is summarized in the following steps.

1. For a given L, H_S pair, a mean drift speed is extracted from Figure 6.4.

2. Similarly, a standard deviation is extracted from Figure 6.5.

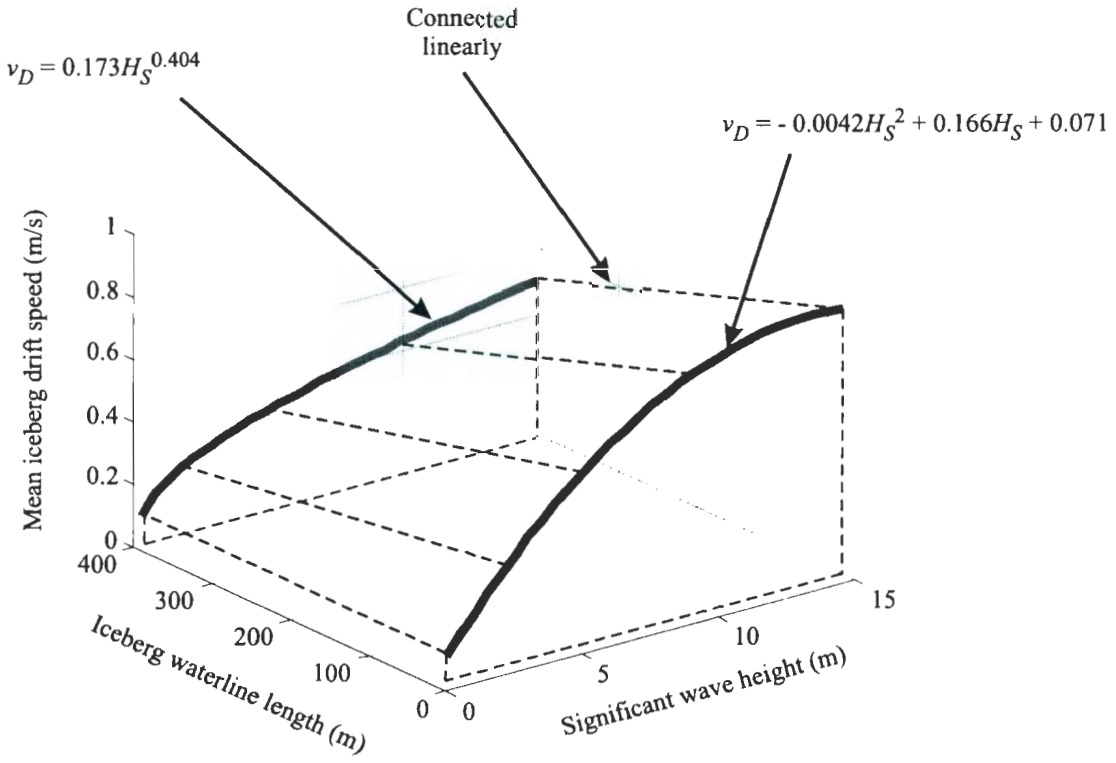

Figure 6.3: Bounding curves for mean iceberg drift speed data

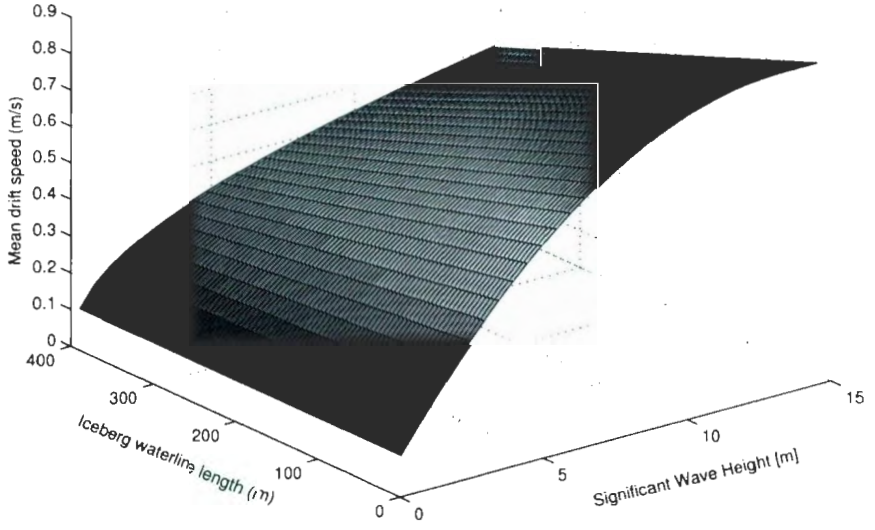

Figure 6.4: Probabilistic model: mean drift speed as a function of L and H_S

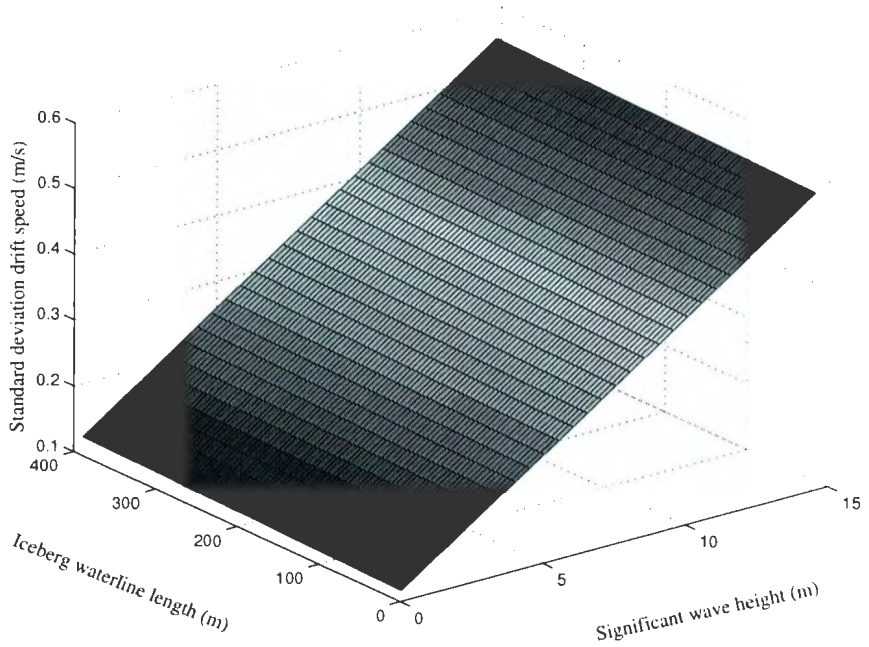

Figure 6.5: Probabilistic model: standard deviation of drift speed as a function of L and H_S

3. A gamma distribution is created using the extracted mean and standard deviation values. This distribution then represents all the possible drift speed values for the given L, H_S pair.

6.3 Comparison with Observed Data

Figure 6.6 compares the output from the model with the observed data. The model output is weighted to account for the observed distribution of waterline lengths and significant wave heights. The figure shows the model fits very well to the data.

In a similar manner, comparisons were made between observed and modelled data based on iceberg size and significant wave height categories. The results indicate the model is a good fit in all iceberg size and significant wave height category. However, for one category, high significant wave height, the probabilistic model does not produce

a good fit. This may be a result of the low number of data in the category. The comparison figures are provided in Appendix E.

6.4 Design Load Sensitivity

Using the iceberg design load methodology outlined in Chapter 2, a sensitivity analysis was performed. Iceberg design loads were estimated using the deterministic drift speed model and the new probabilistic drift speed model. In addition, parameters contributing to the design loads were compared. The GBS and FPSO structures identified in Section 2.6 were used for the sensitivity analysis.

The effect of the drift speed model on ice management effectiveness is also investigated. Ice management effectiveness is defined as the proportion of icebergs that are successfully managed, compared with the overall population that would have otherwise impacted the structure. Iceberg drift speed plays an important role in the iceberg detection model as well as the physical management models. The drift speed is used to determine the range at which an iceberg is detected. An iceberg with a lower drift speed will result in more time available to initiate ice management procedures and attempt to deflect the iceberg.

6.4.1 GBS Results

The GBS described in 2.6.1 was re-analyzed using the new probabilistic drift speed model. The results are summarized in Table 6.1. Incorporating the probabilistic drift speed model results is a 18% reduction in the design load (from 552 MN to 455 MN) at the 10,000 year annual exceedence level when ice management is not included.

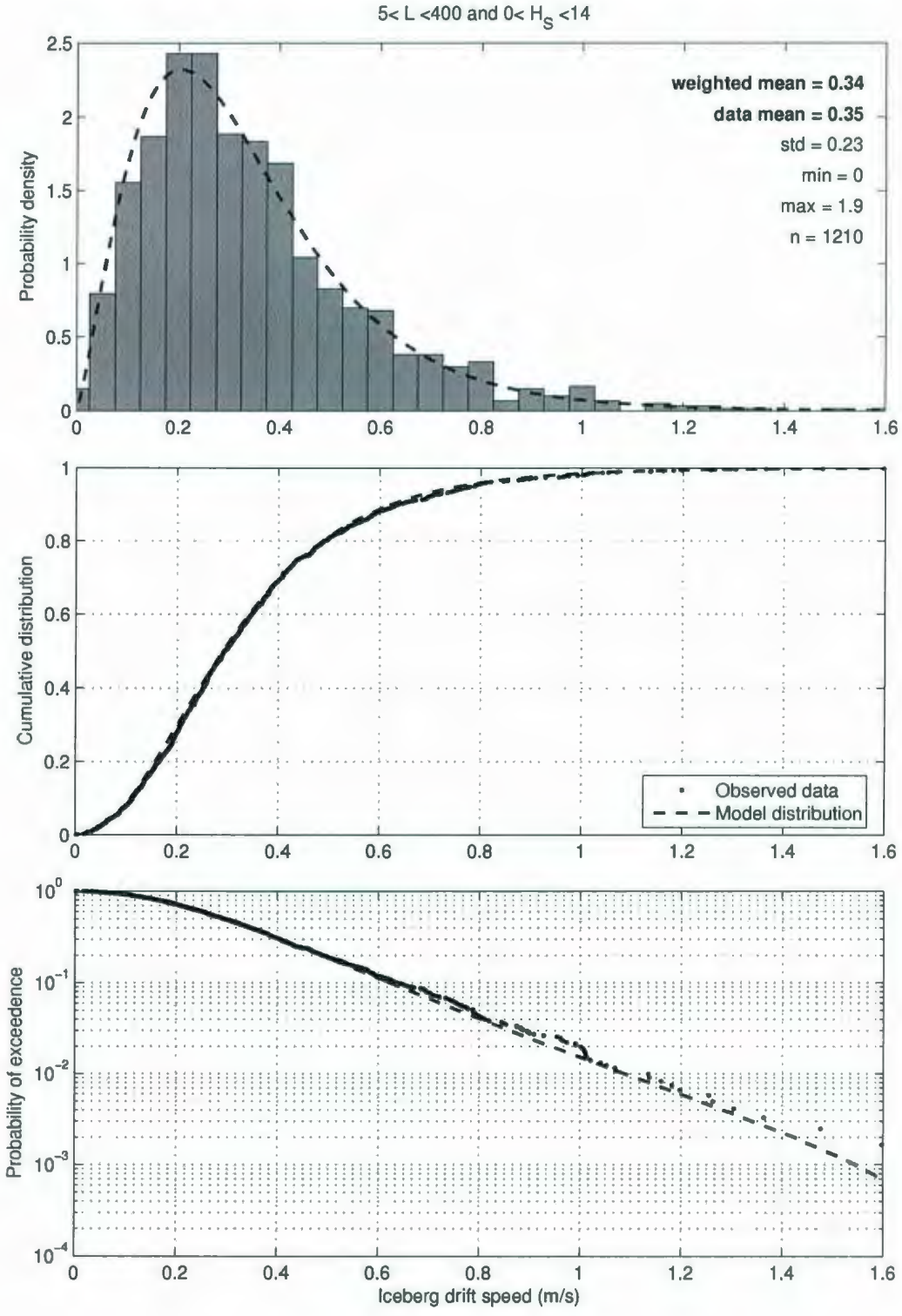

Figure 6.6: Overall comparison

Table 6.1: Summary of generic GBS results using the probabilistic drift speed model; no ice management modelled

	Exceedence Probability		
	10^{-2}	10^{-3}	10^{-4}
Horizontal impact force (MN)	52	184	455
Overturning moment (GN· m)	4.0	14	33
Contributing iceberg length (m)	112	141	166
Contributing significant wave height (m)	3.7	4.2	4.6
Contributing iceberg drift speed ($m\,s^{-1}$)	0.49	0.64	0.77
Contributing iceberg collision speed ($m\,s^{-1}$)	0.49	0.63	0.78
Contributing iceberg mass (1000 tonne)	596	1203	1925
Contributing kinetic energy (MJ)	81	337	825

6.4.2 FPSO Results

The FPSO described in 2.6.2 was re-analyzed using the new probabilistic drift speed model. The results are summarized in Table 6.2. Incorporating the probabilistic drift speed model results in a 16% reduction in design load (from 518 MN to 433 MN) at the 10,000 year annual exceedence level. When ice management is included in the analysis, the design load is reduced 35% (from 415 MN to 269 MN), and the ice management effectiveness is increased from 57% to 66%.

6.4.3 Discussion

The results of the sensitivity analysis, for both the GBS and FPSO, are summarized in Table 6.3. The probabilistic drift speed model resulted in a decrease in design loads for both structures. The lower drift speeds resulted in lower impacting kinetic energies for the icebergs. The impact frequency was lower since slower icebergs will sweep out a smaller area. Ice management effectiveness also increased for both structures; lower

Table 6.2: Summary of generic FPSO results using the probabilistic drift speed model; no ice management modelled

	Exceedence Probability		
	10^{-2}	10^{-3}	10^{-4}
Horizontal impact force (MN)	42	164	433
Contributing iceberg length (m)	110	139	157
Contributing significant wave height (m)	3.6	4.1	4.3
Contributing iceberg drift speed ($m\,s^{-1}$)	0.48	0.58	0.75
Contributing iceberg collision speed ($m\,s^{-1}$)	0.46	0.60	0.78
Contributing iceberg mass (1000 tonne)	555	1102	1574
Contributing kinetic energy (MJ)	72	256	727

drift speeds resulted in more time available between the initial iceberg sighting and the iceberg reaching the structure. The largest reduction was for the FPSO, with ice management.

Table 6.3: Summary of design load sensitivity to iceberg drift speed modelling

Structure	Ice	Design Load at 10^{-4}		%
	Management	Det. v_D Model	Prob. v_D Model	Change
GBS	No	552 MN	455 MN	-18%
FPSO	No	518 MN	433 MN	-16%
FPSO	Yes	415 MN	269 MN	-35%

Chapter 7

Conclusions and Future Work

7.1 Conclusions

With the world demand for hydrocarbons expected to increase, or at least remain relatively high, exploration, development and production activities on the Grand Banks will continue to increase. The presence of icebergs in the region pose a significant risk the facilities, workers and the environment. Facilities must have sufficient resistance to maintain integrity should an iceberg collision occur. In response to industry demand, a comprehensive iceberg design load methodology has been developed. This methodology can be used during the design process to assist the designers in achieving an economical, yet safe, design for the facility. The methodology also allows the designers to incorporate the effectiveness ice management procedures into the design. This results in a lower design load requirement, while still adhering to the guidelines set out in the Canadian Standards Association CAN/CSA-S.471-04, General Requirements, Design Criteria, the Environment, and Loads.

The iceberg drift speed model is a fundamental component of the design load methodology. The model estimates the drift speed of icebergs that may potentially

impact the structure. The drift speed is used to determine the initial kinetic energy of the iceberg, and ultimately the impact force on the structure. The drift speed is also an important variable in the detection and management models.

A deterministic drift speed model was initially developed by Fuglem (1997). This model calculated iceberg drift speeds for each L, H_S combination by balancing the environmental forces acting on the iceberg. The deterministic model predicted well the overall drift speed distribution, given the available data at the time. However, with the availability of more data, it was shown that the model did not adequately capture the randomness in the observed data. This randomness may be due to a number of factors, including localized eddy currents, tidal currents, or the complex underwater shape of the iceberg. If these factors were taken into account, the deterministic model may give a more complete description of the iceberg drift speed distribution with a better description of the physical processes involved. However, such additions would most likely make the model unsuitable for the Monte Carlo type simulation used in the iceberg design load methodology.

A probabilistic iceberg drift speed model has been presented in this thesis. The probabilistic model can be categorized as a statistical model, as outlined in Section 2.7. The mean and standard deviation drift speeds are modelled as functions of the waterline length and significant wave height. Individual drift speed data are then sampled using a gamma distribution. This approach captures more of the randomness in the observed data while still preserving to the overall trends in the observed data.

7.2 Recommended Future Work

During the research and development of the probabilistic drift speed model, several areas were identified which required further research. Several of these areas are outlined below.

1. The addition of a ocean current component may improve the correlation with observed drift velocity data. A detailed study into ocean currents that may affect icebergs on the Grand Banks is required. Based on this study, a random or deterministic component of current may be added to or replace the existing locally generated current component. An example is the diurnal tide current, which have maximum speeds of up to 0.4 m/s near the Hibernia region (Petrie 1982).

2. Further investigate the effect of water depth on the iceberg drift velocity distribution. The onshelf/offshelf analysis revealed that icebergs in deeper water tend to move faster than icebergs in shallower water. This should be taken into account in greater detail in the model. Water depth may be introduced as a third independent variable, and may be closely related to currents.

3. Investigate the effect of Coriolis forces on larger icebergs. The Coriolis effect was considered a secondary effect in the deterministic model.

4. Continue to add new drift speed data as they become available. This may fill in some of the missing areas in the joint $L - H_S$ distribution, as well as strengthen the existing relationships.

5. Conduct a dedicated field program to collect iceberg drift data to fill in gaps in the data matrix given in Figure 6.1

Bibliography

Ainslie, A. and J. Duval (1974). Icebergs and drilling operations. In C. Yorath, E. Parker, and D. Glass (Eds.), *Canada's Continental Margins and Offshore Petroleum Exploration.* Canadian Society of Pretoleum Engineering.

Barr, D. (1985). Matrix procedures for dimensional analysis. *International Journal of Mathematical Education in Science and Technology 16*(5), 629–644.

Bigg, G., M. Wadley, D. Stevens, and J. Johnson (1997). Modelling the dynamics and thermodynamics of icebergs. *Cold Regions Science and Technology 26*(2), 113–135.

Buckingham, E. (1914). On physcially similar systems. *Phys. Rev. 4*, 345–376.

C-CORE (2001). Integrated Ice Management R and D Initiative - Year 2000, Final Report. Technical report, Contract Report for Chevron Canada Resources, Husky Oil Operations Limited, Mobil Oil Canada Properties, Norsk Hydro Canada Oil and Gas Inc., Petro-Canada and Panel on Energy Research and Development. C-CORE Publication 00-C36.

Cammaert, A., I. Jordaan, M. Fuglem, S. Bruneau, G. Crocker, and M. Wishahy (1992). Design Criteria for Ice Loads on Floating Production Systems - Final Report. Contract report 92-c13, C-CORE.

Carrieres, T., M. Sayed, S. Savage, and G. Crocker (2001). Preliminary Verification of an Operational Iceberg Drift Model. In *Proceedings of the International Conference on Port and Ocean Engineering under Arctic Conditions*, Ottawa, Canada.

Carter, J., C. Daley, M. Fuglem, I. Jordaan, A. Keinonen, A. Revill, T. Butler, K. Muggeridge, and B. Zou (1996). Maximum Bow Force for Arctic Shipping Pollution Prevention Regulations - Phase II. Technical report, Memorial University of Newfoundland, Ocean Engineering Research Centre. Submitted for Canadian Coast Guard Arctic Ship Safety.

Crocker, G. (1992). Growler and bergy bit populations on the Grand Banks. Technical report, C-CORE Internal Report.

Crocker, G. and G. Cammaert (1994). Measurements of bergy bit and growler populations off canada's east coast. In *IAHR Symposium*, Volume 1, Trondheim, Norway, pp. 167–176.

Dempster, R. (1974). The measurement and modelling of iceberg drift. In *OCEANS*, Volume 6, pp. 125–129.

Dunwoody, A. (1983). The design, ice island for the impact against an offshore structure. In *Offshore Technology Conference*, pp. 325–330. Paper 4550.

El-Tahan, M., H. El-Tahan, and S. Venkatesh (1983). Forecast of iceberg ensemble drift. In *Proceedings of Offshore Technology Conference*, OTC Paper No 4460, Houston, Texas, pp. 151–158.

Fuglem, M. (1997). *Decision-making for Offshore Resource Development*. Ph. D. thesis, Memorial Univeristy of Newfoundland, St. John's, Newfoundland.

Fuglem, M., G. Crocker, and C. Olsen (1995). Canadian Offshore Design for Ice Environments, First Annual Report, Environment and Routes. Technical report, Ocean Engineering Resource Centre, Memorial University of Newfoundland, St. John's, Newfoundland.

Fuglem, M., I. Jordaan, and G. Crocker (1996). Iceberg-structure interaction probabilities for design. *Canadian Journal of Civil Engineering 23*, 231–241.

Fuglem, M., I. Jordaan, G. Crocker, G. Cammaert, and B. Berry (1996). Environmental factors in iceberg collision risks for floating systems. *Cold Regions Science and Technology 24*, 251–261.

Fuglem, M., K. Muggeridge, and J. Jordaan (1998). Design load calculations for iceberg impacts. In *Proceedings of ISOPE Conference*, Volume 2, Montreal, Canada, pp. 460–467.

Garrett, C. (1985). Statistical prediction of iceberg trajectories. *Cold Regions Science and Technology 11*, 255–266.

Garrett, C., J. Middleton, M. Hazen, and F. Majaess (1985a). Analysis and Prediction of Iceberg Trajectories. Unpublished report, Department of Oceanography, Dalhousie Univeristy, Halifax, NS.

Garrett, C., J. Middleton, M. Hazen, and F. Majaess (1985b). Tidal currents and eddy statistics from iceberg trajectories. *Science 227*, 1333–1335.

Hill, B. (2005). Ship iceberg collision database. http://www.icedata.ca (accessed August, 2007).

Hsiung, C. and A. Aboul-Azm (1982). Iceberg drift affected by wave action. *Ocean Engineering 9*(5), 433–439.

IIP (2007). International Ice Patrol Website. http://www.uscg.mil/lantarea/iip/.

(Accessed August, 2007).

Intera (1980). An Iceberg Motion Prediction Model for Lancaster Sound and West Baffin Bay. Technical report, Intera Environmental Consultants Ltd and Flow Research Inc. Prepared for Petro-Canada.

Isaacson, M. (1988). Influence of wave drift force of ice mass motions. In *Proceedings of the International Offshore Mechanics and Arctic Engineering Symposium*, Volume 2, Houston, TX, USA, pp. 125 130. ASME, New York, NY, USA.

Johnson, M. and J. Ryan (1991). A radar performance prediction model for iceberg detection. In *Proceedings of the 11th International Conference on Port and ocean Engineering under Arctic Conditions*, Volume 2, St. John's, Canada, pp. 989 1003.

Jordaan, I. (1983). Risk analysis with applications to fixed structures in ice. *Seminar/Workshop on Sea ice Management.*

Jordaan, I. (2005). *Decisions under Uncertainy.* Cambridge, U.K.: Cambridge University Press.

Kubat, I. and M. Sayed (2005). An Operational Model of Iceberg Drift. *International Journal of Offshore and Polar Engineering 15*(2), 125 131.

Lever, J., D. Attwood, and D. Sen (1988). Factors affecting the prediction of wave-induced iceberg motion. *Cold Regions Science and Technology 15*, 177 190.

Matskevitch, D. (1996). Eccentric impact of an ice feature: Linearized model. *Cold Regions Science and Technology 25*(3), 159 171.

Matskevitch, D. (1997a). Analytical model of iceberg impact accounting for 3d effects. (submitted paper #274, Cold Regions Science and Technology).

Matskevitch, D. (1997b). Eccentric impact of an ice feature: Non-linear model. *Cold Regions Science and Technology 26*, 55–66.

McKenna, R., F. Ralph, D. Power, I. Jordaan, and S. Churchill (2003). Modelling iceberg management strategy. In *Proceedings of the 17trh Conference on Port and Ocean Engineering under Arctic Conditions.*

MEDS (1997). Canadian Offshore Oil and Gas Environmental Data. Marine Environmental Data Service, National Energy Board (CD-ROM).

Mellor, G. (1997). User's guide for a three-dimensional primitive equation, numerical ocean models. Technical report, Atmospheric and Ocean Sciences Program, Princeton University, Princeton, New Jersey.

Moore, M. (1985). Modelling Iceberg Motion: A Multiple-time-series Approach. *Canadian Journal of Statistics 13*(2), 88 94.

Moore, M. (1987). Exponential smoothing to predict iceberg trajectories. *Cold Regions Science and Technology 41*, 263 272.

Mountain, D. (1980). On predicting iceberg drift. *Cold Regions Science and Technology 1*(1), 273–282.

Muggeridge, K., M. Fuglem, I. Jordaan, D. Matskevitch, G. Crocker, and R. McKenna (1998). Canadian Offshore Design for Ice Environments, Final Report, Ice Environment and Model Framework. Technical report, Ocean Engineering Resource Centre, Memorial University of Newfoundland, St. John's, Newfoundland.

Murray, J. E. (1969). The drift, deterioration and distribution of icebergs in the North Atlantic. In *Ice Seminars CIMM*, Volume 10, Calgary, Alberta, pp. 3 18. The canadian Institute of Mining and Metallurgy.

PAL (2000). The 2000 iceberg season on the Grand Banks,. Final Report for the Grand Banks Management Team. PAL Environmental Services.

PAL (2001). The 2001 iceberg season on the Grand Banks,. Final Report for the Grand Banks Management Team. PAL Environmental Services.

PAL (2002). The 2002 iceberg season on the Grand Banks,. Final Report for the Grand Banks Management Team. PAL Environmental Services.

PAL (2003). The 2003 iceberg season on the Grand Banks,. Final Report for the Grand Banks Management Team. PAL Environmental Services.

PAL (2004). The 2004 iceberg season on the Grand Banks,. Final Report for the Grand Banks Management Team. PAL Environmental Services.

PERD (2003). PERD Comprehensive Iceberg Management Database. Technical report, PERD/CHC Report 20-69 prepared by PAL Environmental Services, July.

Petrie, B. (1982). Aspects of the Circulation on the Newfoundland Continental Shelf. Canadian Technical Report Hydrography Ocean Sciences, Number 11, Bedford Institute of Oceanography, Dartmouth, Nova Scotia.

Pond, S. and G. Pickard (1983). *Introductory Dynamical Oceanography.* New York, New York: Pergamon Press.

Rayleigh, L. (1915). The principle of similitude. *Nature 95*(66), 396–397.

Sanderson, T. (1988). *Ice Mechanics: Risks to Offshore Structures.* London, U.K.: Graham and Trotman Ltd.

Savage, S. (1999). State of the Art Review-Prediction of Iceberg Deterioration and Drift. Report for Canadian Ice Services (CIS), Environment Canada, Contract KM149-8-S028/001/SS.

Savage, S. B. (2001). Aspects of Iceberg Deterioration and Drift. In N. J. Balmforth and A. Provenzale (Eds.), *Geomorphological Fluid Mechanics*, Volume 582 of *Lecture Notes in Physics, Berlin Springer Verlag*, pp. 279–318.

Sayed, M. (2000). Implementation of Iceberg Drift and Deterioration Model. Technical Report HYD-TR-049, Canadian Hydraulics Centre, National Research Council of Canada, Ottawa, ON.

Seaconsult (1988). Physical Environmental Data for Productions Systems at Terra Nova. Technical report, Tecnical report prepared for Petro-Canada Inc.

Sharp, J. and E. Moore (1988). A systematic approach to the development of echelon matrices for dimensional analysis. *International Journal of Mathematical Education in Science and Technology 19*(3), 461–467.

Smith, S. and E. Banke (1981). A numerical model of iceberg drift. In *Proceedings of the 6th International Conference on Port and Ocean Engineering under Arctic Conditions*, Volume 2, pp. 1001–1011. POAC.

Smith, S. and N. Donaldson (1987). Dynamic Modelling of Iceberg Drift Using Current Profiles. Canadian Technical Report of Hydrogrpahy and Ocean Sciences No. 91, Bedford Institute of Oceanography, Dartmouth, Canada.

Sodhi, D. and M. El-Tahan (1980). Prediction of an iceberg drift trajectory during a storm. *Annals of Glaciology 1*, 77–82.

Soulis, E. (1976). Modelling of iceberg drift using wind and current measurements at a fixed station. Master's thesis, Faculty of Engineering and Applied Science, Memorial University of Newfoundland, St. John's, Canada.

Swail, V., E. Ceccacci, and T. Cox (2000). The AES40 North Atlantic wave analysis: validation and climate assessment. PERD Workshop, Environmental Factors

and Loads Related to Petroleum Development on the Grand Banks, September 25-26, 2000, St. John's, Newfoundland.

Appendix A

Comparison Between Observed and Modelled Drift Speed Data Sets Based on Iceberg Size

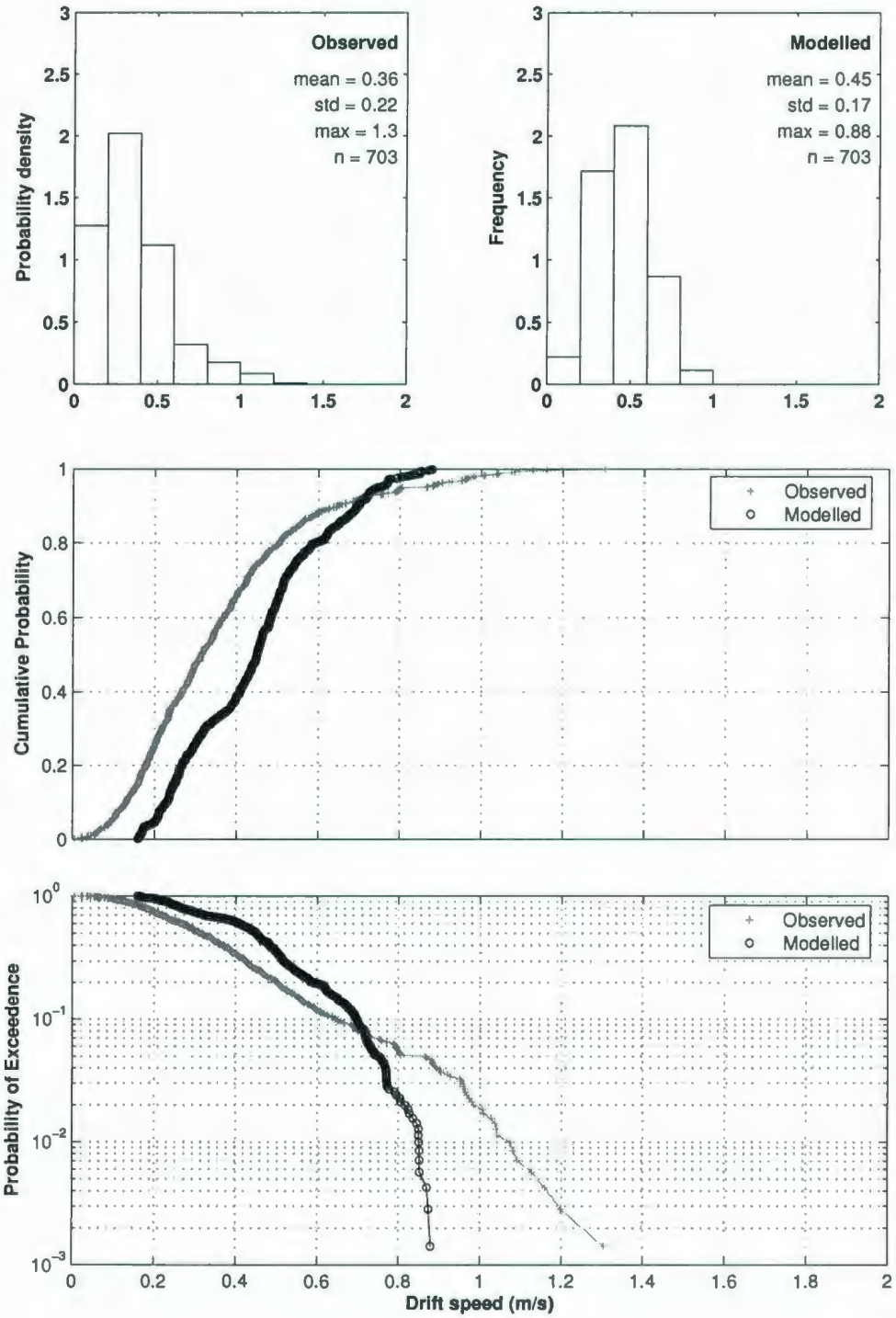

Figure A.1: Comparison of observed and modelled drift speed distributions for bergy bits and growlers

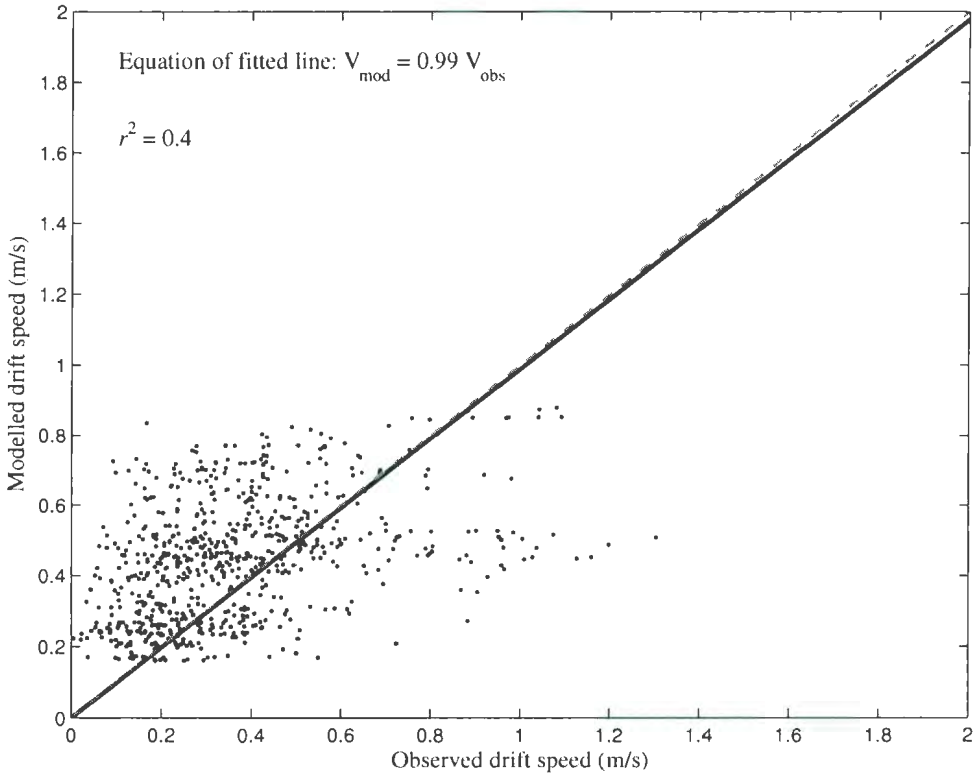

Figure A.2: Correlation between observed and modelled drift speed data for bergy bits and growlers

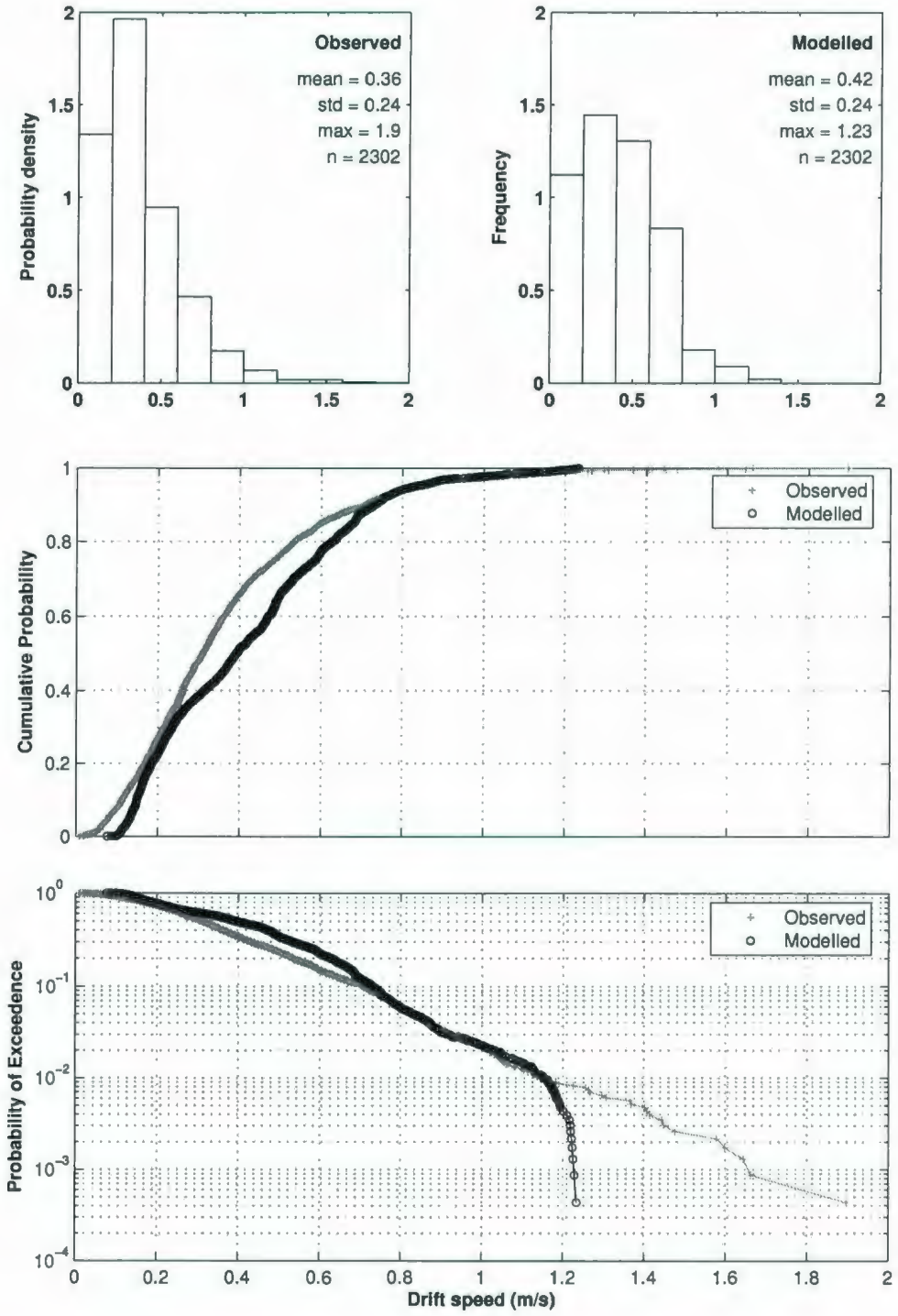

Figure A.3: Comparison of observed and modelled drift speed distributions for small icebergs

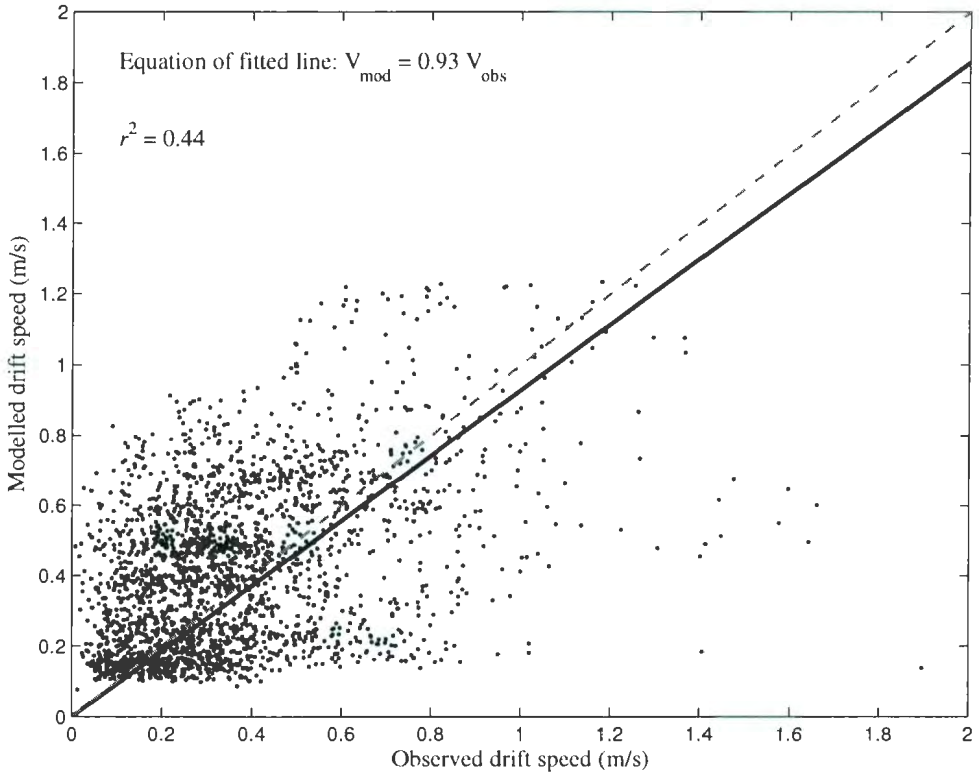

Figure A.4: Correlation between observed and modelled drift speed data for small icebergs

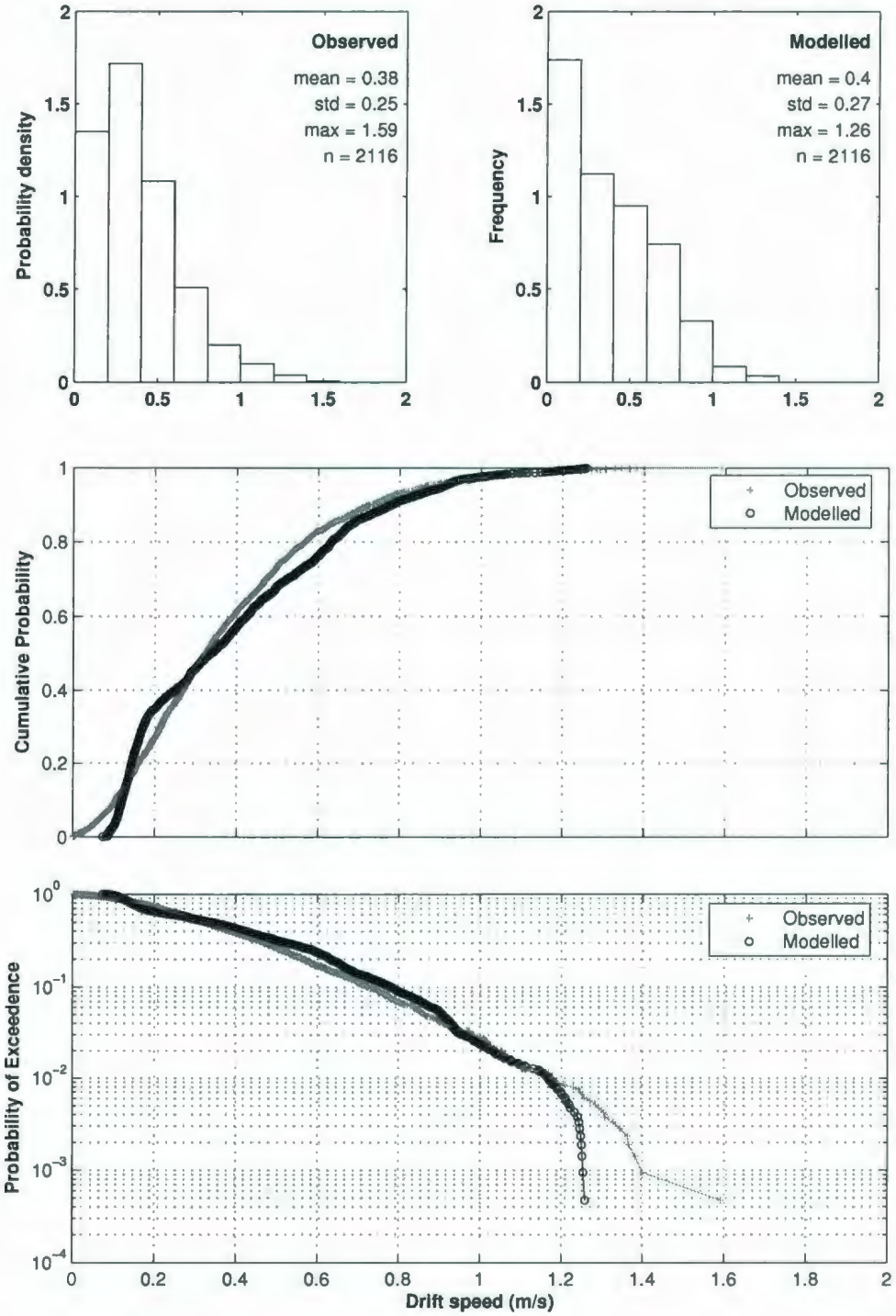

Figure A.5: Comparison of observed and modelled drift speed distributions for medium icebergs

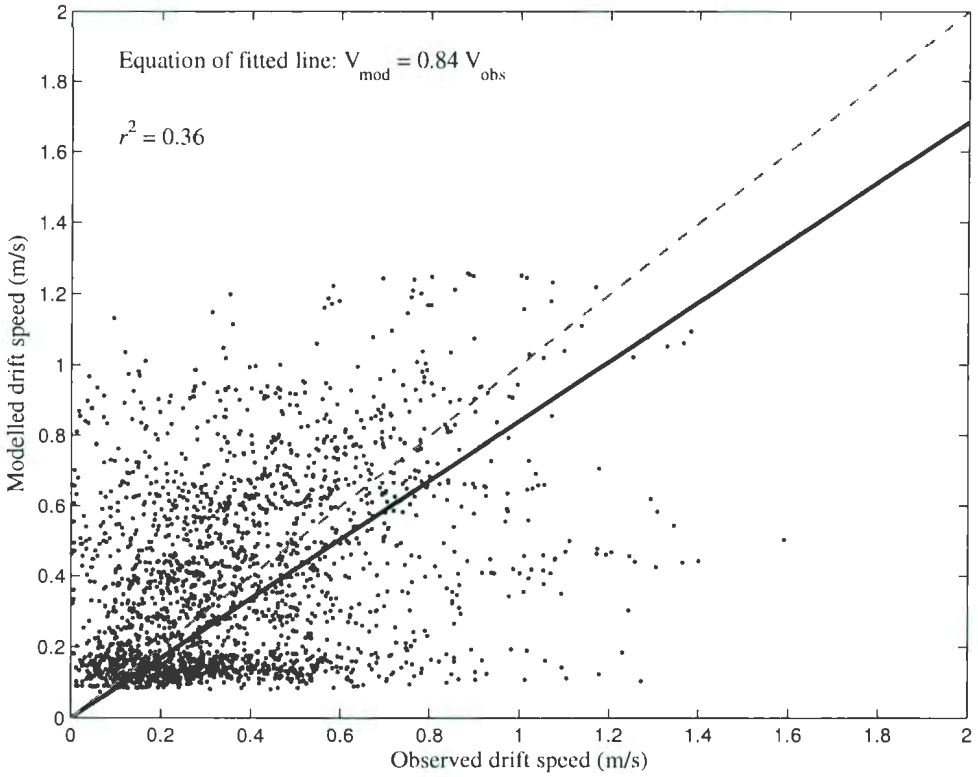

Figure A.6: Correlation between observed and modelled drift speed data for medium icebergs

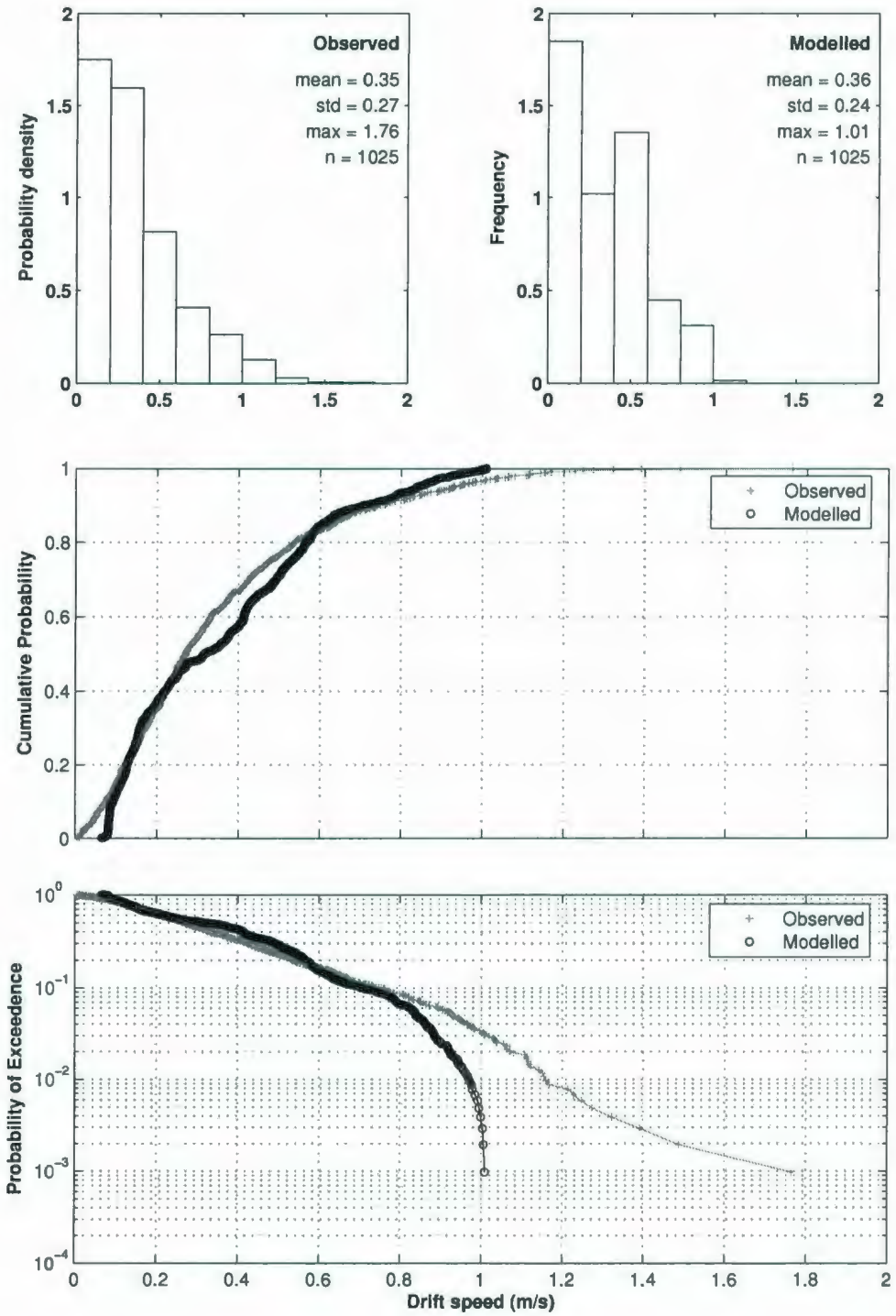

Figure A.7: Comparison of observed and modelled drift speed distributions for large and extra-large icebergs

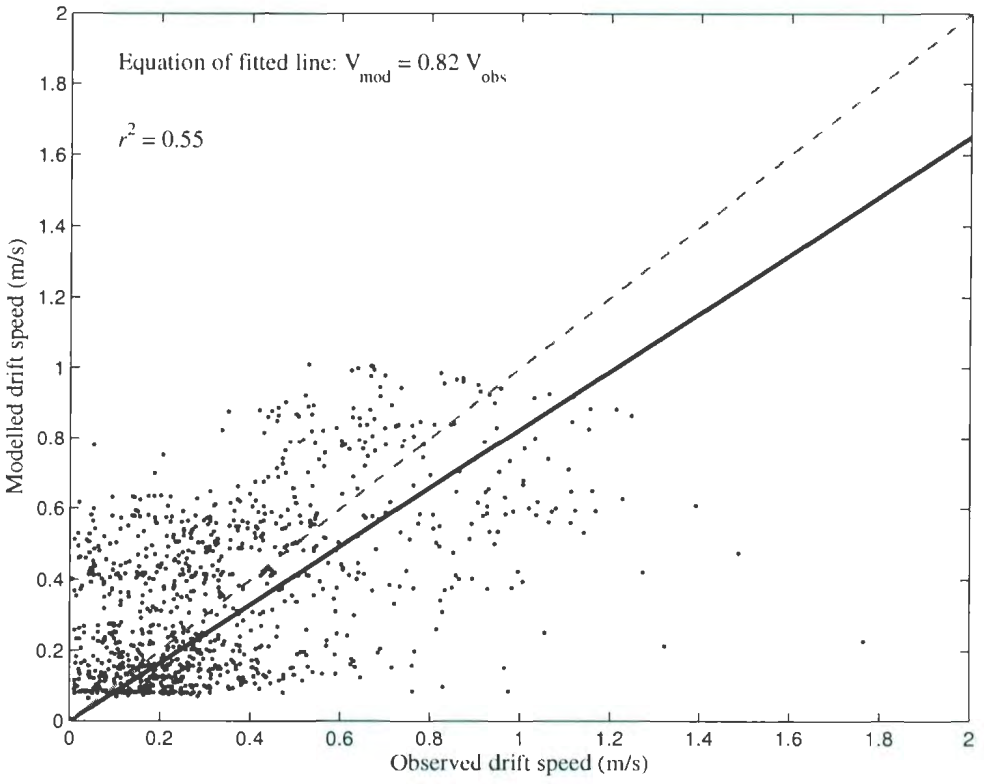

Figure A.8: Correlation between observed and modelled drift speed data for large and extra-large icebergs

Appendix B

Comparison Between Observed and Modelled Drift Speed Data Sets Based on Significant Wave Height

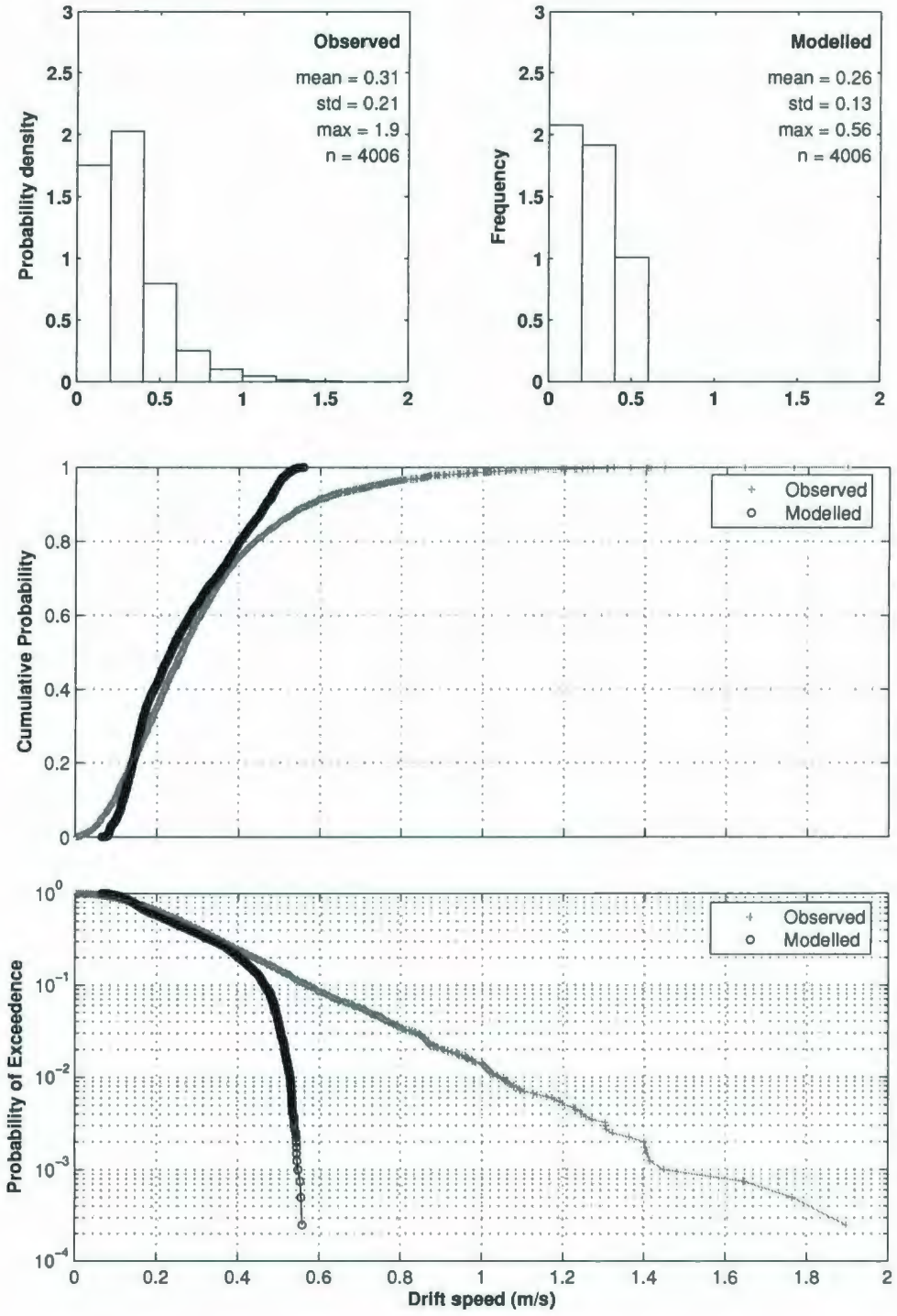

Figure B.1: Comparison of observed and modelled drift speed distributions for low sea state conditions

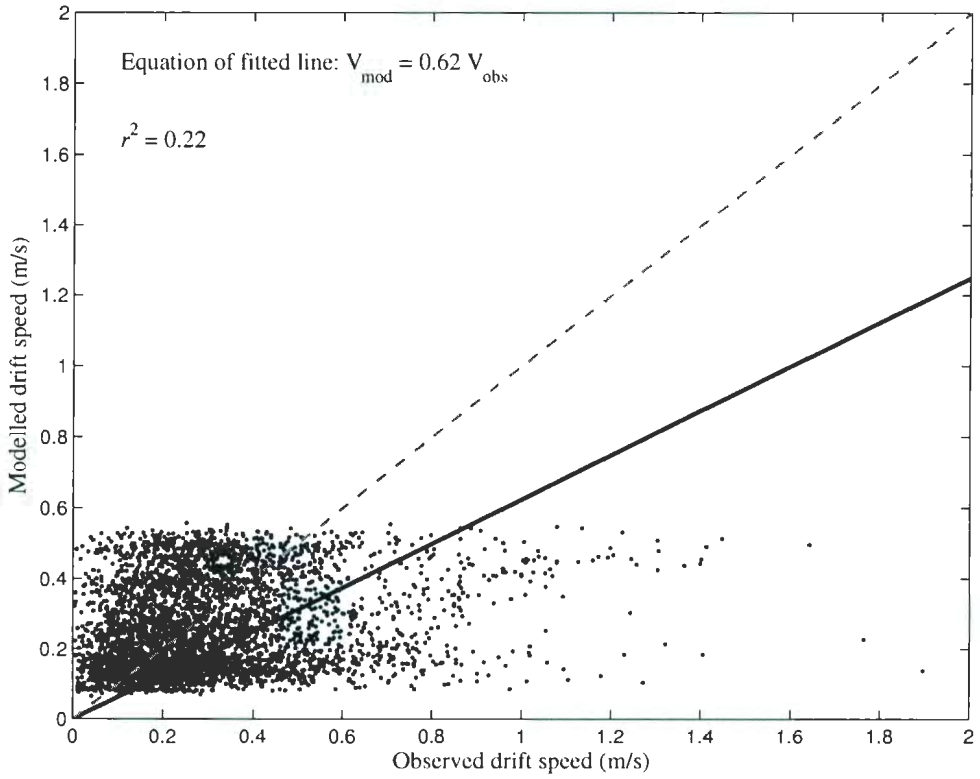

Figure B.2: Correlation between observed and modelled drift speed data for low sea state conditions

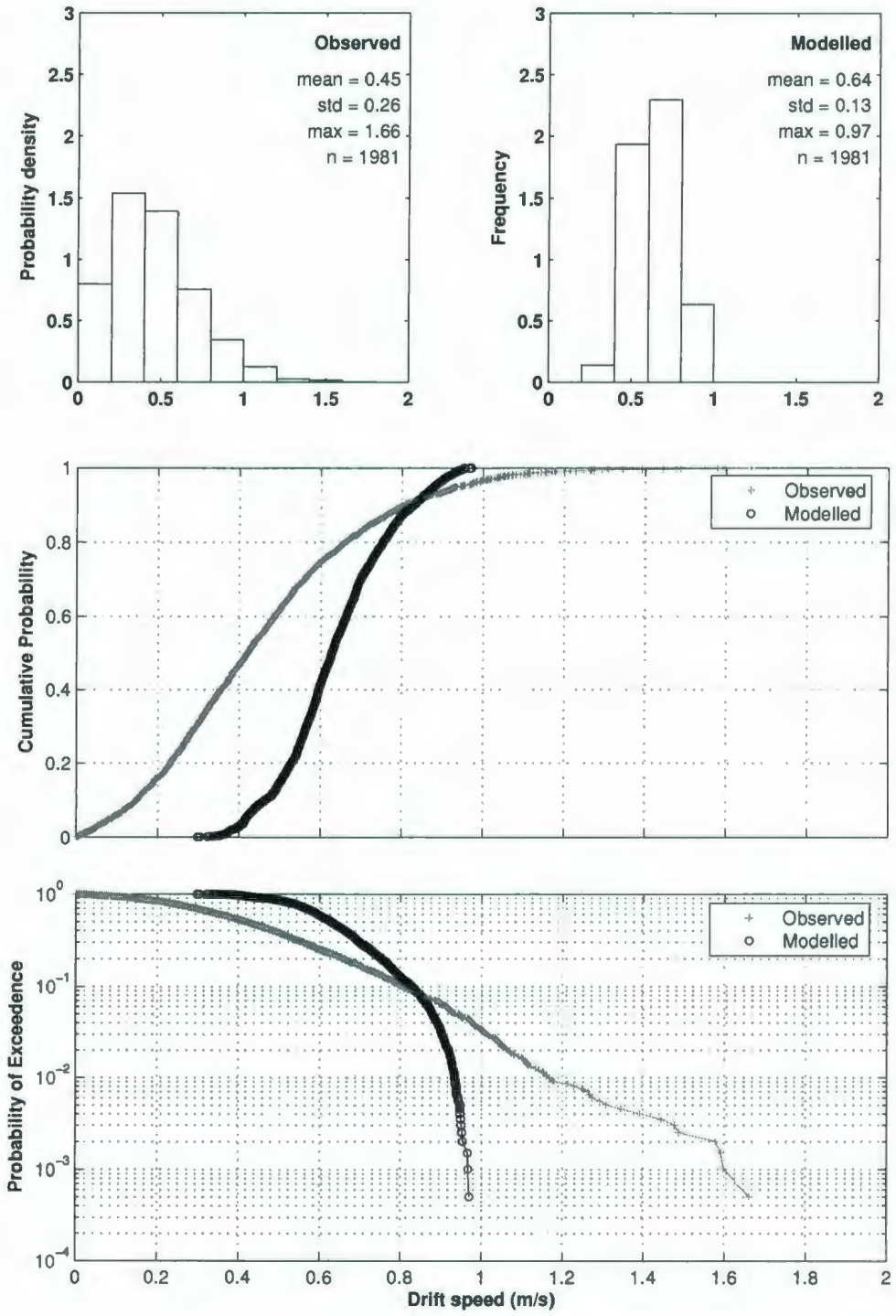

Figure B.3: Comparison of observed and modelled drift speed distributions for medium sea state conditions

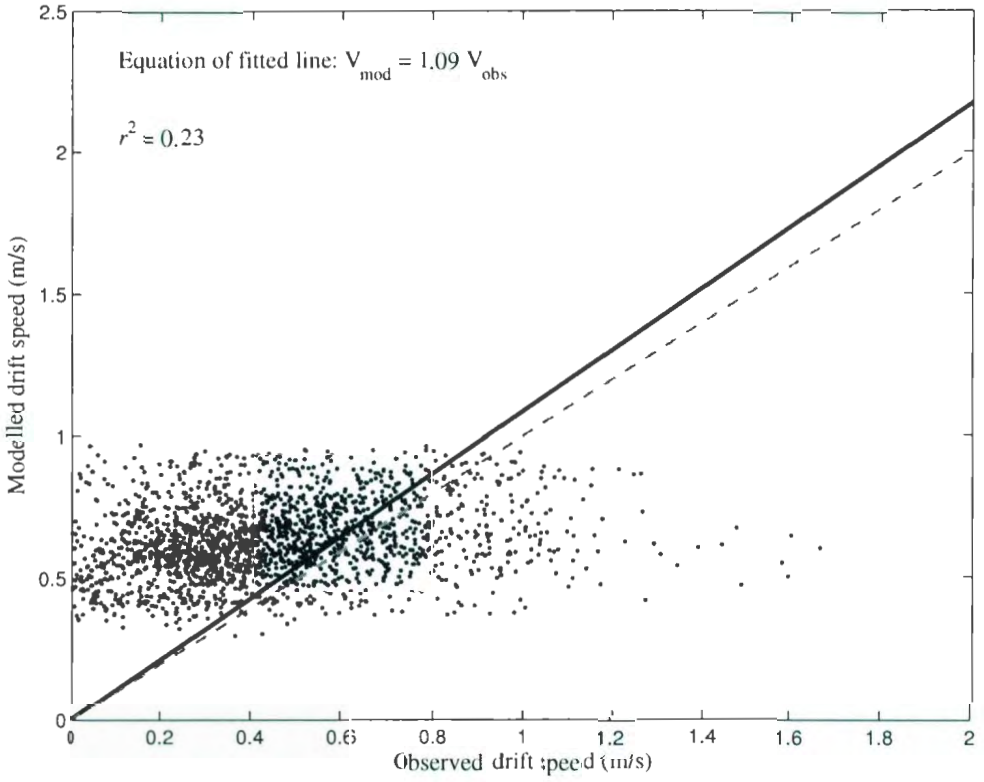

Figure B.4: Correlation between observed and modelled drift speed data for medium sea state conditions

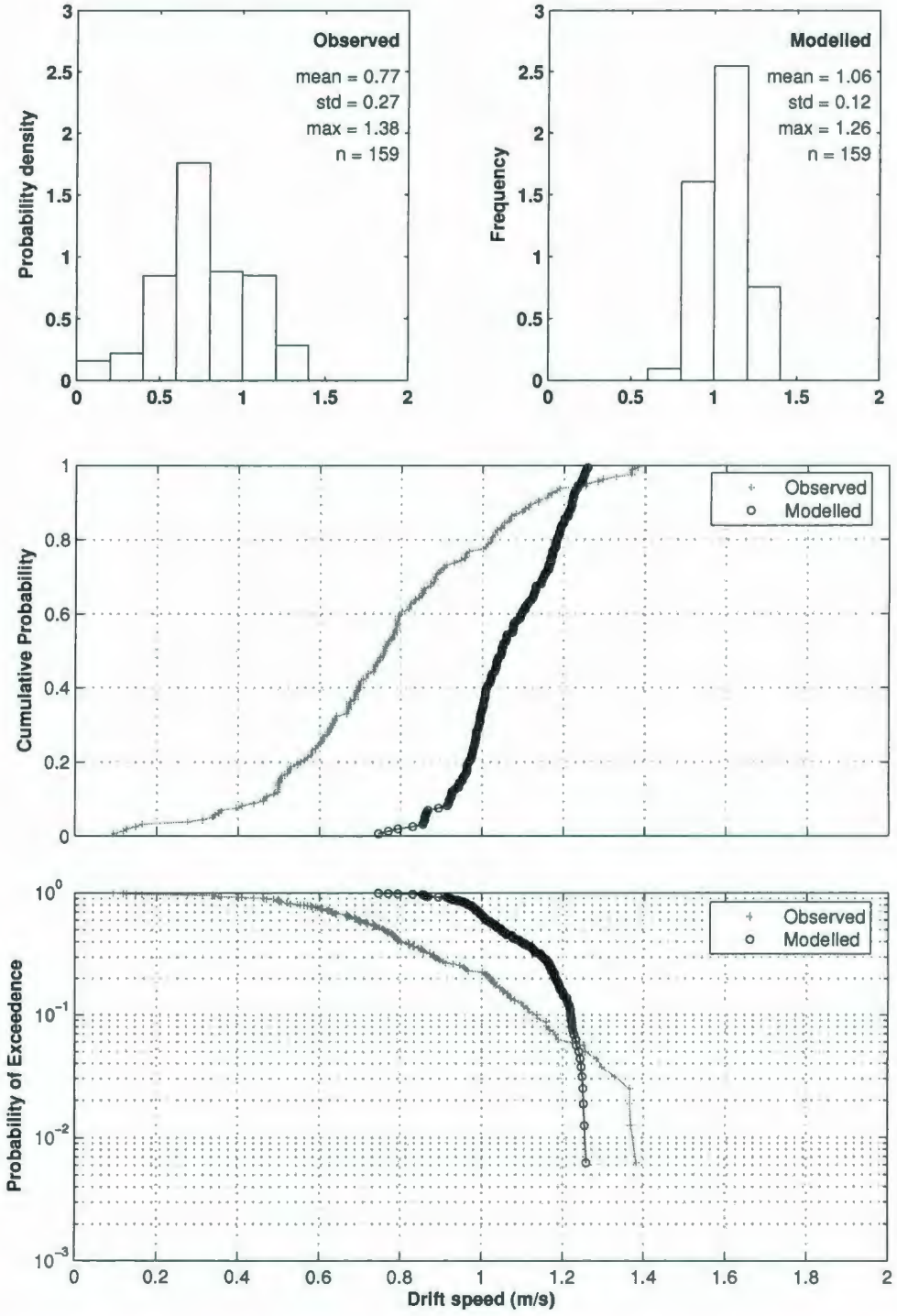

Figure B.5: Comparison of observed and modelled drift speed distributions for high sea state conditions

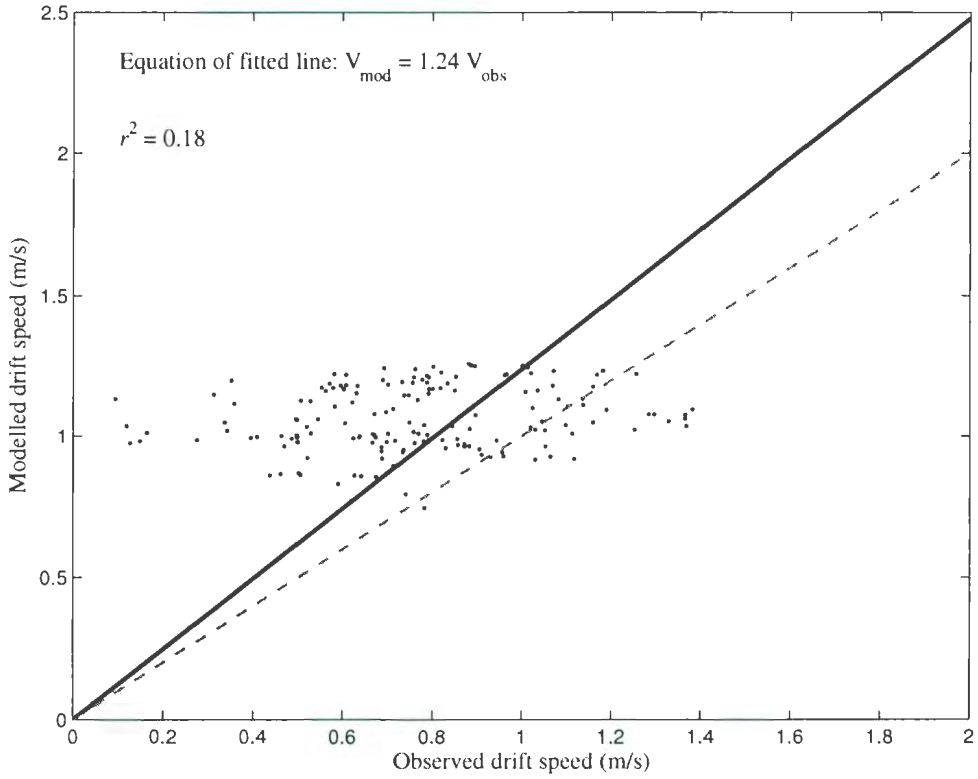

Figure B.6: Correlation between observed and modelled drift speed data for high sea state conditions

Appendix C

Comparison Between Observed and Modelled Drift Speed Data Sets Based on Joint Distribution

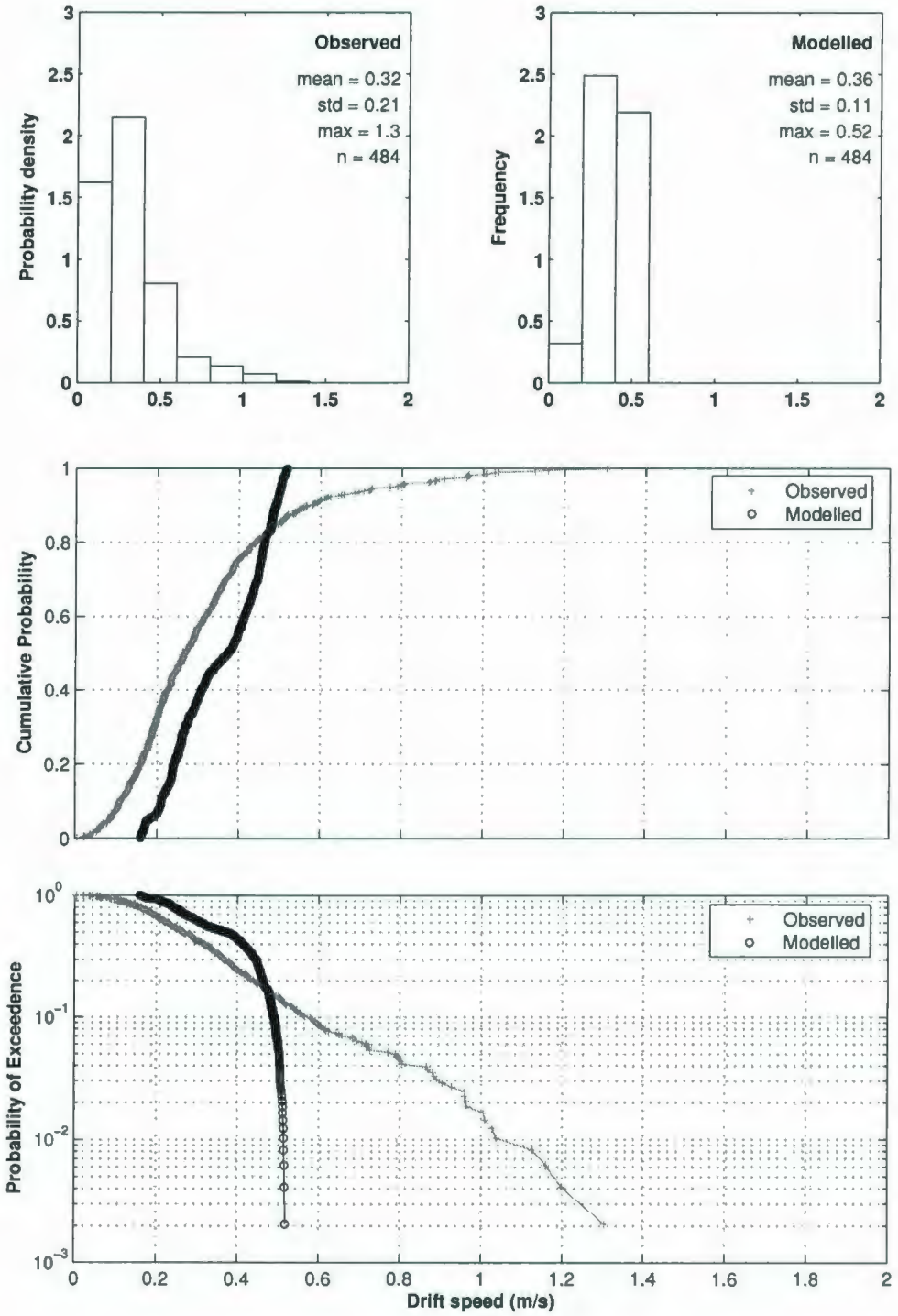

Figure C.1: Comparison of observed and modelled drift speed distributions for bergy bits and growlers in low sea state

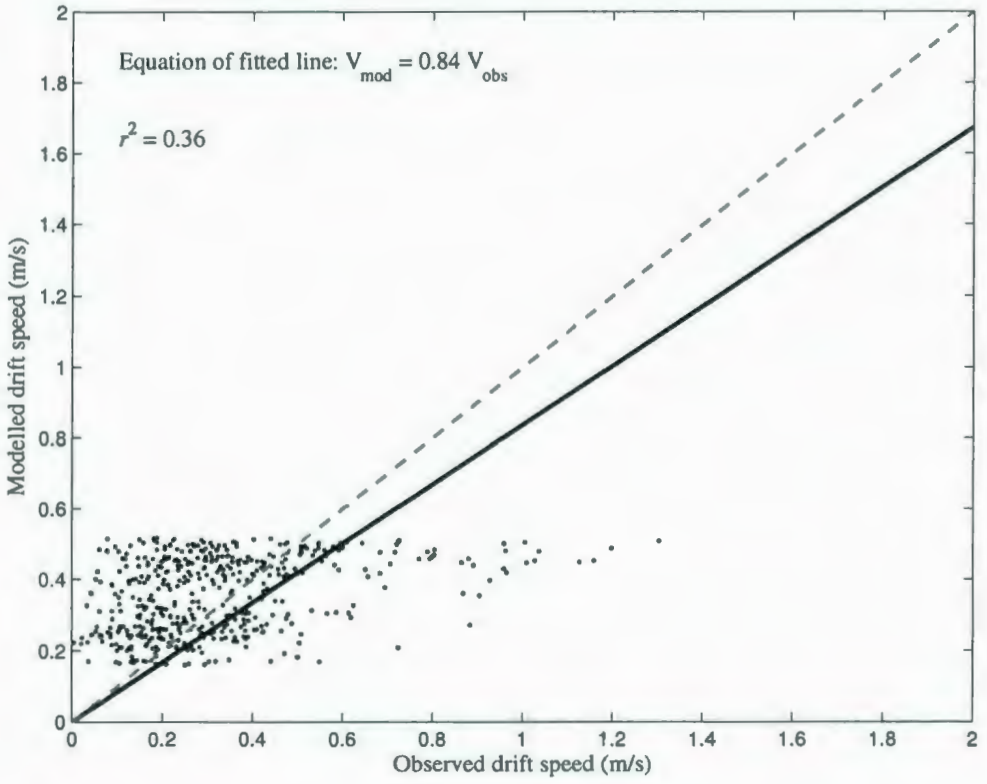

Figure C.2: Correlation between observed and modelled drift speed data for bergy bits and growlers in low sea state

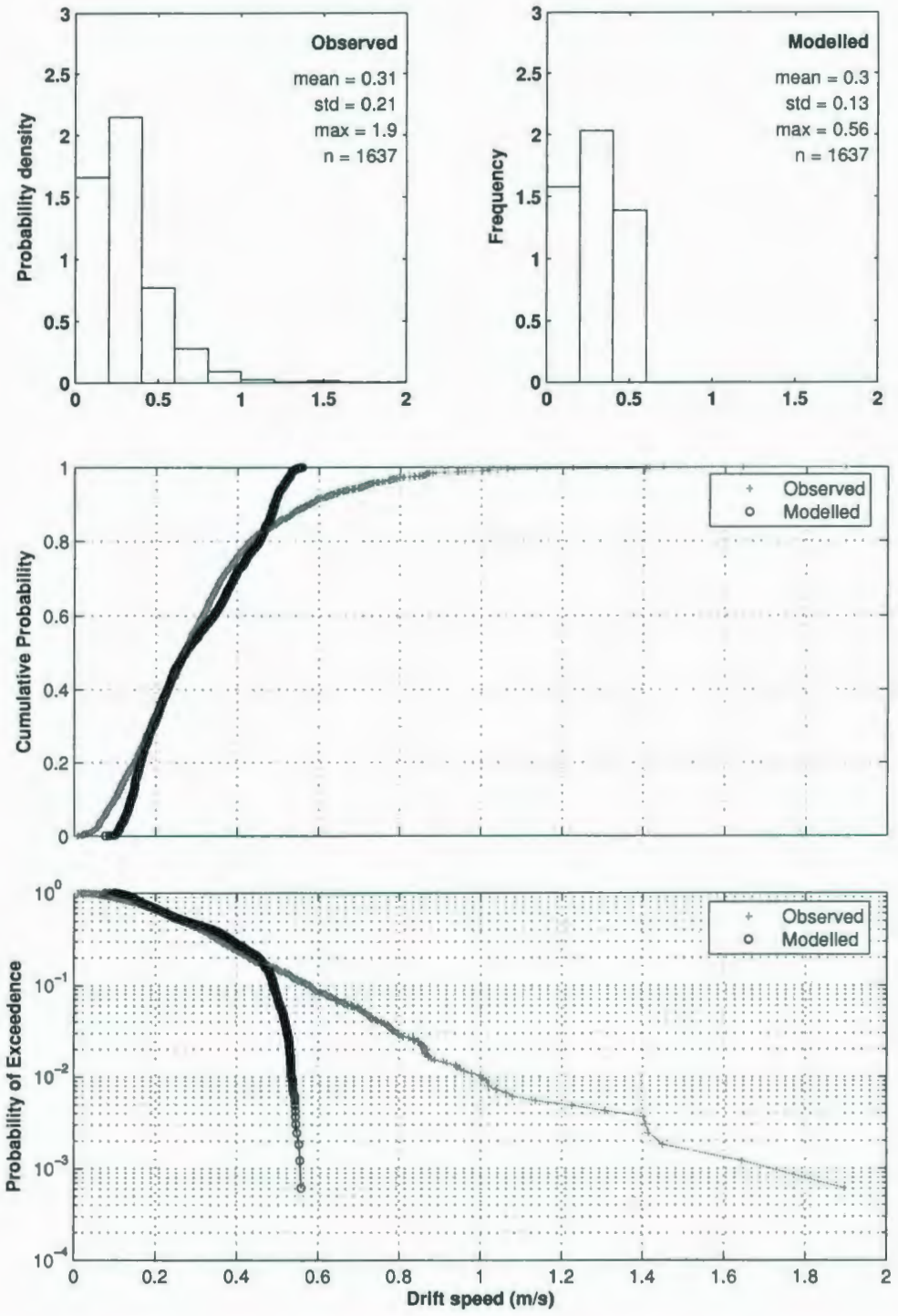

Figure C.3: Comparison of observed and modelled drift speed distributions for small icebergs in low sea states

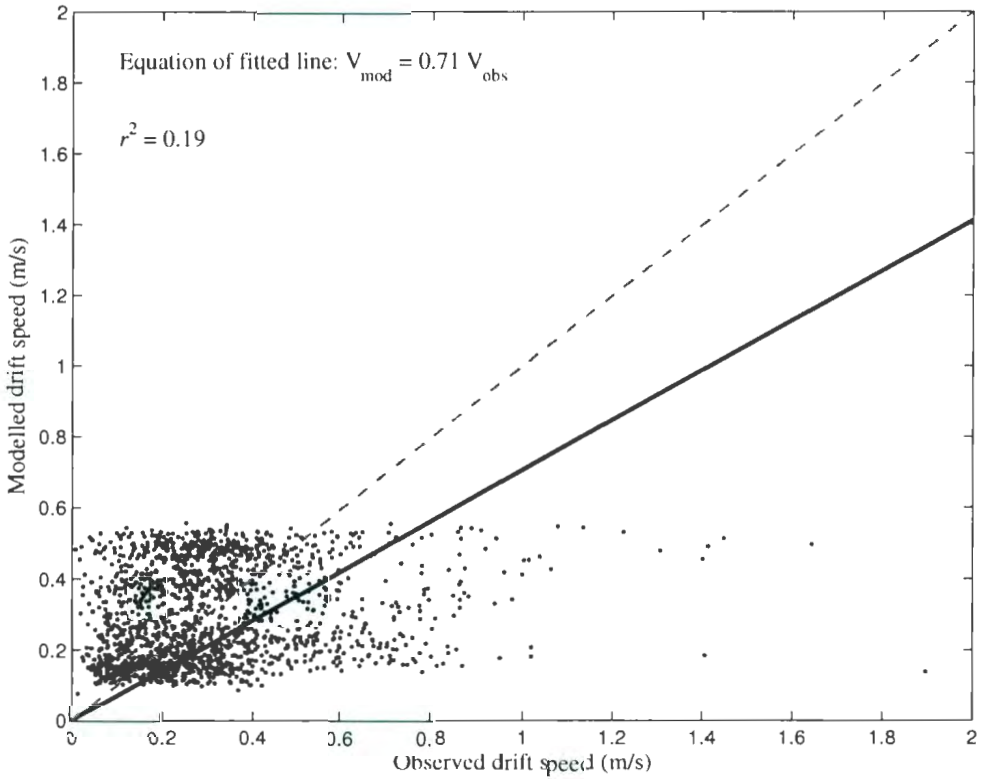

Figure C.4: Correlation between observed and modelled drift speed data for small icebergs in low sea state

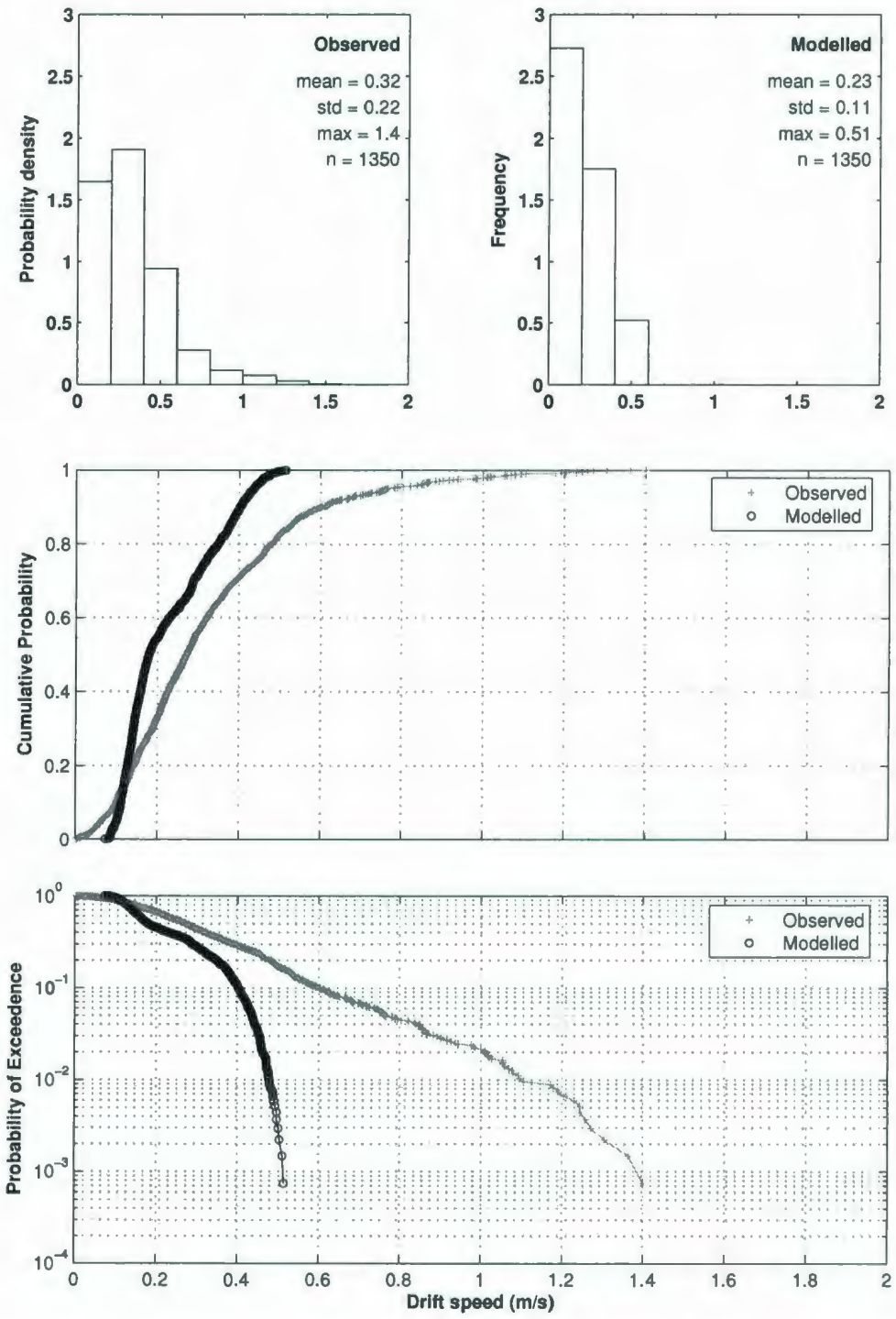

Figure C.5: Comparison of observed and modelled drift speed distributions for medium icebergs in low sea state

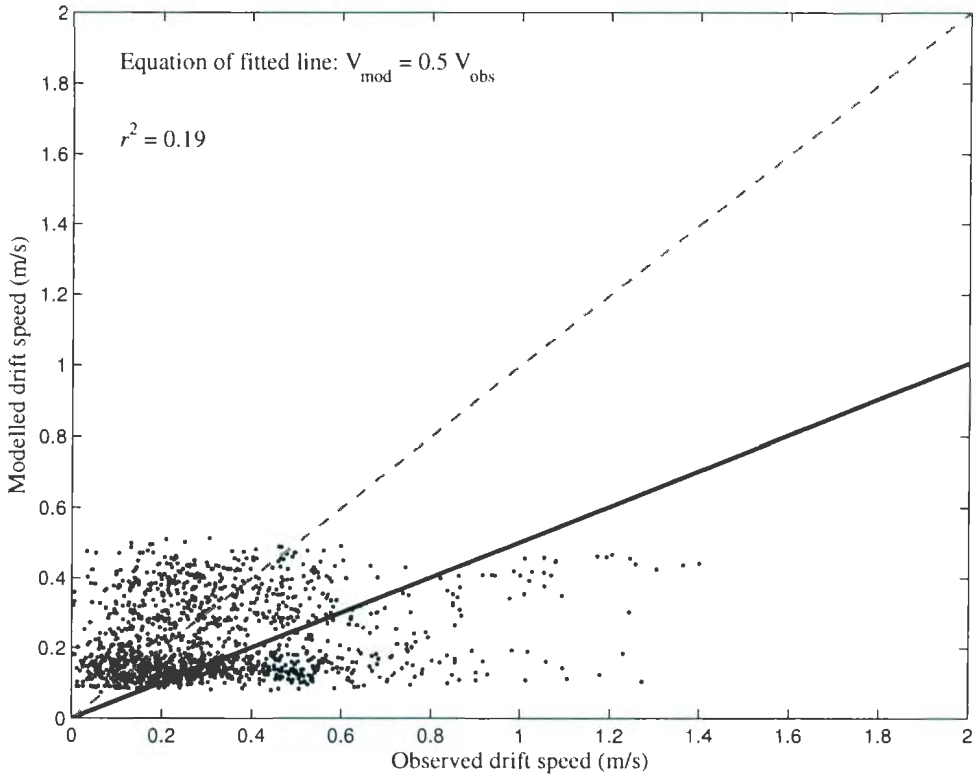

Figure C.6: Correlation between observed and modelled drift speed data for medium icebergs in low sea state

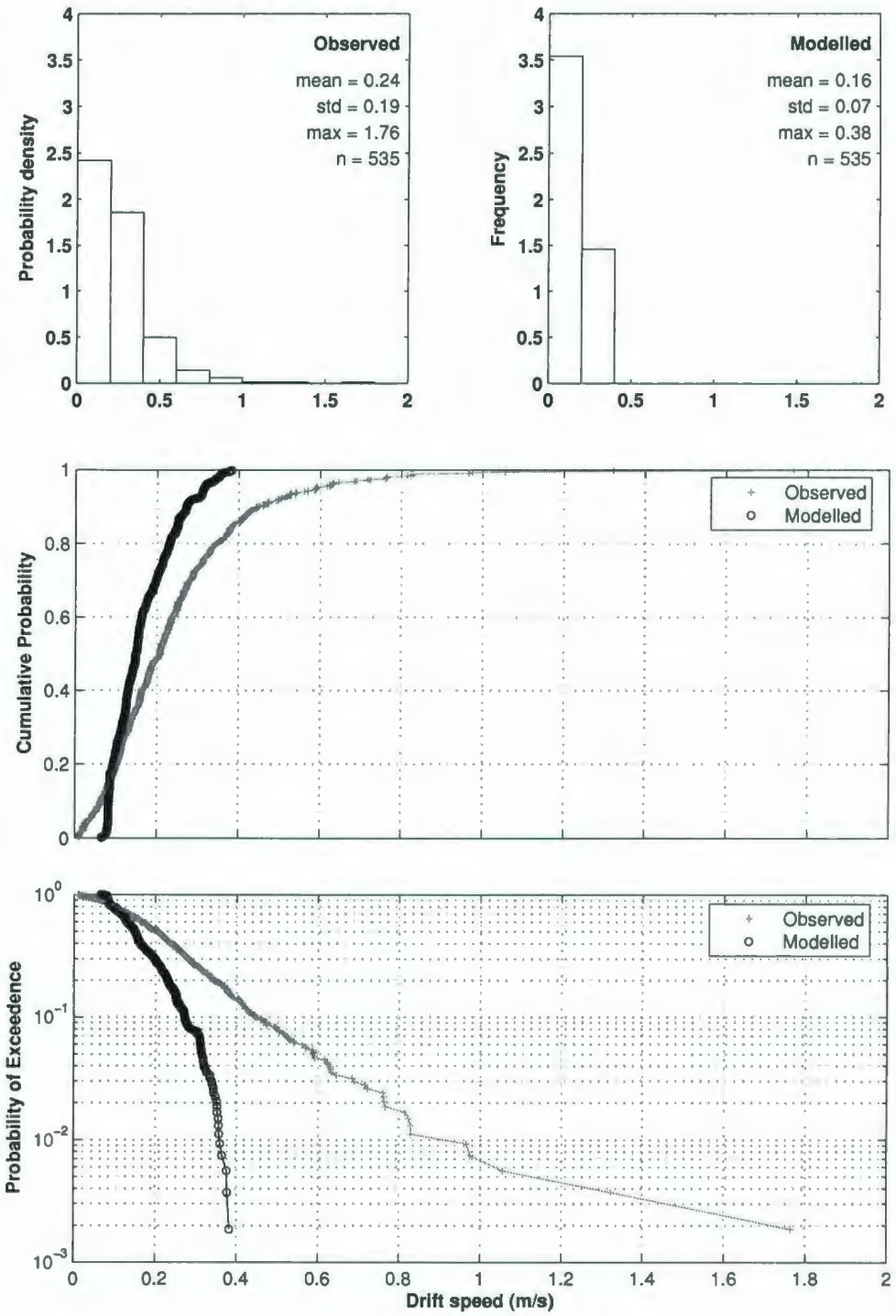

Figure C.7: Comparison of observed and modelled drift speed distributions for large and extra-large icebergs in low sea state

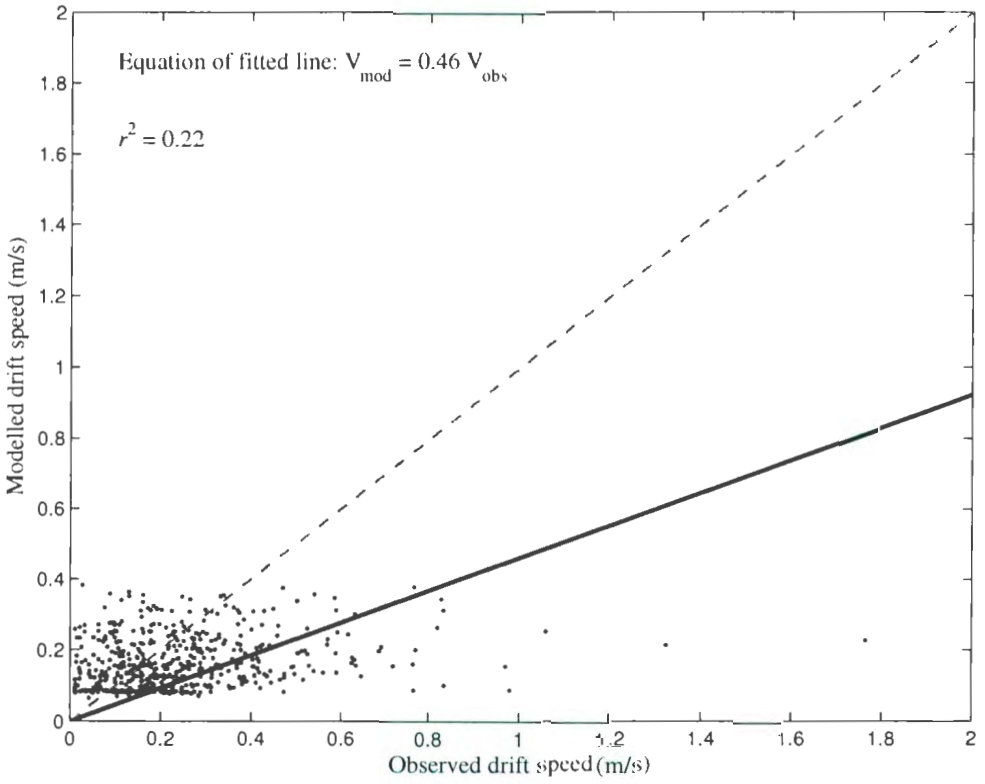

Figure C.8: Correlation between observed and modelled drift speed data for large and extra-large icebergs in low sea state

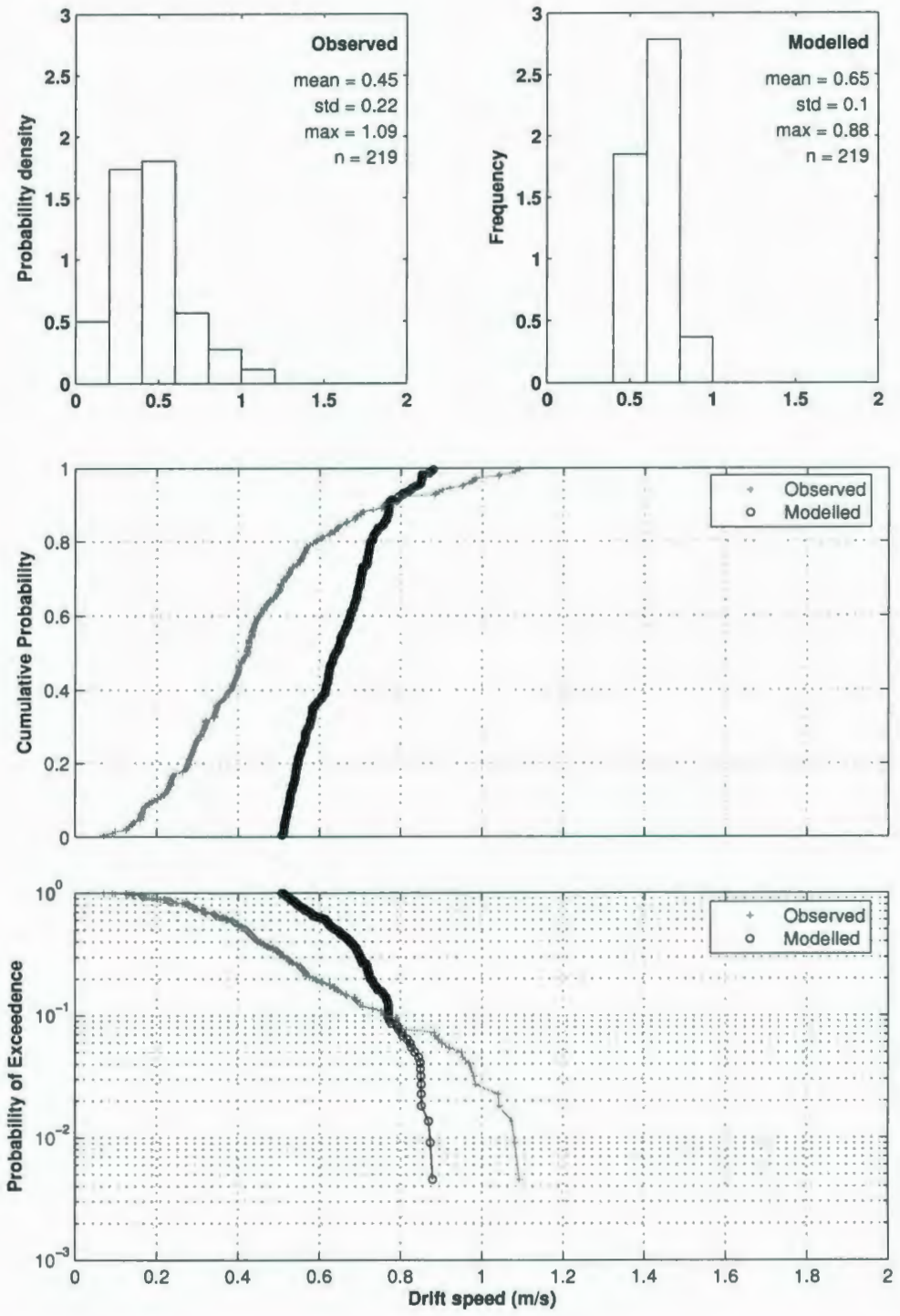

Figure C.9: Comparison of observed and modelled drift speed distributions for bergy bits and growlers in medium sea states

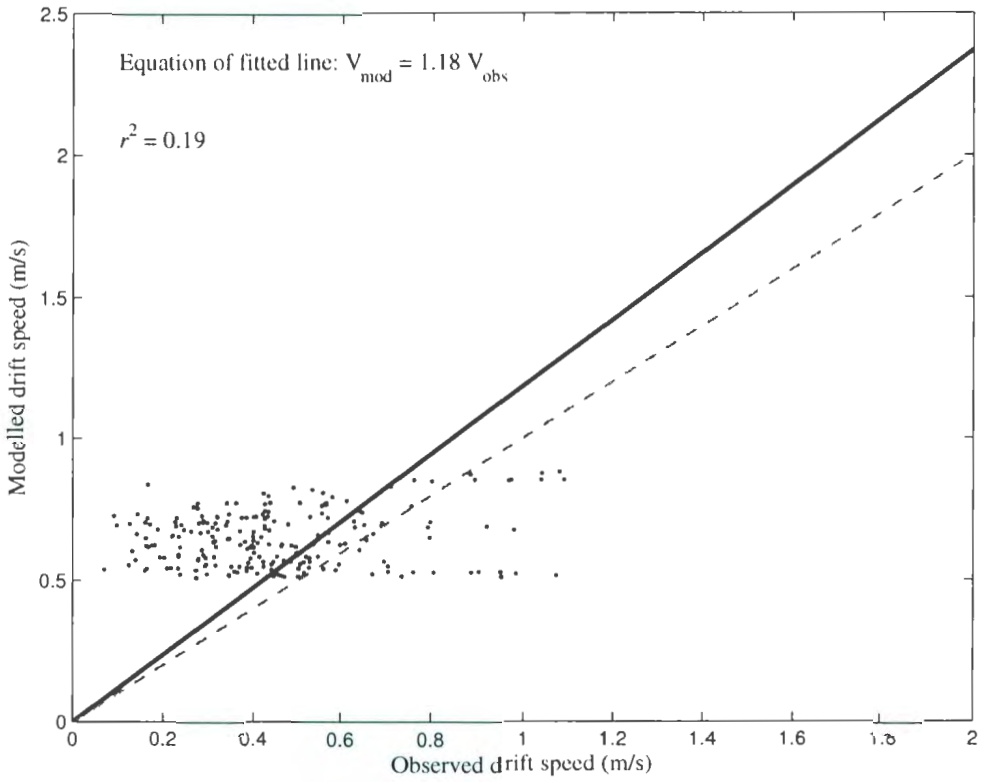

Figure C.10: Correlation between observed and modelled drift speed data for bergy bits and growlers in medium sea states

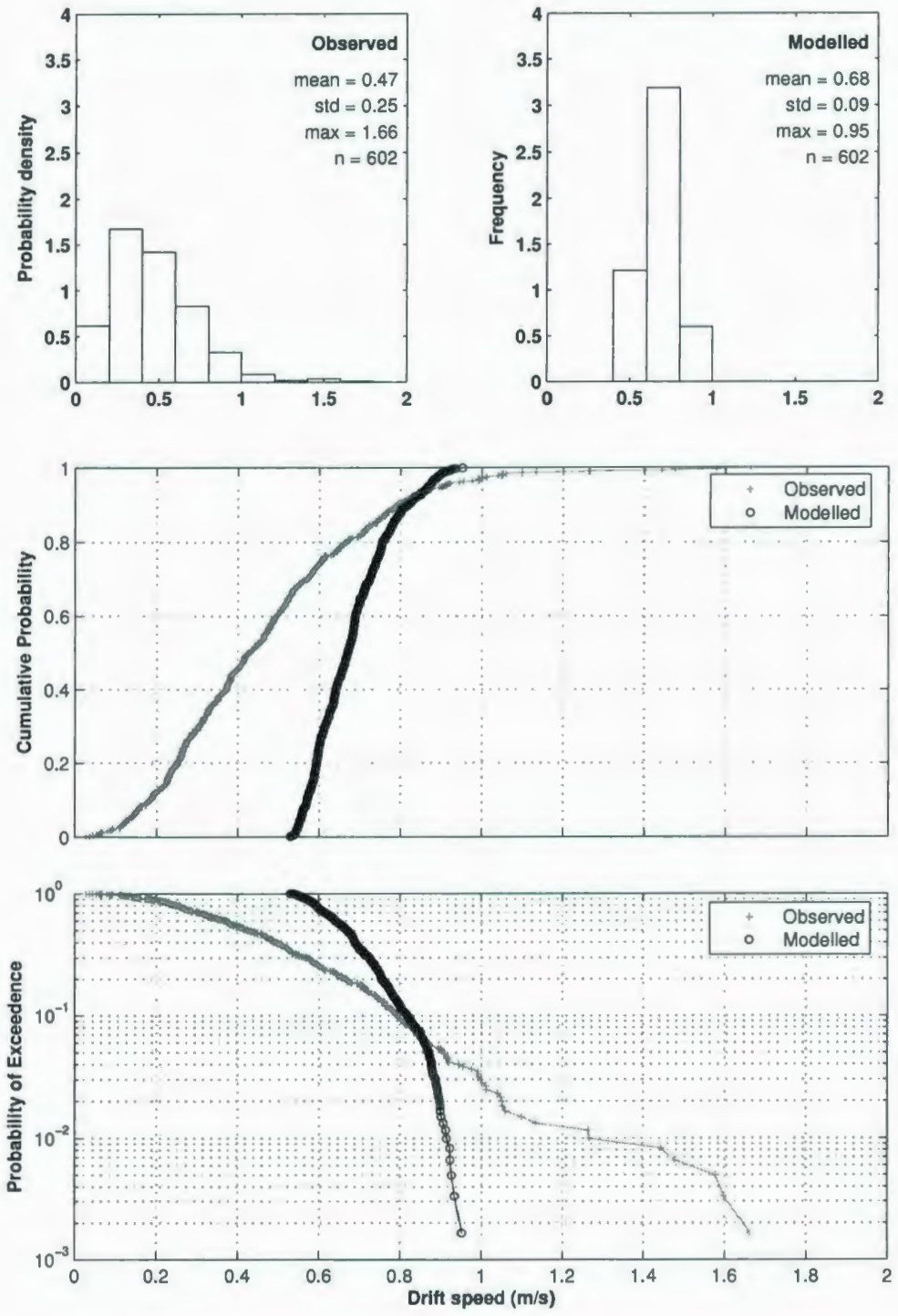

Figure C.11: Comparison of observed and modelled drift speed distributions for small icebergs in medium sea states

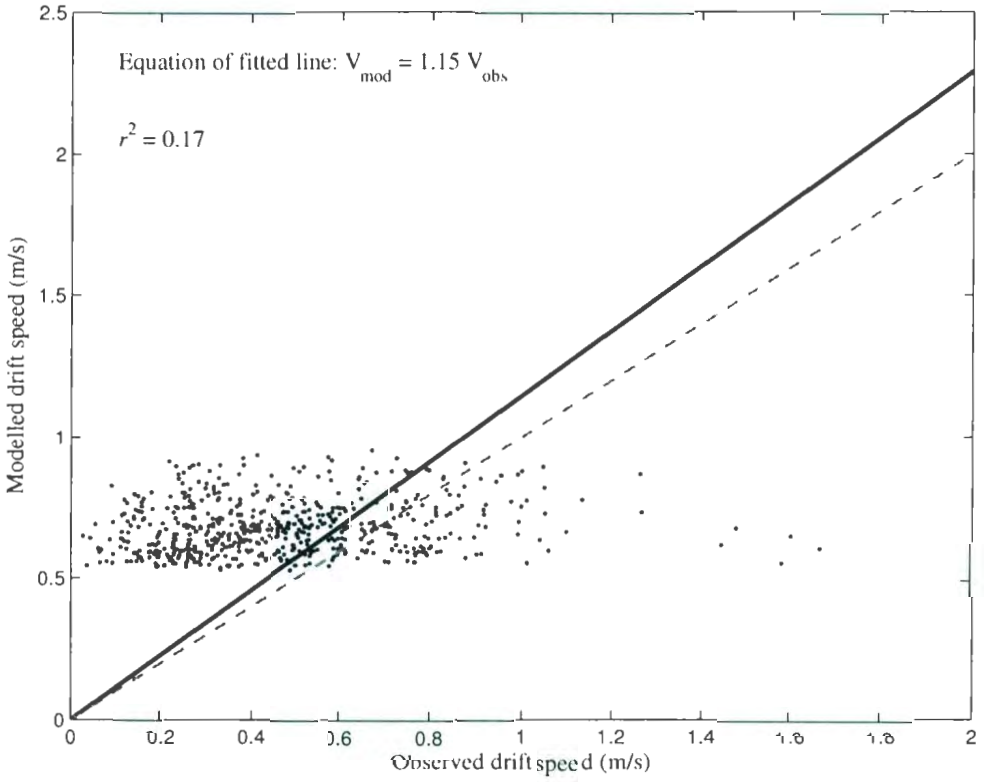

Figure C.12: Correlation between observed and modelled drift speed data for small icebergs in medium sea states

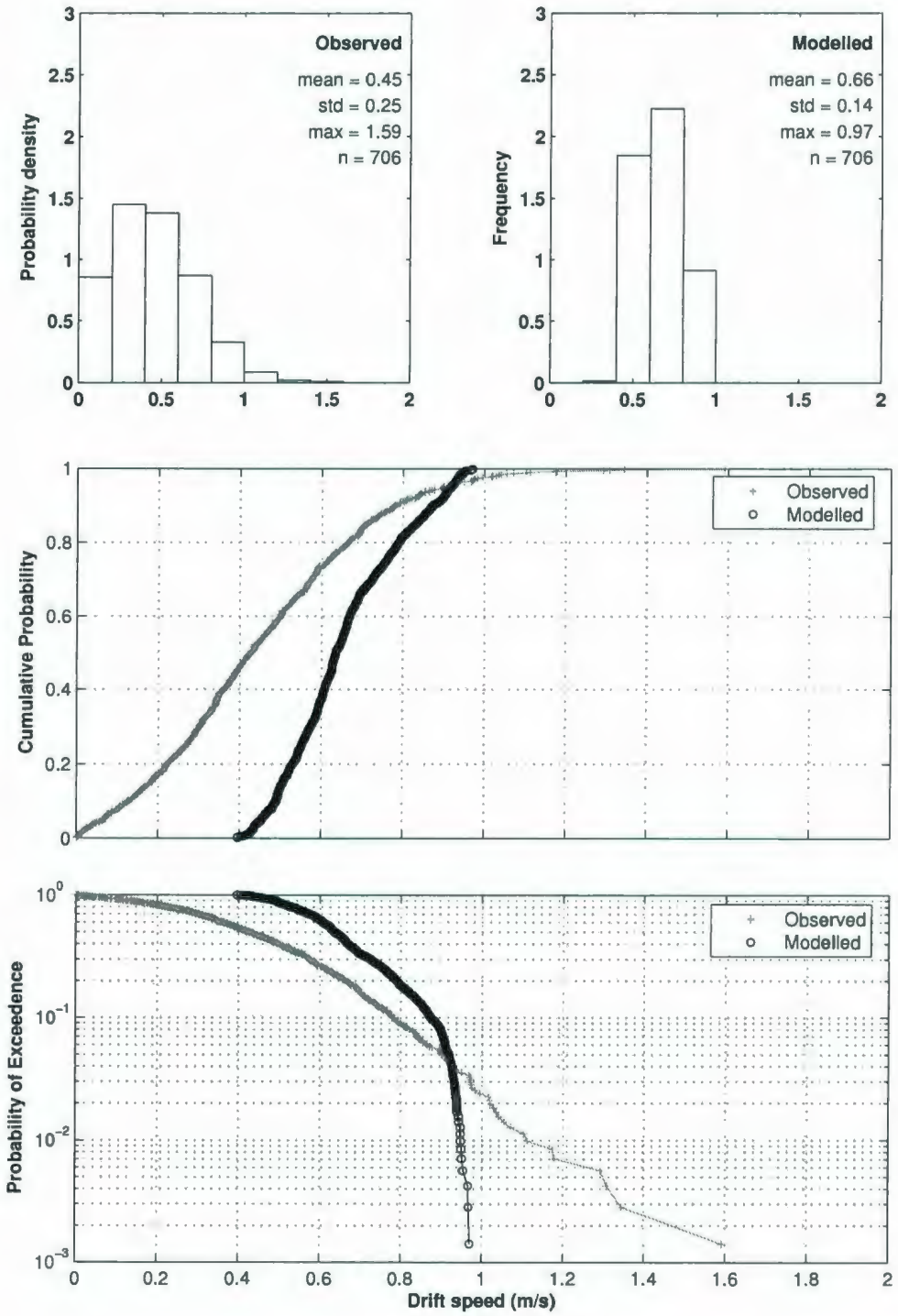

Figure C.13: Comparison of observed and modelled drift speed distributions for medium icebergs in medium sea states

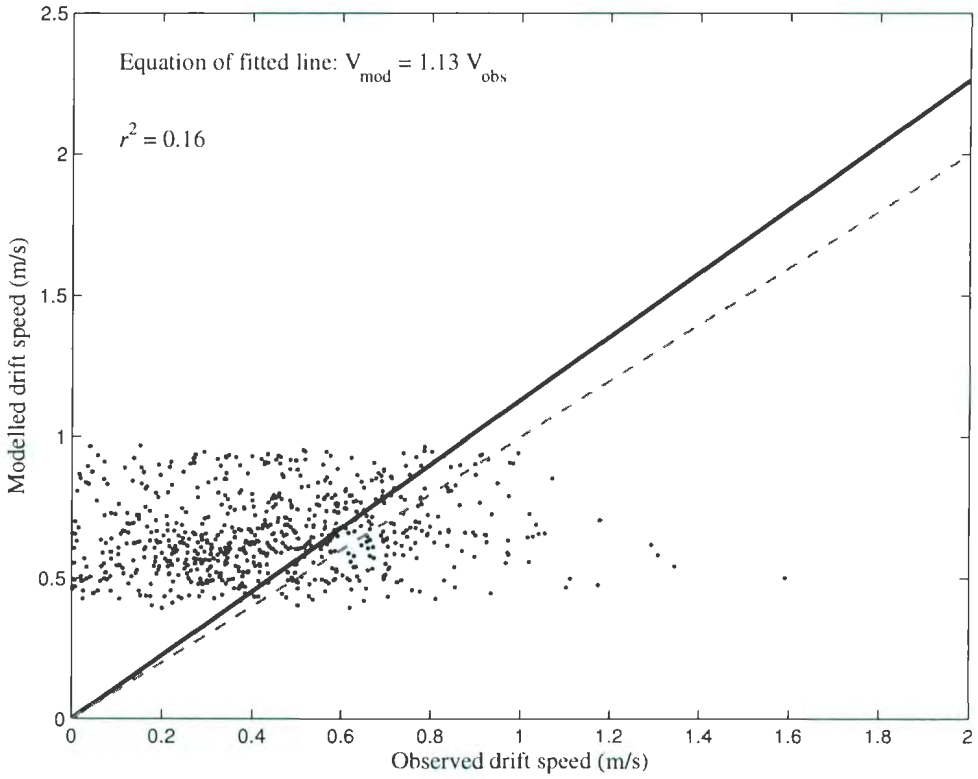

Figure C.14: Correlation between observed and modelled drift speed data for medium icebergs in medium sea states

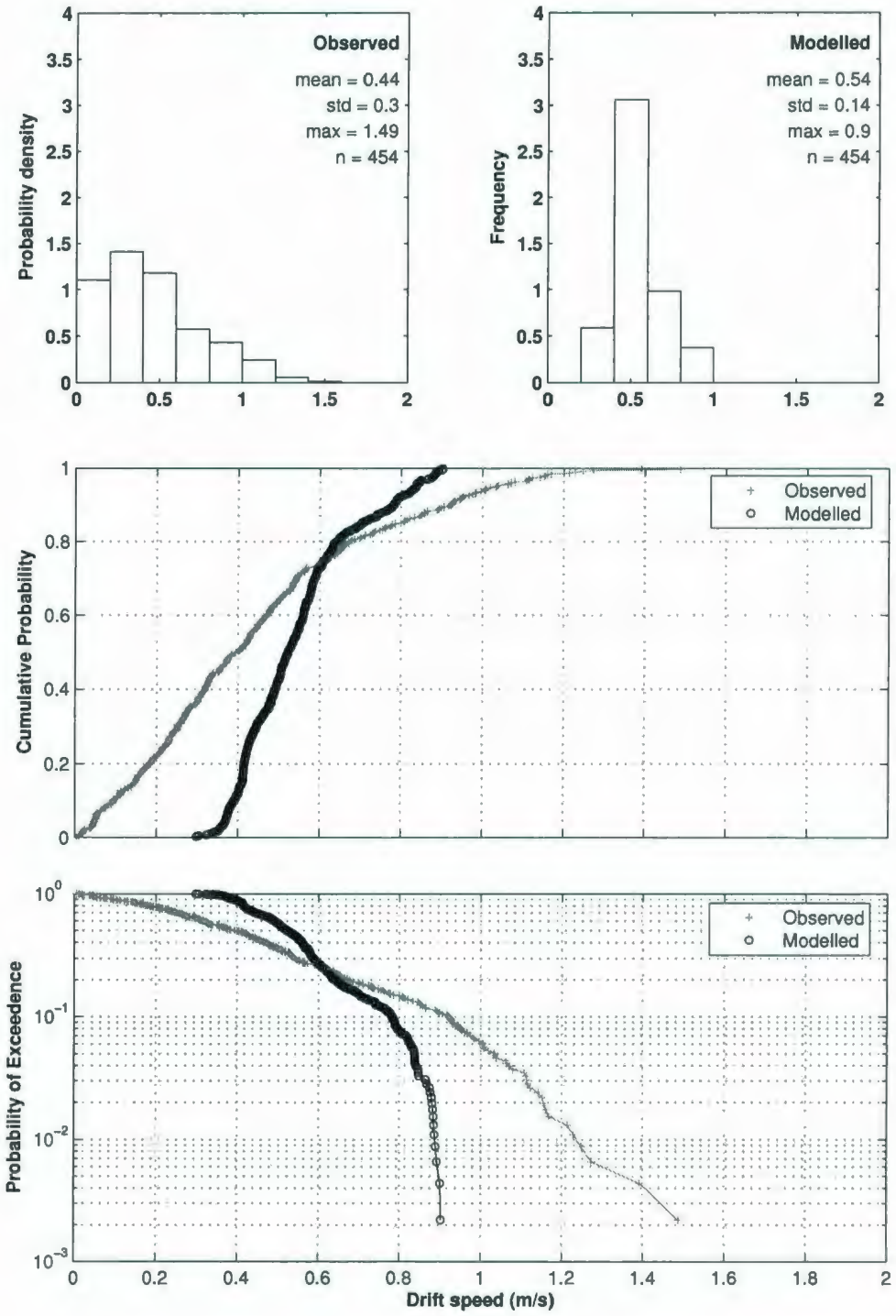

Figure C.15: Comparison of observed and modelled drift speed distributions for large and extra-large icebergs in medium sea states

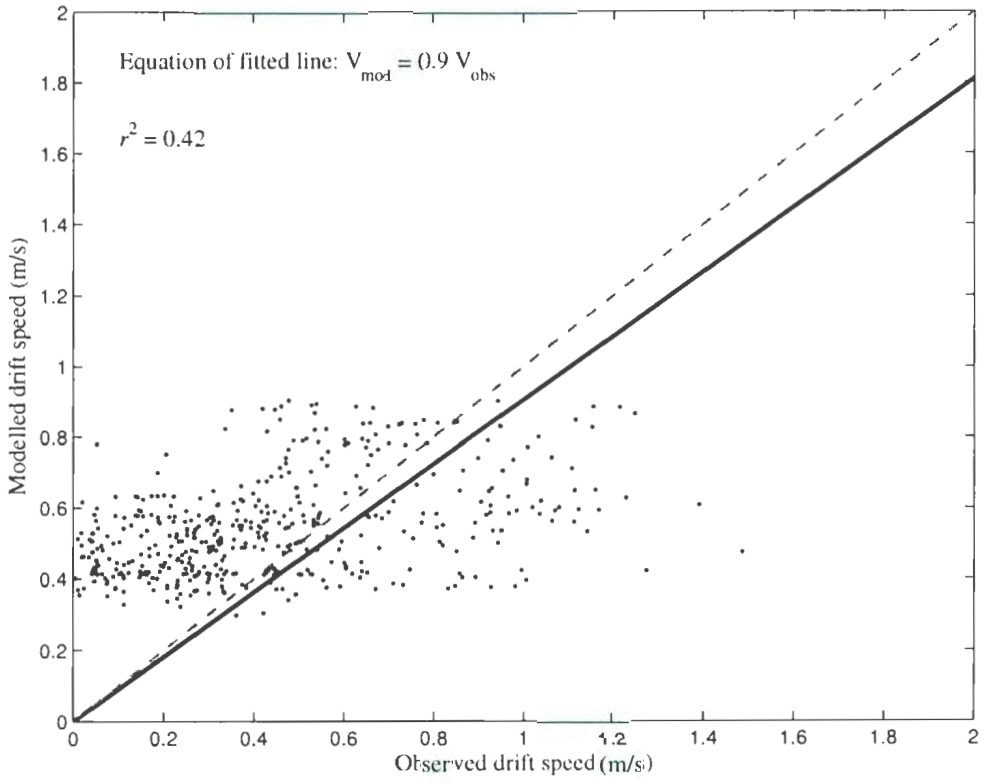

Figure C.16: Correlation between observed and modelled drift speed data for large and extra-large icebergs in medium sea states

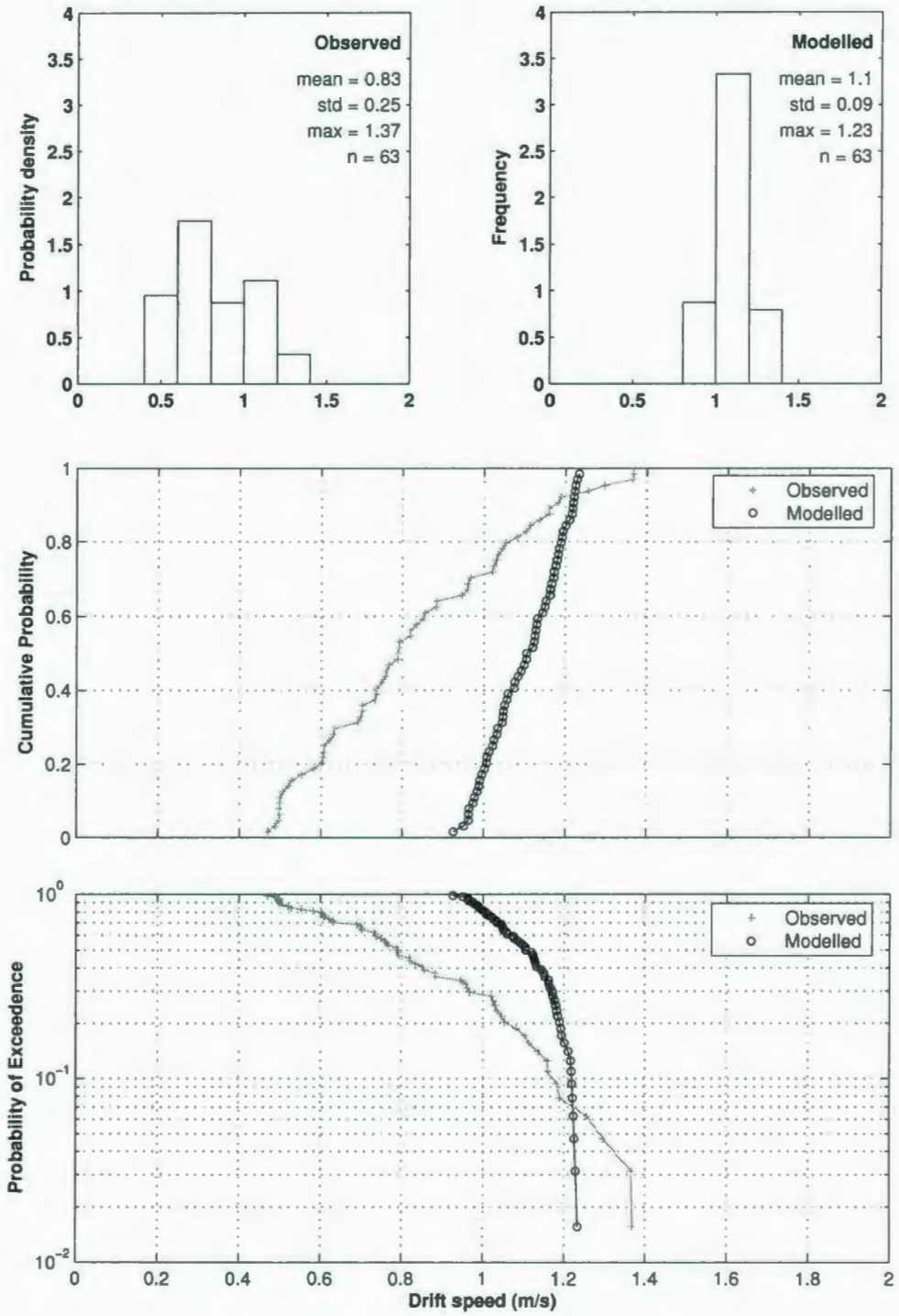

Figure C.17: Comparison of observed and modelled drift speed distributions for small icebergs in high sea states

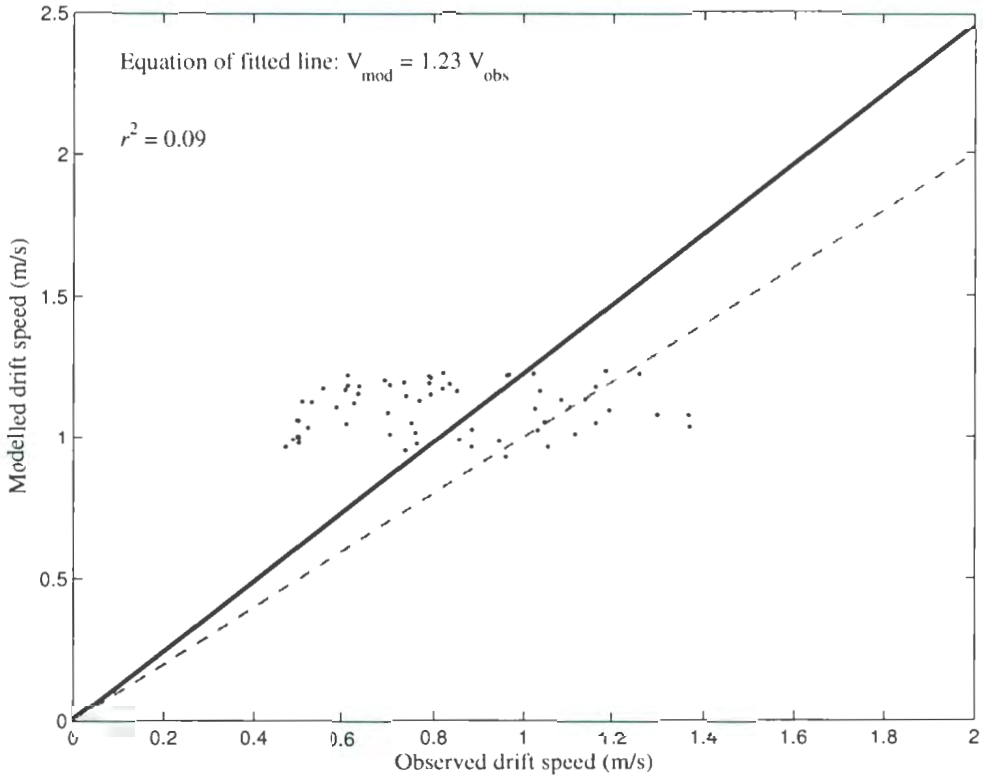

Figure C.18: Correlation between observed and modelled drift speed data for small icebergs in high sea states

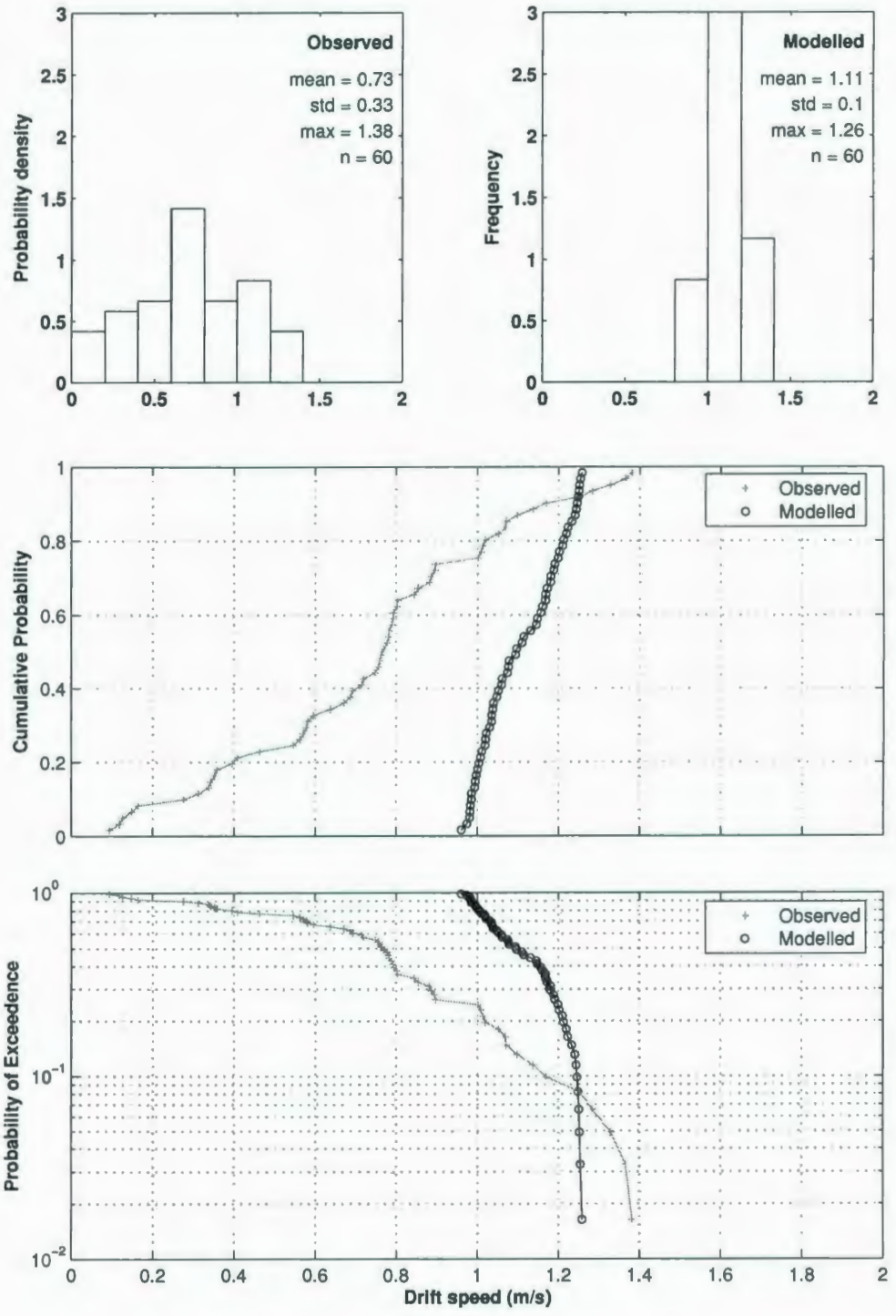

Figure C.19: Comparison of observed and modelled drift speed distributions for medium icebergs in high sea states

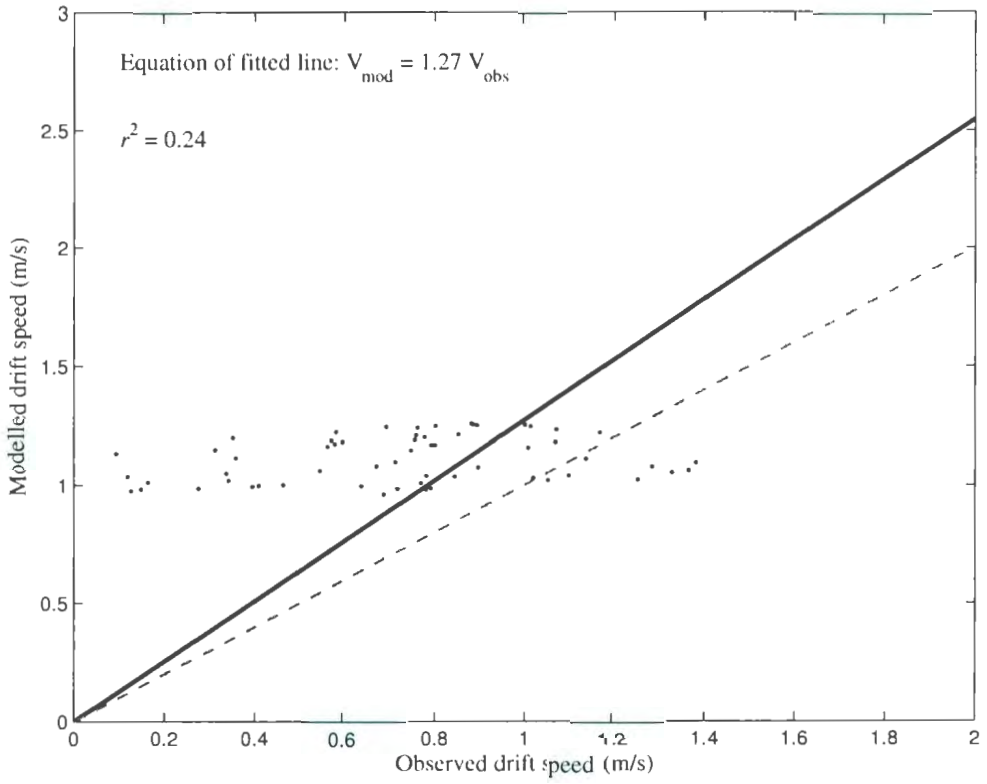

Figure C.20: Correlation between observed and modelled drift speed data for medium icebergs in high sea states

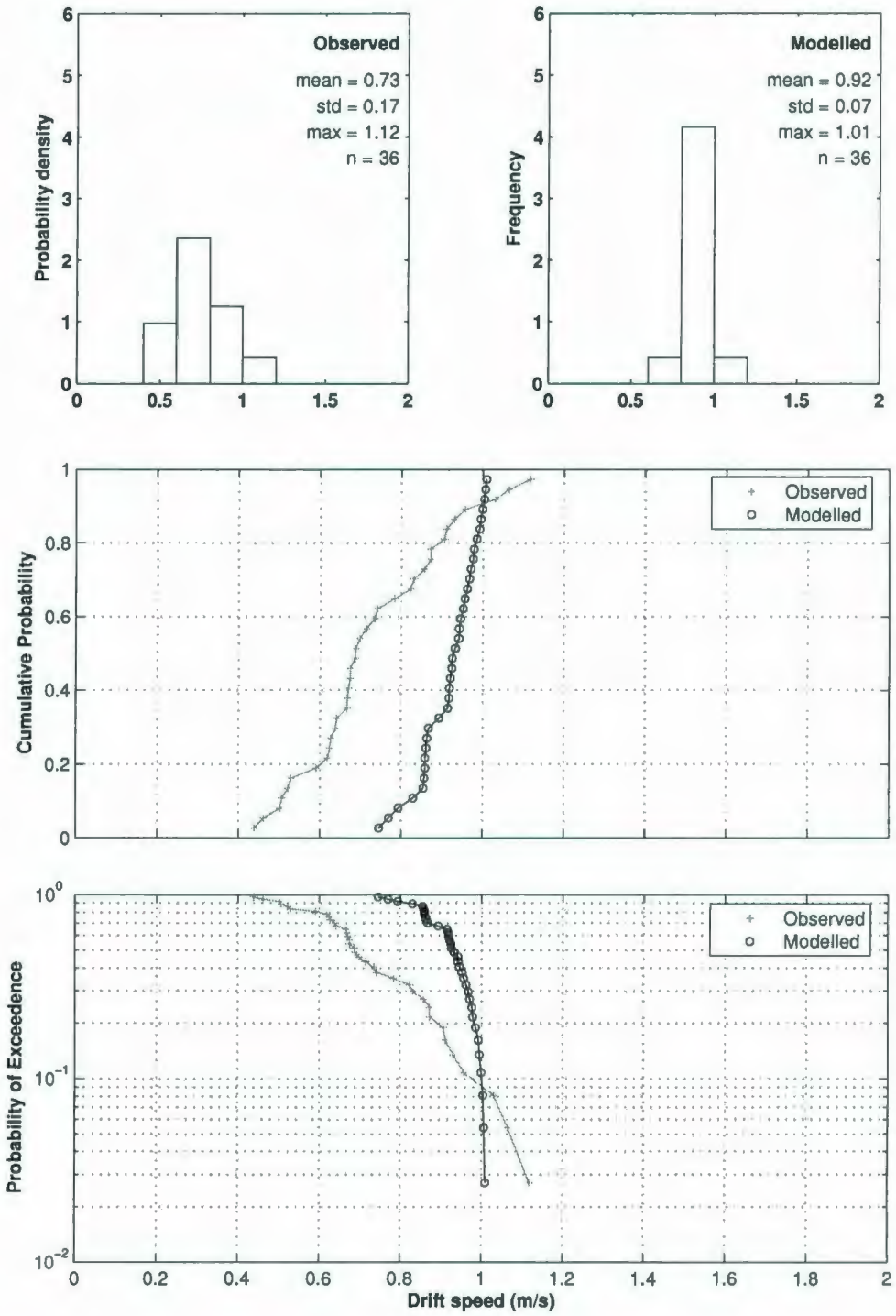

Figure C.21: Comparison of observed and modelled drift speed distributions for large and extra-large icebergs in high sea states

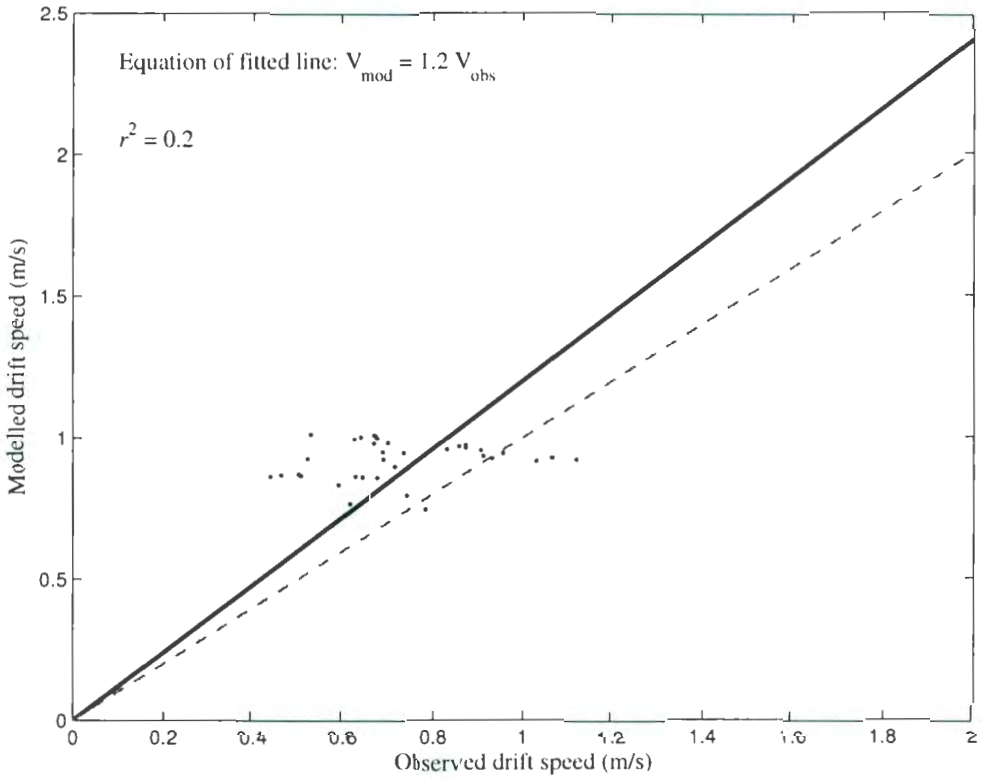

Figure C.22: Correlation between observed and modelled drift speed data for large and extra-large icebergs in high sea states

Appendix D

Comparison Between Observed and Modelled Drift Speed Data Sets Based on Water Depth

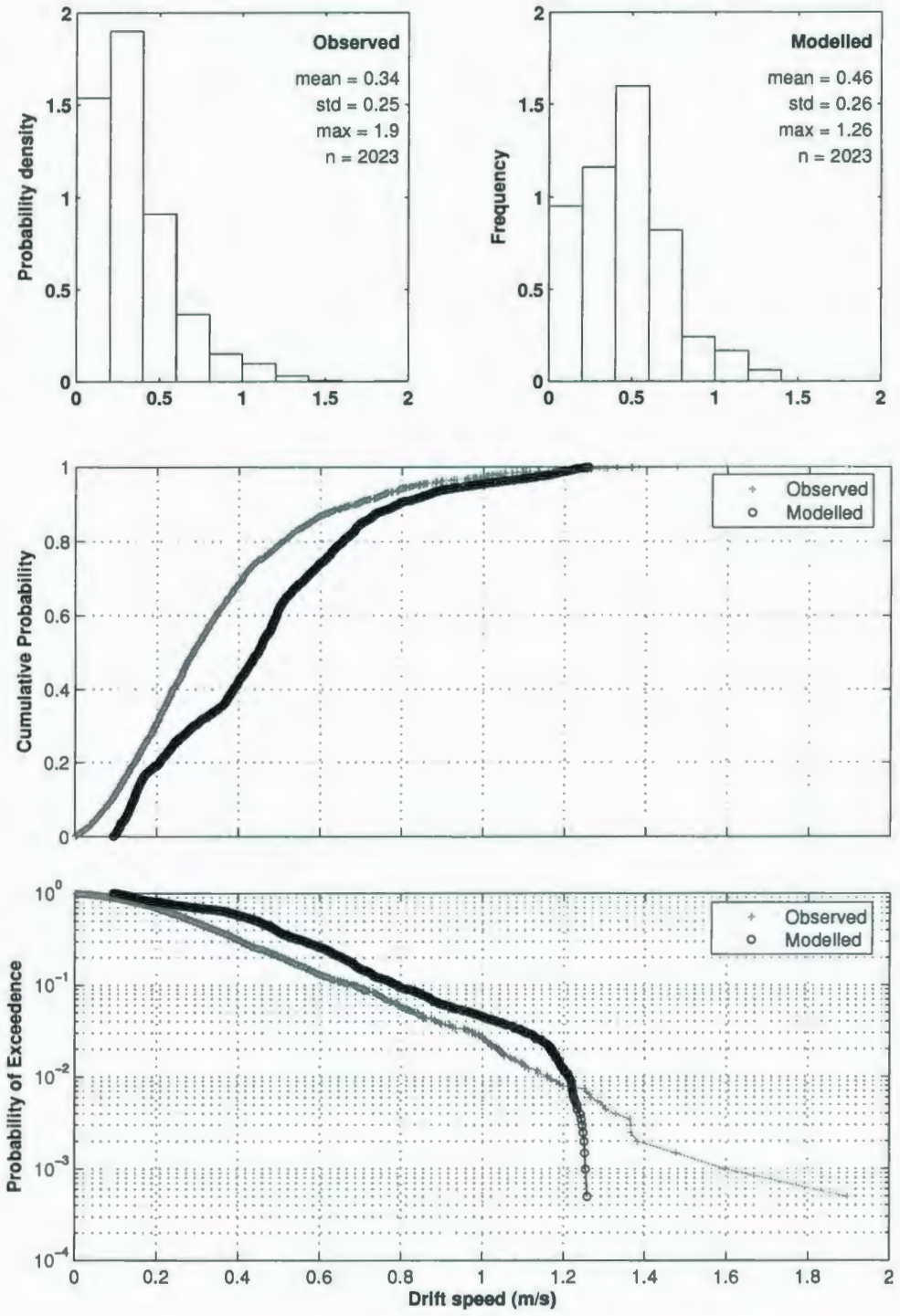

Figure D.1: Comparison of observed and modelled drift speed distributions for onshelf icebergs

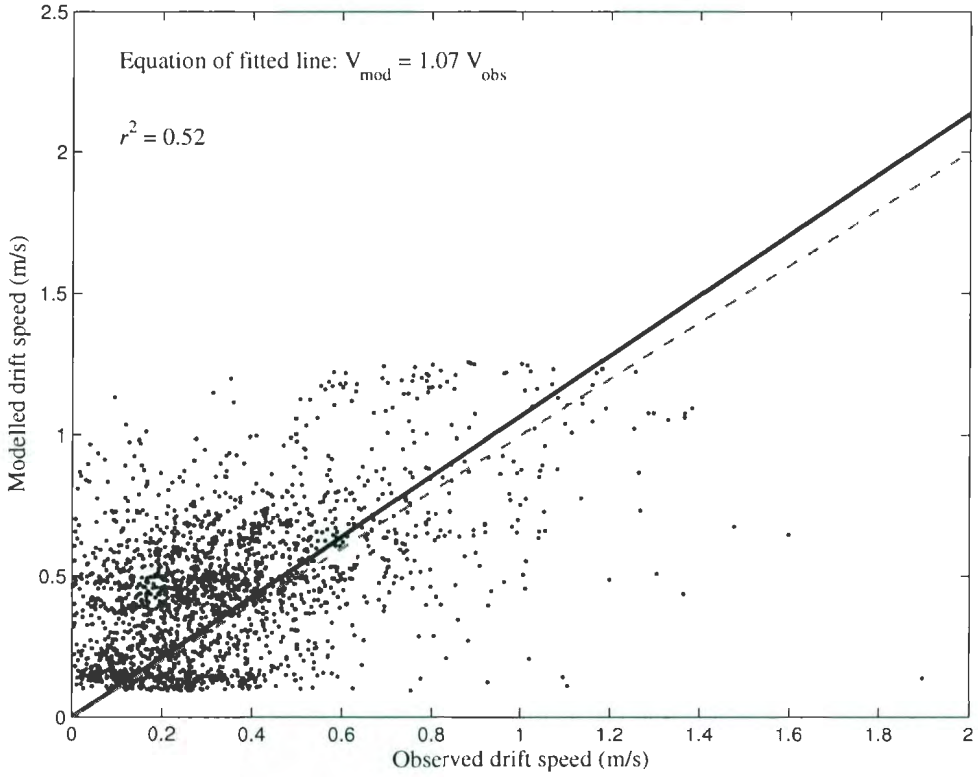

Figure D.2: Correlation between observed and modelled drift speed data for onshelf icebergs

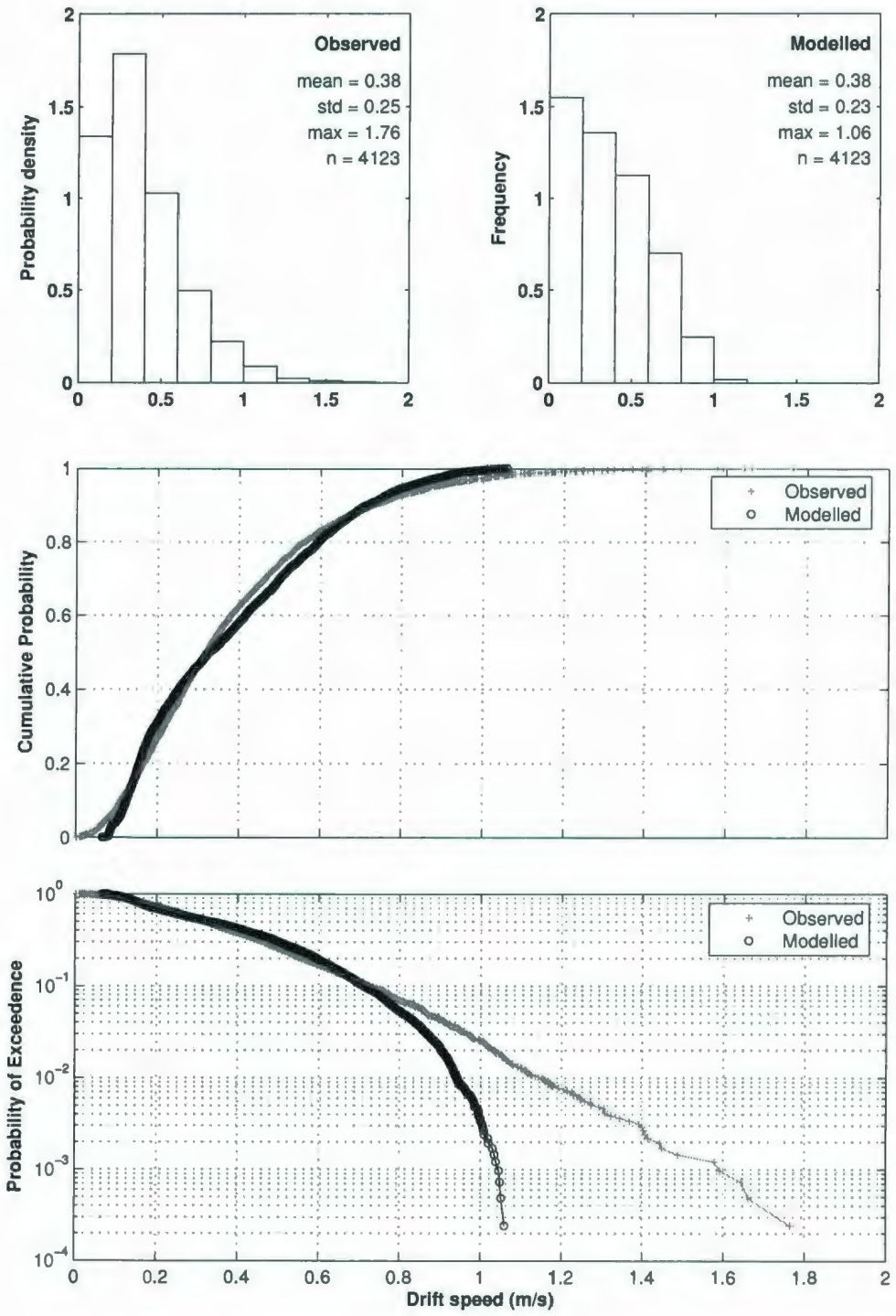

Figure D.3: Comparison of observed and modelled drift speed distributions for offshelf icebergs

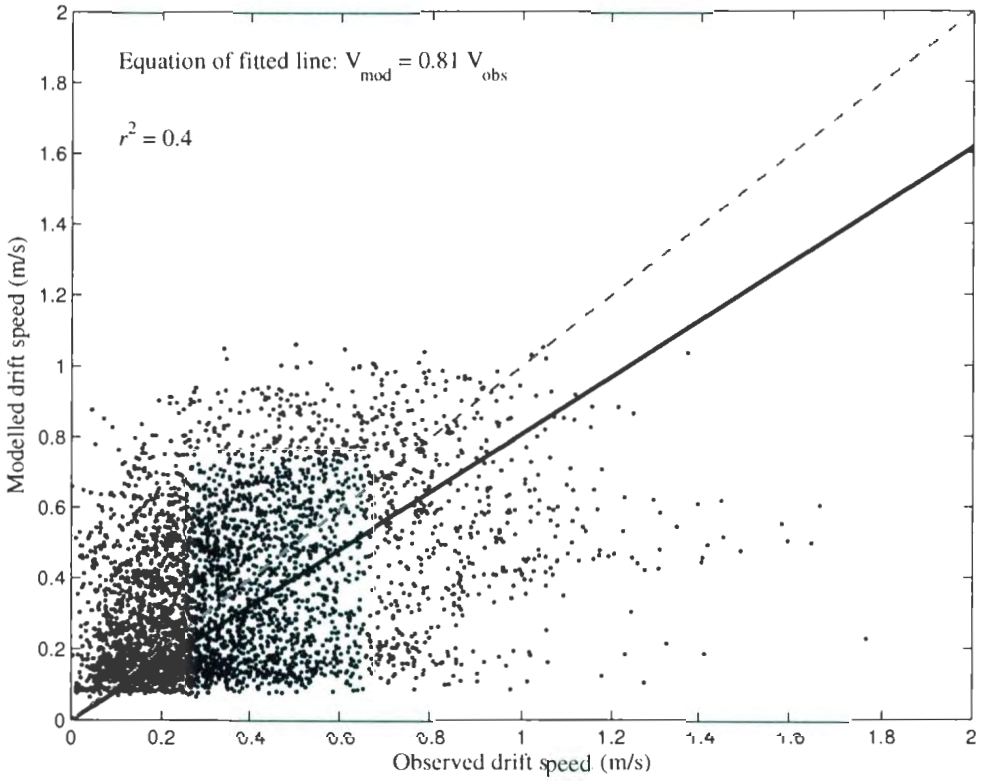

Figure D.4: Correlation between observed and modelled drift speed data for offshelf icebergs

Appendix E

Comparison Between Observed and Modelled Drift Speed Data Sets Using Probabilistic Drift Speed Model

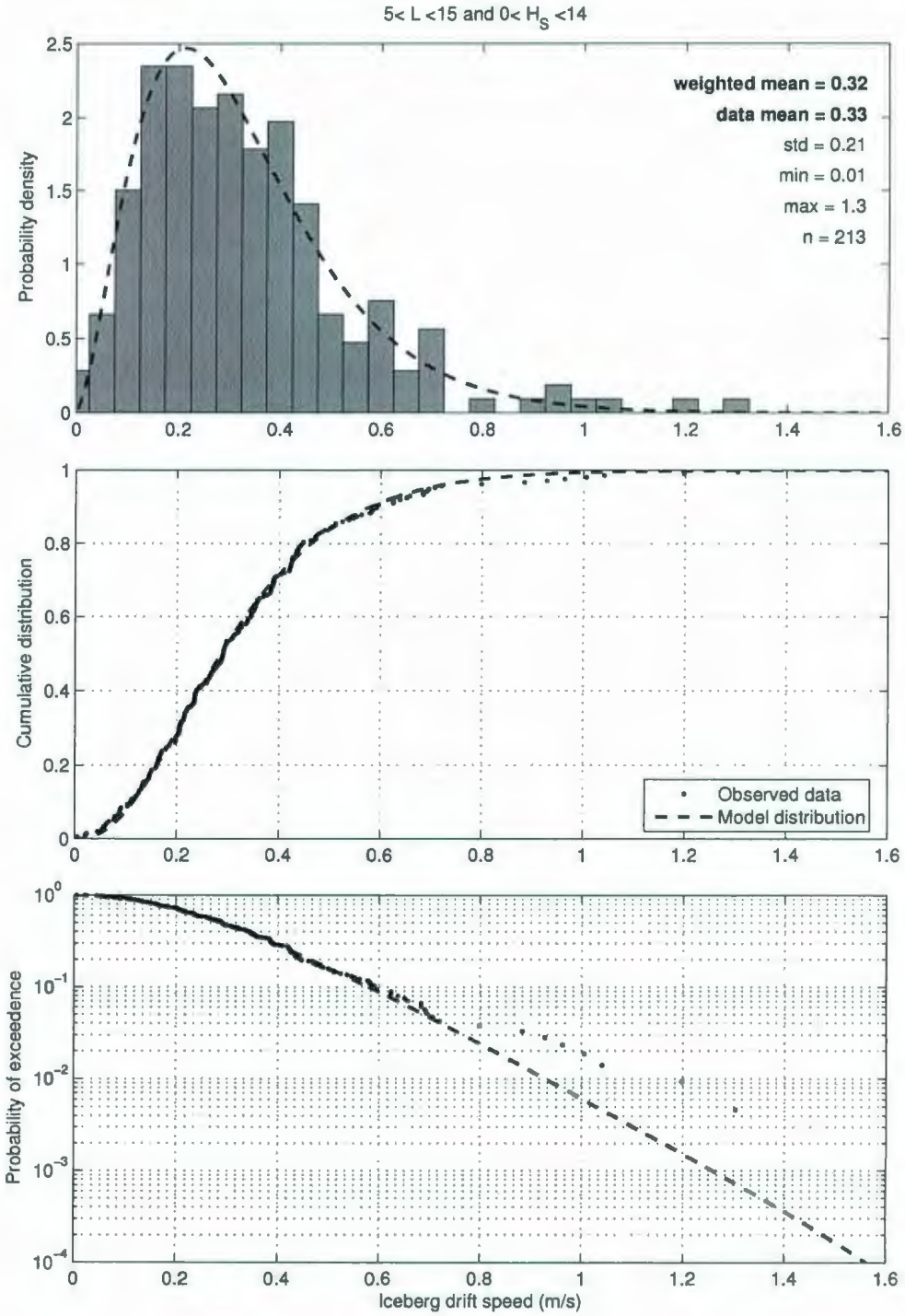

Figure E.1: Comparison of observed and newly modelled drift speed distributions for bergy bits and growlers

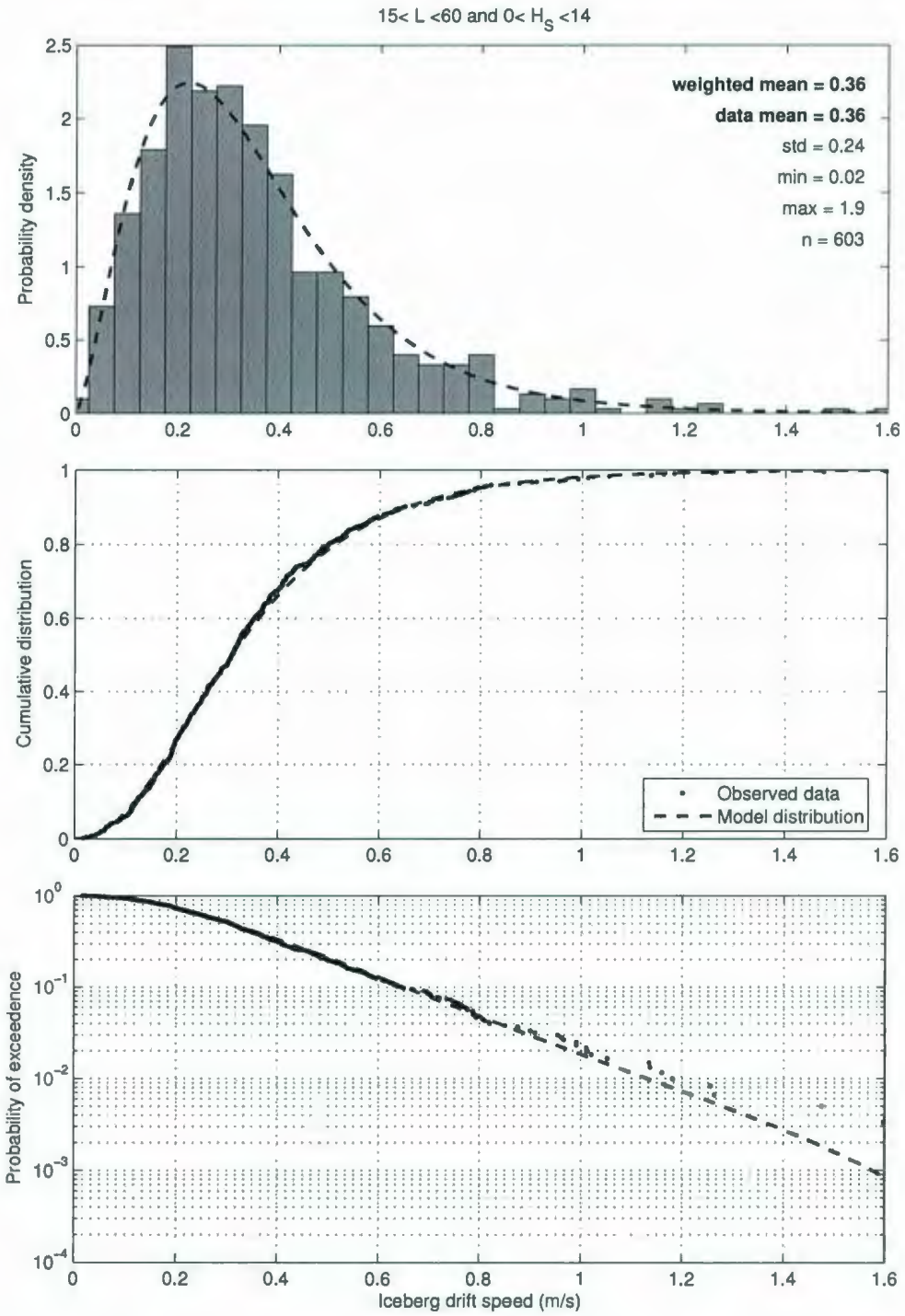

Figure E.2: Comparison of observed and newly modelled drift speed distributions for small icebergs

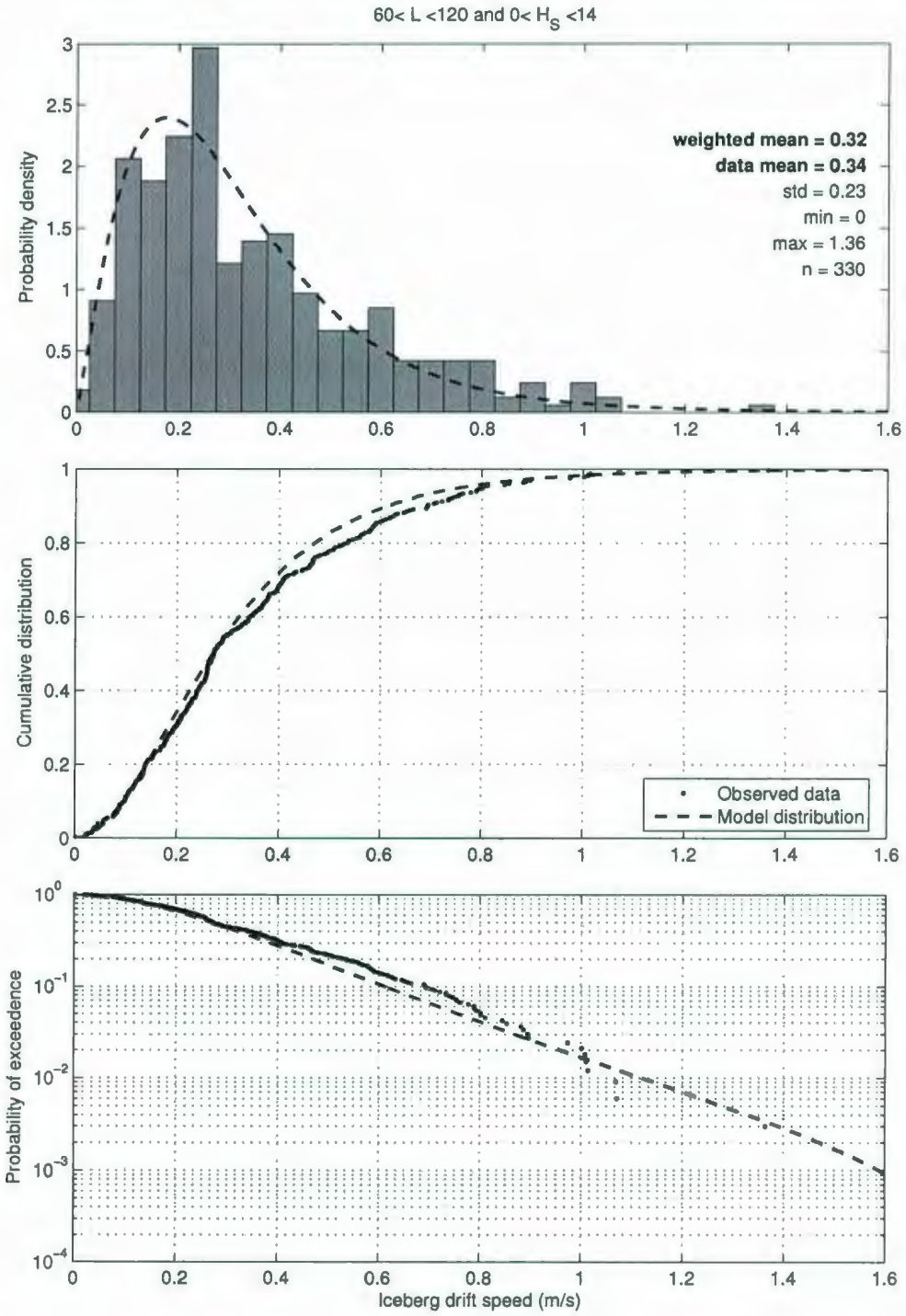

Figure E.3: Comparison of observed and newly modelled drift speed distributions for medium icebergs

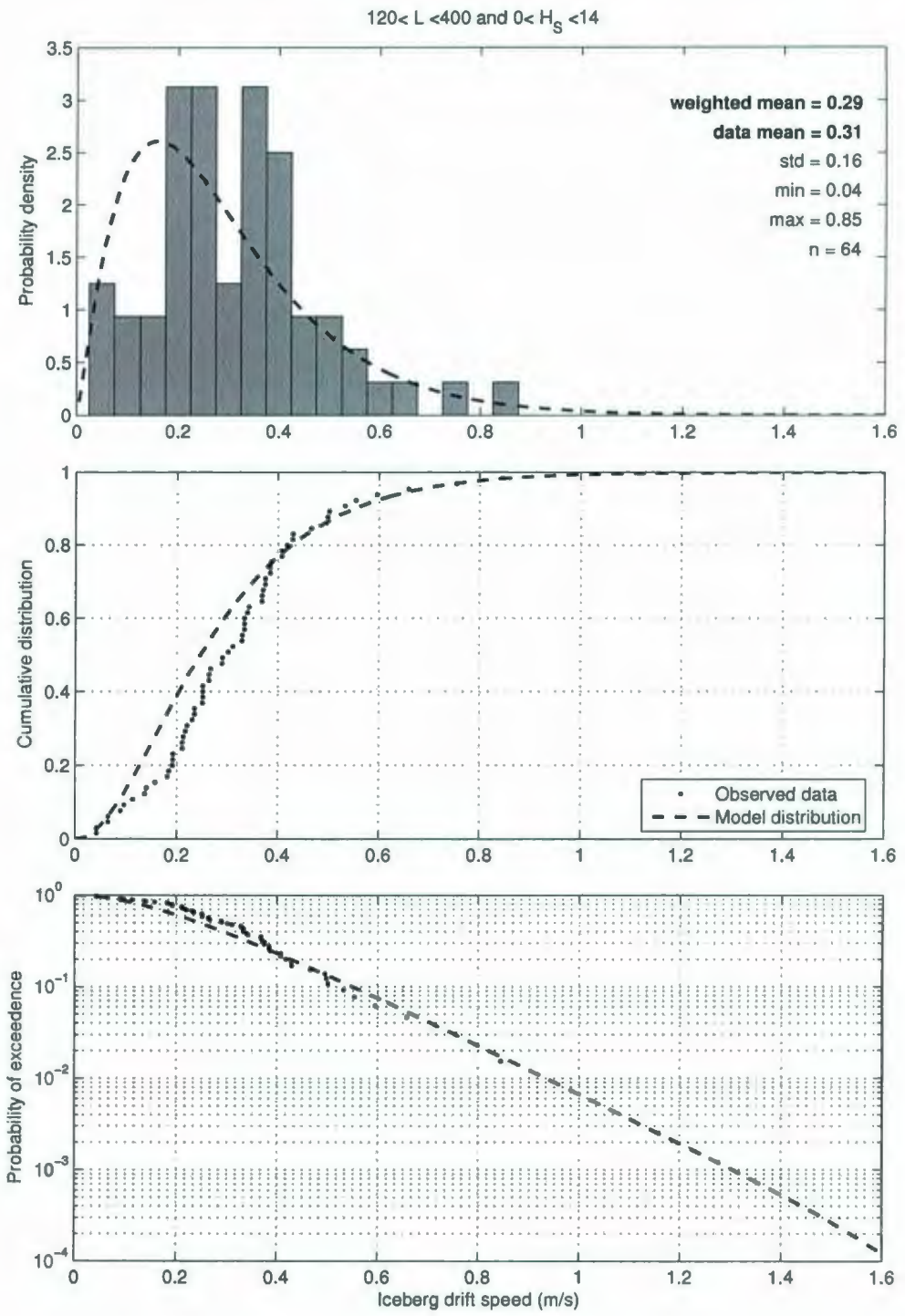

Figure E.4: Comparison of observed and newly modelled drift speed distributions for large icebergs

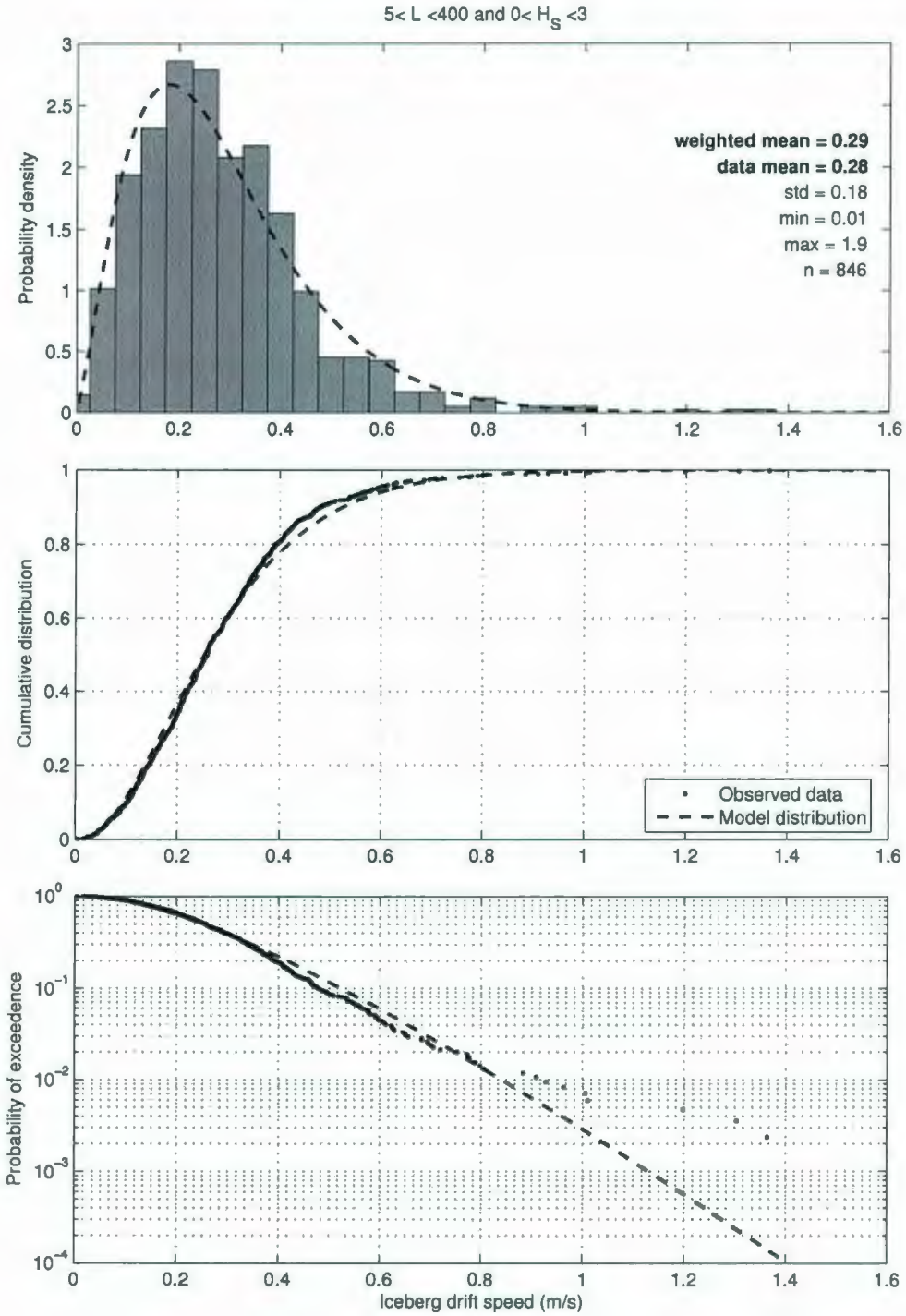

Figure E.5: Comparison of observed and newly modelled drift speed distributions for low significant wave heights

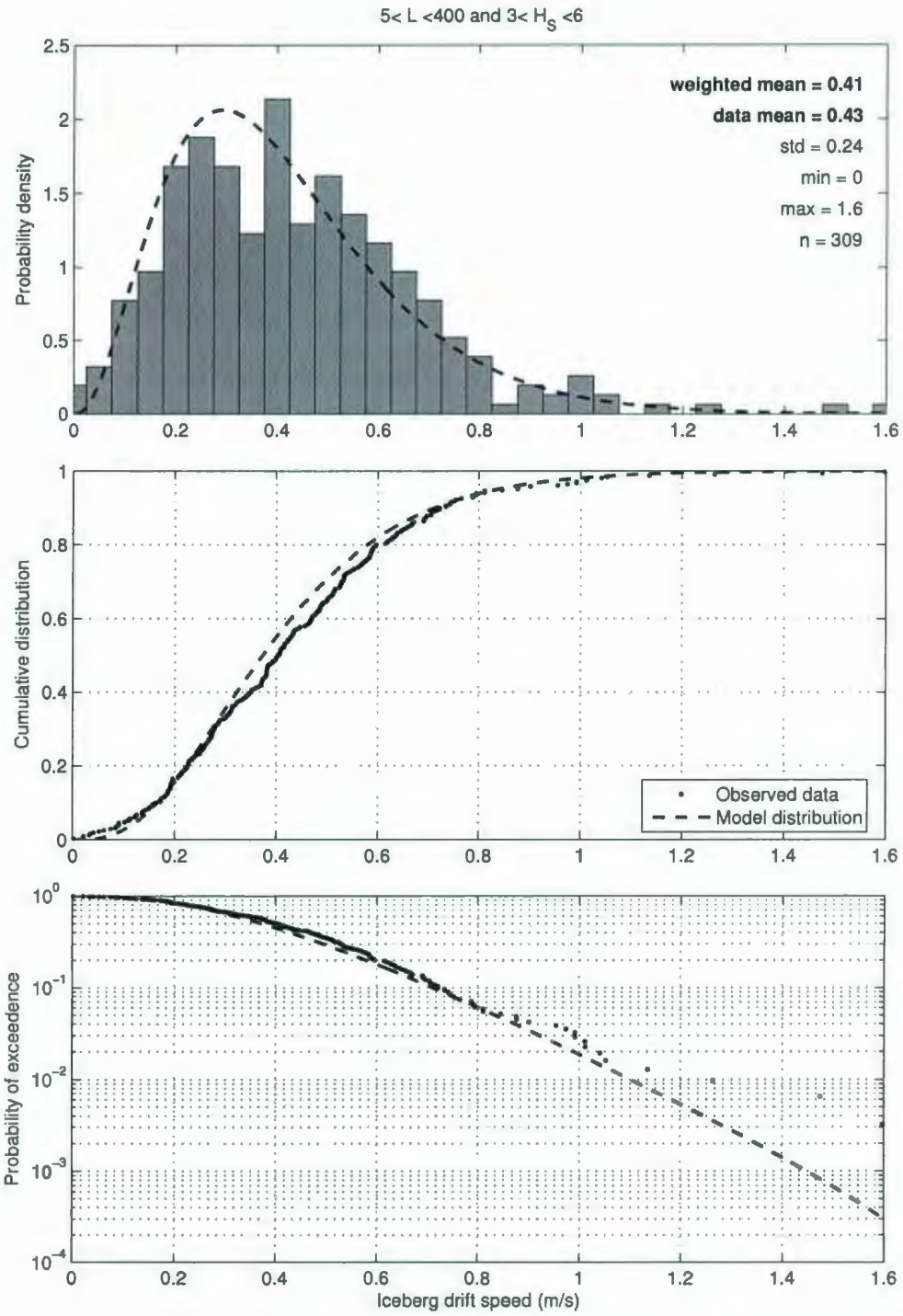

Figure E.6: Comparison of observed and newly modelled drift speed distributions for medium significant wave heights

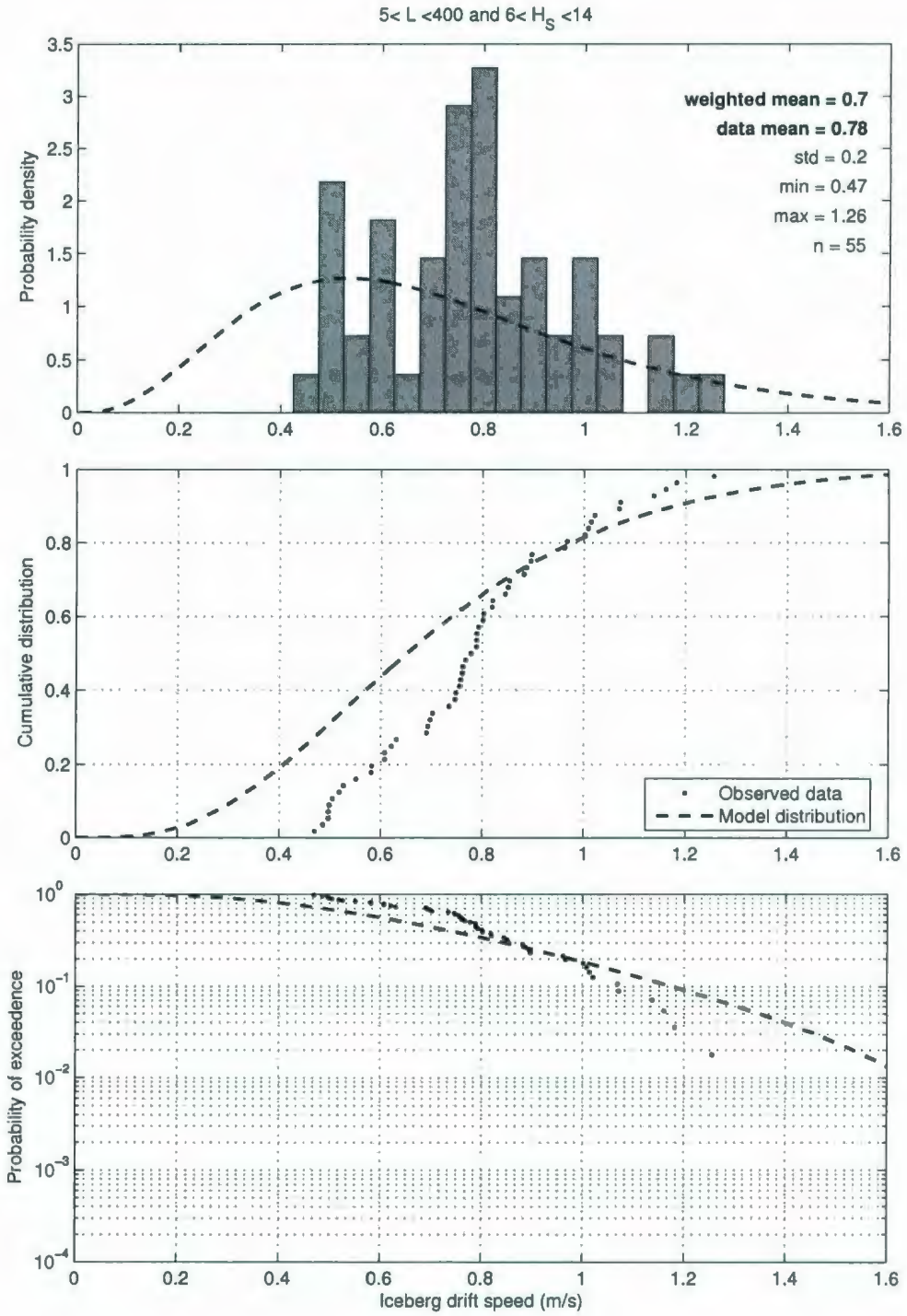

Figure E.7: Comparison of observed and newly modelled drift speed distributions for high significant wave heights